SPIN DYNAMICS
NEAR
THE CRITICAL POINT

Yuichi OKUDA

1978

Synopsis

Spin dynamics near the critical point was studied by the dispersion-absorption technique, which is the complex susceptibility measurement, on a quasi two dimensional ferrimagnet $Mn(CH_3COO)_2 \cdot 4H_2O$ and a quasi two dimensional Heisenberg ferromagnet $(CH_3NH_3)_2CuCl_4$.

The critical slowing down, which is the most fundamental phenomenon near the critical point, was observed as a dip just at T_c in $\chi'(\omega)$ in $Mn(CH_3COO)_2 \cdot 4H_2O$ for the frequency higher than 180 MHz. This was the first observation of the dip in $\chi'(\omega)$ just at T_c due to the critical slowing down in the spin system. The critical exponent of the relaxation time for the uniform mode, Δ, was revealed to be 1.30 ± 0.03 for $0.06 < \varepsilon < 1$ ($\varepsilon = T/T_N - 1$) in the paramagnetic region. This value is smaller than that of the static susceptibility, γ, which is 1.53 ± 0.03 for the same ε region. This fact indicates that the Onsager's kinetic coefficient L, which is defined as $L = \chi_0/\tau$, definitely increases as the transition point is approached. The increase of L means the development of the torque which acts on the uniform mode. Another important result is a small but definite deviation of the Cole=Cole figure from the semi-circle to the Cole-Cole arc as the transition temperature is approached. The deviation reaches to $\beta = 0.9$ at T_N from $\beta = 1.0$ for the high temperature region, where β is the measure of the deviation from the Cole-Cole semi-circle, in the notation of the phenomenological theory of Matsubara and Yoshimitsu.

In $(CH_3NH_3)_2CuCl_4$, the dip was also observed in $\chi'(\omega)$ just at T_c for the frequency higher than 9.8 MHz. The critical exponent Δ is 1.05 ± 0.05 for $0.003<\varepsilon<0.1$. The critical exponent γ is 1.73 for $0.05<\varepsilon<0.3$ and 1.2 for $0.003<\varepsilon<0.05$ (crossover from 2d Ising to 3d Ising). The crossover phenomenon was not observed in the dynamic quantity τ. γ is larger than Δ for the whole ε region, which means a definite divergence of the Onsager's kinetic coefficient L, though it is weaker than that of χ_0 and τ. The deviation from the Debye type semi-circle to the Cole-Cole arc was also observed when the transition point was approached. β decreases from 1 for ε smaller than 0.01 where χ_0 is diverging with a definite critical exponent. β finally reaches to 0.9 at T_c. The decrease of β from 1 is understood as the polydispersive relaxation.

The spin dynamics in the random diluted ferromagnet $(CH_3NH_3)_2Cu_{1-x}Cd_xCl_4$ (x=0.08, 0.11) was studied by the Cole-Cole plot. The Cole-Cole figure is approximated by a semi-circle or a symmetric Cole-Cole arc in the high temperature region, but as the transition point is approached it becomes anomalously depressed, especially in the low frequency region. The angle between the abscissa ($\chi'(\omega)$-axis) and the tangent at $\omega=0$ is about $\pi/4$, which implys that the asymptotic form for $t\to\infty$ of the relaxation function is $t^{-1/2}$.

The relaxation time near T_c under the external field was studied in $Mn(CH_3COO)_2\cdot4H_2O$ and $(CH_3NH_3)_2CuCl_4$. The relaxation time, which gets slow down sufficiently near T_c, makes a quick recovery to a fast relaxation time when the field is applied along

the second easy axis. The Onsager's kinetic coefficient L drastically increases when the field is applied along the second easy axis. The experimental results are discussed comparing the case when the field is applied along the easy axis which is the same direction of the susceptibility measurement.

CONTENTS

Chapter I.	General introduction	1
	References	7
Chapter II.	Experimental procedures	
§II-1.	Measurement of high frequency susceptibility	8
§II-2.	Cryostat design	12
§II-3.	Sample preparation	14
§II-4.	Correction for demagnetization	15
	References	18
Chapter III.	Critical slowing down in $Mn(CH_3COO)_2 \cdot 4H_2O$	
§III-1.	Introduction	19
§III-2.	Static susceptibility	22
§III-3.	Dynamic susceptibility	27
§III-4.	Discussion	38
	References	40
Chapter IV.	Critical slowing down in $(CH_3NH_3)_2CuCl_4$	
§IV-1.	Introduction	41
§IV-2.	Static susceptibility	45
§IV-3.	Dynamic susceptibility	49
§IV-4.	Analysis and discussion of the polydispersive relaxation	60
	References	64
Chapter V.	Dynamics in a randomly diluted ferromagnetic system $(CH_3NH_3)_2Cu_{1-x}Cd_xCl_4$	
§V-1.	Introduction	65
§V-2.	Experimental results	67

§V-3. Comparison with the theory of the spin glass 73

References 77

Chapter VI. Relaxation time near T_c under external field

§VI-1. Introduction 78

§VI-2. Experimental results 82

References 98

Appendix Non-linearity and polydispersive relaxation 99

References 100

Acknowledgments 103

I. General introduction

The investigation of the critical phenomena near the second order phase transition point has made a great strides in recent years. We have reached the deep understanding of singularities of various physical quantities at the critical point in the static case. The most transparent result is the hypothesis of the universality, which has been supported by various experiments.[1,2] The hypothesis states that the critical exponents must be identical for all systems which belong to the same universality class. The crossover phenomena from one universality class to another, which can be detected as a change of the exponent of one universality class to another, are also found in some experiments[3] when the transition temperature is extremely approached; for instance, quasi two dimensional system comes to order into three dimensional system as T_c is extremely approached. Although there remain some problems concerning the static universality, for example the exponents in the random system which is being reformulated as a weak universality,[4] there is a tendency in these days that some of the interests shift to the dynamical phenomena in the critical region. It is not only because time dependent phenomena themselves are brilliant, but also because they would promisingly give much more microscopic informations than the static phenomena.

Dynamical properties are reflected in the quantities such as relaxation time, relaxation function and the kinetic coefficient. The detailed sudy of the relaxation time and of the

relaxation function of the uniform magnetization will give the microscopic picture how the uniform mode fluctuation is decomposed into the random noise. The value and the temperature dependence of the relaxation time will reflect the elementary relaxation process. Exponential decay function corresponds to a single relaxation process. Non-exponential decay function, for instance, some power decay function of t, suggests the possibility of the existence of the multi-decay process which will come out just at T_c.[5,6] The Onsager's kinetic coefficient L is defined phenomenologically as $\frac{dM}{dt}=-L\frac{\partial F}{\partial M}$, where F is the free energy and M is the order parameter of a ferromagnet. L contains the informations of the microscopic torque acting on the unifom magnetization. As is shown by Mori and Kawasaki,[7] L is expressed as the time integral of the torque correlation function. The torque correlation function contains the coupling between q=0 mode and $q\neq 0$ modes via some anisotropic interaction or non-linear interactions, where q denotes the wave vector. The temperature dependence of L will reveal how this coupling develops near T_c. So the study on dynamics will lead to the more profound and general understanding of the phase transition or the critical phenomena from the microscopic view point.

In the study of the dynamics near the critical point, the most *fundamental* phenomenon is the critical slowing down. The phenomenon that the relaxation time of the order parameter becomes enormously long is closely connected with the divergence of the correlation length in the static sense at the critical point. The thermodynamic restoring force to the equilibrium

state vanishes at T_c as a result that the curvature of the free energy becomes flatter, which corresponds to the large fluctuation not to easily decay and which in turn corresponds to the divergence of the susceptibility.

The critical slowing down of the uniform mode has been found as a dip in $\varepsilon^*(\omega)$ at T_c in the ferroelectrics.[8,9] When we study the critical dynamics *in the spin system*, we would like to begin with this phenomenon of the dip in $\chi^*(\omega)$ which is a direct observation of the critical slowing down in the low frequency region. It might be due to the effect of the xy components in the spin system that there has not been any observation of this dip in $\chi'(\omega)$ at T_c.

Next problem is to check experimentally the longest limit of the relaxation time at T_c. Does the relaxation time diverge to infinity, or turn out to be constant, or change to speed up? If it diverges, what is the numerical value of the critical exponent?

The third is the temperature dependence of the Onsager's kinetic coefficient L. L is expressed as $1/\tau=L/\chi_0$ phenomenologically. According to the conventional theory[10] which states that L is constant and is not singular at the critical point because only short wave fluctuation contribute to L, the relaxation time diverges as the static susceptibility and the exponent of the critical slowing down of the ferromagnetic order parameter is the same as that of the static susceptibility. Does the coventional theory hold in the real magnetic system or not? If L diverges more strongly than the static susceptibility, the critical slowing down is replaced by the critical speeding up.

As L originates in the interaction which does not conserve the total magnetization, it must be sensitive to the anisotropy or something in the Hamiltonian which does not commute with the uniform mode in the Heisenberg system. How do the xy components in the spin system affect L?

The fourth is to examine whether the relaxation function does deviate from the exponential type decay in the extreme vicinity of the critical point. Does the relaxation of the order parameter continue to follow the exponential decay or change to a slower type for large t such as some power law of t? This can be manifested by the shape of the Cole-Cole plots of $\chi'(\omega)$ and $\chi''(\omega)$. If the asymptotic form of the decay function for large t is described by some power law, the Cole-Cole figure becomes depressed in the lower frequency range. The non-exponential relaxation has been suggested by a phenomenological approach[6] which has the asymptotic form of $t^{-1/2}$ for $t\to\infty$ just at T_c. This may be interpreted as a polydispersive relaxation which means that there are many slowly varying modes. Kinzel and Fischer[11] also showed that the same $t^{-1/2}$ behavior of the uniform magnetization could appear at the freezing point in the spin glass. Their result is based on the random distribution of the exchange interaction which leads to the polydispersive behavior near the transition point. These theories must be checked experimentally in the real system.

There have been some experiments focussed on the dynamical critical phenomena.[12, 13] The most popular and powerful experiment is the neutron inelastic scattering.[14, 15] As the energy

of the thermal neutron is comparable with that of the excitation in the magnetic system, this measurement is fitted for obtaining the microscopic time-scale informations. And it also has an advantage to obtain wave vector dependent phenomena. So it has been a leading experiment, providing the verification of the dynamic scaling law and of the existence of the new modes such as sloppy spin waves in the paramagnetic region. But owing to neutron's high energy, it is difficult to probe into the phenomena near the origin of (q,ω) space, which are the most important and interesting in the critical spin dynamics. We would like to attack the region near the origin of (q,ω), bearing the problems mentioned above in mind.

ESR line width experiment is another popular experiment. Anomalous line broadening near T_N in some antiferromagnets[16] was one of the brilliant results. The external field inherent to the magnetic resonance brings an inevitable difficulty on the study of the singular behavior in the ferromagnetic phase transition, although the recent report by Koetzler et al.[17] on a ferromagnetic Cr compound insisted that in the low field limit the line width was independent of the external field and it would bring about the imformation compatible with that of zero field. It seems actually that the results of the resonance and those of the nonresonant relaxation measurement are different. Line width measures the angular average of the fluctuation perpendicular to the static field, while the nonresonant relaxation measurement can measure the fluctuation of the order parameter M_z itself without the external field.

Here we are interested in the relaxation of the ferromagnetic order parameter itself. So we have adopted the so-called dispersion-absorption technique, in other words, the frequency dependent complex susceptibility measurement. This technique is fitted for low frequency phenomena up to 10^9 Hz, though limited q=0 mode only. It also has a merit to take the external field as an independent parameter. This technique would bring about essentially important informations concerning the problems mentioned in the preceding paragraph.

In this thesis, the critical spin dynamics by the dispersion-absorption technique is studied in some salts which can be approximated to the two dimensional ferromagnets. Low dimensional materials have a wide temperature region for the critical phenomena which brings the fruitful results.

A brief explanation of the experimental procedures and the sample preparations is written in chapter II.

The experimental results on $Mn(CH_3COO)_2 \cdot 4H_2O$ which is approximated to a two dimensional ferrimagnet are presented in chapter III.

Chapter IV gives the experimental results on $(CH_3NH_3)_2CuCl_4$ which is a quasi-two-dimensional Heisenberg ferromagnet. Some phenomenological analysis is done in this chapter.

Chapter V is devoted to the experiment on the random diluted ferromagnetic system $(CH_3NH_3)_2Cu_{1-x}Cd_xCl_4$. The randomness effect on the dynamics is aimed at. The discussion is made by the recent theoretical work on the dynamics of the spin glass.

Final chapter concerns with the relaxation under the external fields. Main attention is on the Onsager's kinetic coefficient L under the external field $H_\perp$ and $H_{//}$.

References

1) H. Ikeda: J. Phys. Soc. Japan 37 (1974) 660.

2) J. Als-Nielsen, R. J. Birgeneau, H. J. Guggenheim and G. Shirane: J. Phys. C9 (1976) L121.

3) L. J. de Jongh: Physica 82B (1976) 247.

4) M. Suzuki: Progr. theor. Phys. 51 (1974) 1992.

5) M. Suzuki and R. Kubo: J. Phys. Soc. Japan 24 (1968) 51.

6) R. Kubo, K. Matsuo and K. Kitahara: J. Statistical Phys. 9 (1973) 51.

7) H. Mori and K. Kawasaki: Progr. theor. Phys. 27 (1962) 529.

8) E. Nakamura and M. Hosoya: J. Phys. Soc. Japan 23 (1967) 844.

9) F. Sandy and R. V. Jones: Phys. Rev. 168 (1968) 481.

10) L. Van Hove: Phys. Rev. 93 (1954) 1374.

11) W. Kinzel and K. H. Fischer: Solid State Commun. 23 (1977) 687.

12) T. Hashimoto and A. Sato: J. Phys. Soc. Japan 38 (1975) 345.

13) R. Nathans, F. Menzinger and S. J. Pickart: J. appl. Phys. 39 (1968) 1237.

14) M. P. Schulhof, P. Heller, R. Nathans and A. Linz: Phys. Rev. Letters 24 (1970) 1184.

15) O. W. Dietrich, J. Als-Nielsen and L. Passel: Phys. Rev. B 14 (1976) 4923.

16) J. C. Burgiel and M. W. P. Strandberg: J. Phys. Chem. Solids 26 (1965) 865.

17) J. Koetzler and H. von Philipsborn: Phys. Rev. Letters 40 (1978) 790.

II. Experimental procedures

§II-1. Measurement of high frequency susceptibility $\chi^*(\omega)$

Measurement of the high frequency magnetic susceptibility, $\chi'(\omega)$ and $\chi''(\omega)$, was performed from 1 MHz up to 450 MHz using Hewlett Packard vector voltmeter A-8504. Figure II-1 displays the block diagram of the apparatus for high frequency susceptibility measurement. The principle of the measurement is as follows. The high frequency wave generated by the signal generator is splitted into two branches by the hybrid Tee†, one of which is fed to the reference probe A of the vector voltmeter and the other to the helical resonator[1] in the cryostat and then is guided to the test probe B. When the circuit is tuned, reactive components are canceled out, so the impedance of the resonator is always resistive, and there exists no phase shift of the propagating wave through the resonator. Whatever the frequency is, the phase difference between A and B is constant so long as the circuit is tuned. The vector voltmeter is used to detect the phase difference between A and B. The frequency of the signal generator is locked to the resonant frequency by the servo-system so that the phase difference between A and B is unchanged when the susceptibility of the sample varies as T approaches T_c. The lengths of transmission lines from the signal generator to A and B are set equal using the line-stretcher,†† in order to minimize the possible error resulting from the change of the resonance frequency due to $\chi^*(\omega)$.

---

† Anzac Electronics, model HH-107.

†† Japan High Frequency Co., Ltd., SRC-S-222P.

This phase detection method is more sensitive and accurate than the conventional Q-meter method, because the phase changes drastically when the frequency is swept across the resonant point, while the amplitude variation in the Q-meter method is often flat, and besides it becomes almost imperceptible near the critical point as the magnetic absorption increases and the Q-value gets worse.

For the measurement of lower frequency (1 MHz<f<50 MHz), the usual LC circuit was used in place of the helical resonator.

Real and imaginary part of $\chi^*(\omega)$ are obtained from the following relation, which are calculated from the impedance of the circuit.

$$4\pi\chi'(\omega)\eta=\Delta-1,$$

$$4\pi\chi''(\omega)\eta=(\Delta-1)/ZQ_0\Omega,$$

$$\Delta=(Q_0^2+1)/(1/Z^2+Q_0^2\Omega^2),$$

$$\Omega=\omega_S/\omega_B,$$

$$Z=V_S/V_B,$$

where ω and V denote the resonant frequencies and the amplitudes of the output of B. The suffix S and B stand for the presence and the absence of the sample in the resonator, respectively. Q_0 is unloaded Q-value of the resonator and η is a filling factor. The dielectric constant of the sample is so small compared with magnetic susceptibility which increases enormously near the transition point that it has a negligible effect on the data.

Magnetic susceptibility for lower frequencies (<100 kHz) was performed by using the modified AC Hartshorn bridge method, whose block diagram is shown in Fig. II-2. The induced voltage

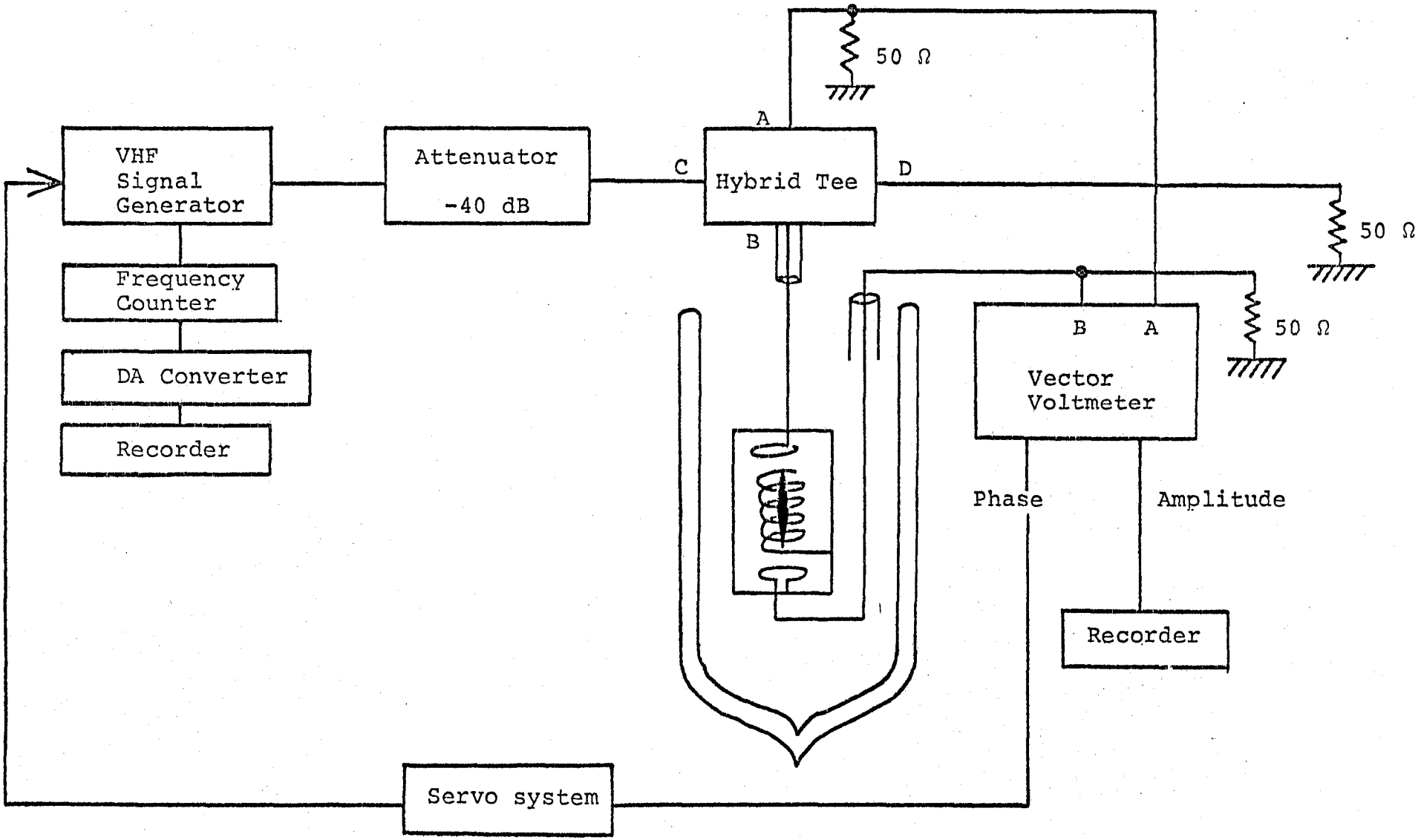

Fig. II-1. Block diagram of the apparatus for the high frequency susceptibility measurement.

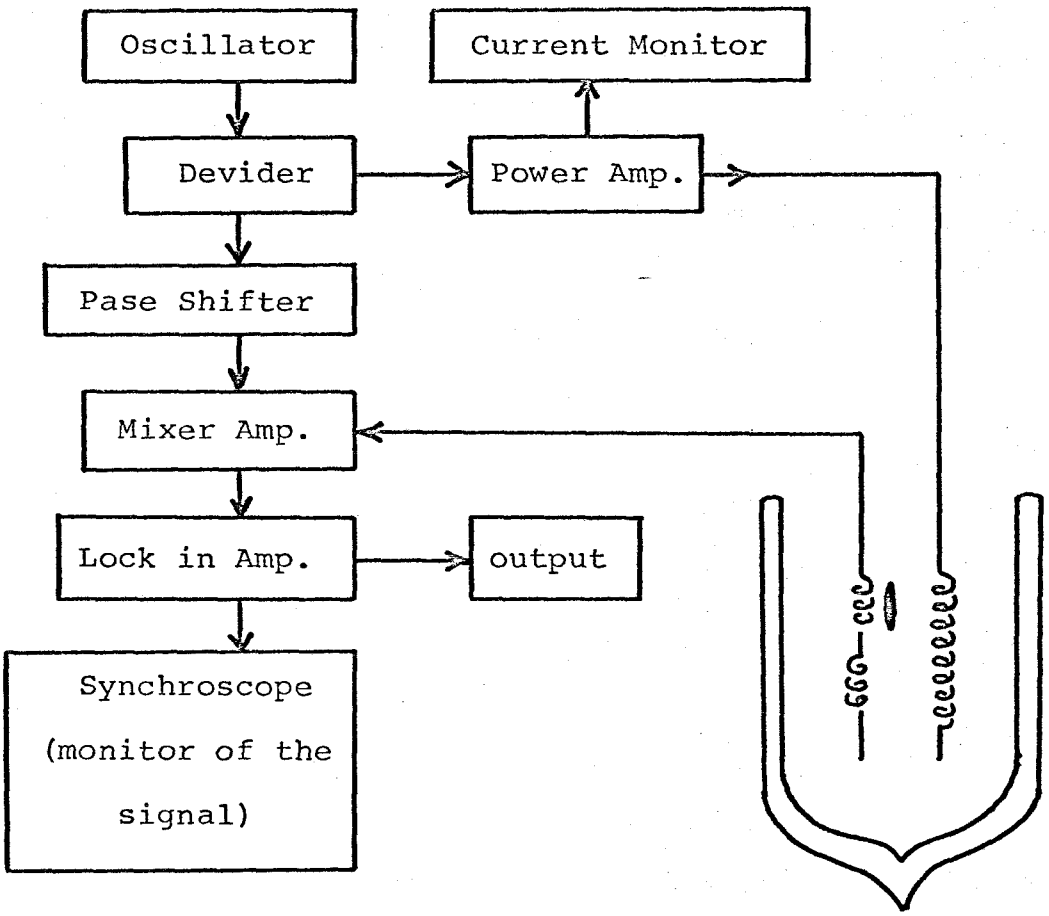

Fig. II-2. Block diagram of the modified Hartshorn Bridge method of the susceptibility measurement in the lower frequency region (<100 kHz).

across the secondary coil is proportional to the susceptibility if the compensation of the coil is perfect. $\chi'(\omega)$ and $\chi''(\omega)$ are detected by the usual lock-in detection.

The absolute value of the magnetic susceptibility was calculated by the well known value of $Mn(NH_4)_2(SO_4)_2 \cdot 6H_2O$, which is given near 4.2 K as

$$\chi = \frac{4.378}{T} \qquad \text{(emu/mol.)}.$$

§II-2. Cryostat design

The measurement for higher temperature than 4.2 K, in the case of $(CH_3NH_3)_2CuCl_4$ and $Mn(CH_3COO)_2 \cdot 4H_2O$, was done by using the adiabatic cell which is shown in Fig. II-3. And for precise temperature control even below 4.2 K it is necessary to construct the adiabatic cell to control temperature electronically. Allen Bradley 100 Ω carbon resistor was used as a thermometer and a temperature sensor as well, and 1 kΩ manganin wire as a heater. The carbon resistor was calibrated against ^4He and H_2 vapor pressure and the superconducting transition point of Pb (six nines) using the empirical formula,

$$T^{-1} = A/\ln R + B + C\ln R.$$

As the susceptibility measurement was performed up to 450 MHz, the adiabatic cell and heat link to the sample must be made of non-metallic materials in order to avoid eddy current losses. Double glass cell and quartz plate were used. Quartz has an excellent heat conductivity below 50 K which is almost compara-

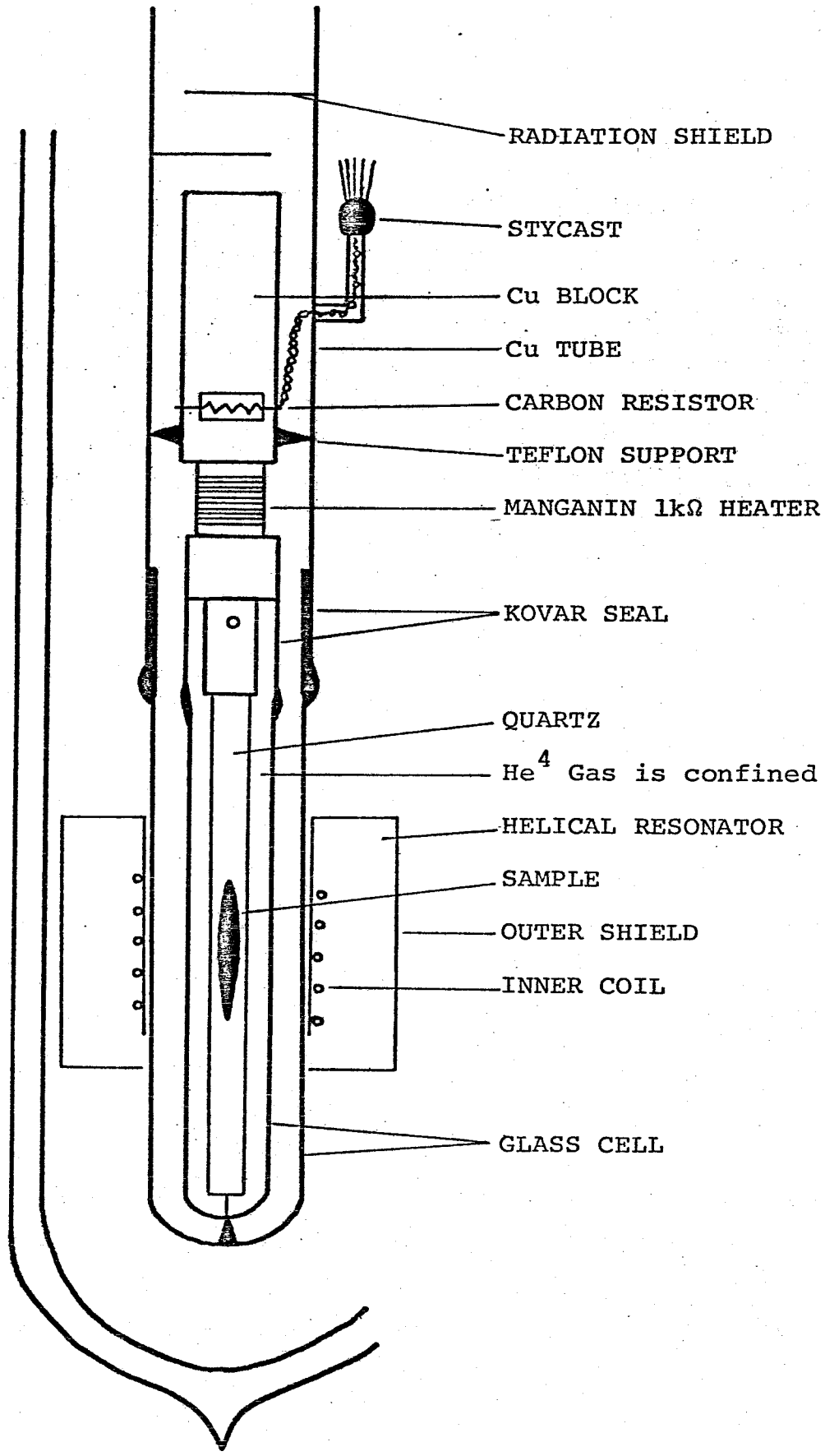

Fig. II-3. Schematic view of the cryostat.

ble with that of Cu metal. It contains little paramagnetic impurities. The sample adhered to the quartz plate by Apiezon N grease was confined in an inner glass cell with ^{4}He gas which not only brings a better thermal contact between the sample and the Cu block but also helps the sample from dehydration or oxidation through a run of experiments. The crystals of $Mn(CH_3COO)_2 \cdot 4H_2O$ were also coated with silicon oil. The adiabatic cell was so constructed as to be movable vertically by the gear at the top of the cryostat for the purpose of getting the resonant frequency of the resonator without the sample. The whole system was made rigidly so that any spurious errors might not come in when moving the adiabatic cell.

§II-3. Sample preparation

The crystals of $Mn(CH_3COO)_2 \cdot 4H_2O$ used in this study were grown from the aqueous solution by slow evaporation at 15∿25°C. The points to make a big crystal are precise temperature control, slow evaporation and using large Schales. Chemically analyzed concentration of Mn ion in $Mn(CH_3COO)_2 \cdot 4H_2O$ prepared in this way is 22.3_5 wt. % while the calculated one is 22.4_3 wt. %.

Crystals of $(CH_3NH_3)_2CuCl_4$ were prepared by slow evaporation from methyl alcohol solution of CH_3NH_3Cl and $CuCl_2$ (stoichiometric mixture) at 35∿40°C. In this case, the essential point is also very slow evaporation.

§II-4. Correction for demagnetization effect

It should be noted that divergence of the susceptibility along the easy axis is stopped at the value of N^{-1}, where N denotes the demagnetization factor depending on the shape of the sample. This fact comes from the well known relation,

$$H = H_{ext} - NM, \qquad (2\text{-}1)$$

where H is the internal field and H_{ext} is the external field. The relation between the intrinsic susceptibility χ and the apparent susceptibility χ_{app} is

$$\chi^{-1} = \chi_{app}^{-1} - N. \qquad (2\text{-}2)$$

The relation (2-1) could be extended to the time dependent field as

$$H(t) = H_{ext}(t) - NM(t). \qquad (2\text{-}3)$$

The similar relation with (2-2) will be obtained for the complex susceptibility $\chi^*(\omega)$.

$$\chi^*(\omega)^{-1} = \chi^*_{app}(\omega)^{-1} - N. \qquad (2\text{-}4)$$

Although N can be obtained from the calculation if the sample shape is ellipsoidal, it is very difficult to shape the present crystals exactly ellipsoidal. So we determined N as follows. It is usually found in various ferromagnetic materials[2, 3] that the static susceptibility along the easy axis of the ellipsoidal crystal is constant below T_c and that the constant value is equal to N^{-1} which is calculated from the shape. In the case of $(CH_3NH_3)_2CuCl_4$ the constant value of the static susceptibility (the measurement was done at 50 Hz which can be regarded as static in this case) was found to be consistent with the calculated one. So we used the value obtained from the static susceptibility measurement for the demagnetization factor. In the case

of $Mn(CH_3COO)_2 \cdot 4H_2O$ we used the calculated value from the sample shape.

The dimensional ratio of the sample, the ratio of the longer axis to the shorter one, lies between 8 and 11 for each sample.

The ellipsoidal shape would be the most preferable, because this makes it easy to set the specimen along the axis of the measuring coil (parallel to the easy axis) and because the demagnetization correction is small so long as the dimensional ratio is large enough. If the sample is shaped toroidally, there exists no need for the demagnetization correction, but the susceptibility reflects fluctuations along the toroid, which are not what we want to know at the critical point.

Next, let us see how the relaxation time and the type of the dispersion obtained from the experimental $\chi'_{app}(\omega)$ and $\chi''_{app}(\omega)$ are corrected by the demagnetization effect. If the dispersion is the Debye-type which expresses $\chi^*_{app}(\omega)$ as

$$\chi^*_{app}(\omega) = \frac{\chi_{0\,app}}{1+i\omega\tau_{app}} ,$$

the intrinsic susceptibility $\chi^*(\omega)$ is given by (2-4) as

$$\chi^*(\omega)^{-1} = \frac{1+i\omega\tau_{app}}{\chi_{0\,app}} - N$$

$$= \frac{1+i\omega\left[\frac{\tau_{app}}{1-N\chi_{0\,app}}\right]}{\left[\frac{\chi_{0\,app}}{1-N\chi_{0\,app}}\right]} .$$

Therefore

$$\chi_0 = \frac{\chi_{0\,app}}{1-N\chi_{0\,app}} ,$$

$$\tau = \frac{\tau_{app}}{1-N\chi_{0\,app}} ,$$

$$L = \frac{\chi_0}{\tau} = \frac{\chi_{0\,app}}{\tau_{app}} .$$

It is easily seen that if the dispersion is the Debye-type, the corrected dispersion is also the Debye-type. In other words the Cole-Cole semi-circle is not changed by the demagnetization correction. Only the absolute value τ_{app} is transformed to $\tau_{app}/(1-N\chi_{0\,app})$. This feature is also found in the case of the Cole-Cole arc.

$$\chi^*(\omega)^{-1} = \left[\frac{\chi_{0\,app}}{1+(i\omega\tau_{app})^{\beta}}\right]^{-1} - N$$

$$= \frac{1+i\omega\left[\frac{\tau_{app}}{(1-N\chi_{0\,app})^{1/\beta}}\right]^{\beta}}{\left[\frac{\chi_{0\,app}}{1-N\chi_{0\,app}}\right]} .$$

The figure of the Cole-Cole arc is unchanged. τ_{app} is transformed to $\tau_{app}/[1-N\chi_{0_{app}}]^{1/\beta}$. It is not an easy matter to verify the above feature for the general polydispersive case.

Koetzler et al.[4] devised the ingenious formula to derive L from $\chi_{0_{app}}$ and $\chi'_{app}(\omega)$ free from the demagnetization effect. But in order to investigate the relaxation time directly and to look into the Cole-Cole figures at the critical point, the tedious demagnetization correction is inevitable.

III. Critical slowing down in $Mn(CH_3COO)_2 \cdot 4H_2O$

§III-1. Introduction

Manganese acetate tetrahydrate (Mn·acetate) is monoclinic and has a crystallographic layer (a-b plane) structure. Figure III-1 shows the crystal structure projected on the a-b plane obtained by the neutron diffraction.[1] There are two sites of Mn ions designated Mn_1 and Mn_2. Inequivalence of the numbers of Mn_1 and Mn_2 in the same plane makes each plane ferrimagnetic. The plane is made up of groups of three Mn ions which are coupled to each other by a linkage of Mn_2-O-Mn_1-O-Mn_2. According to the saturation magnetization measurement[2] and the neutron diffraction[3] the exchange interaction within this trimer is antiferromagnetic and relatively strong which might be a comparable situation to that in MnO. The coupling between these trimers in the same plane is ferromagnetic and the coupling between adjacent layers is antiferromagnetic. Consequently in a low temperature region (near the transition point) this salt is assumed to consist of resultant ferromagnetic layers which are weakly coupled antiferromagnetically with each other. The ferromagnetic interaction J_F in a layer is much stronger than the antiferromagnetic interaction J'_{AF} between adjacent layers ($J'_{AF}/J_F \sim 10^{-3}$).[4]

The spin alignment in the ordered state is shown in Fig. III-2.[5] The easy axis is a-axis. The static susceptibility along this axis exhibits a divergent peak at T_N (3.186 K), reflecting the ferromagnetic intralyer interaction and the weak ($\sim$6 Oe) anti-

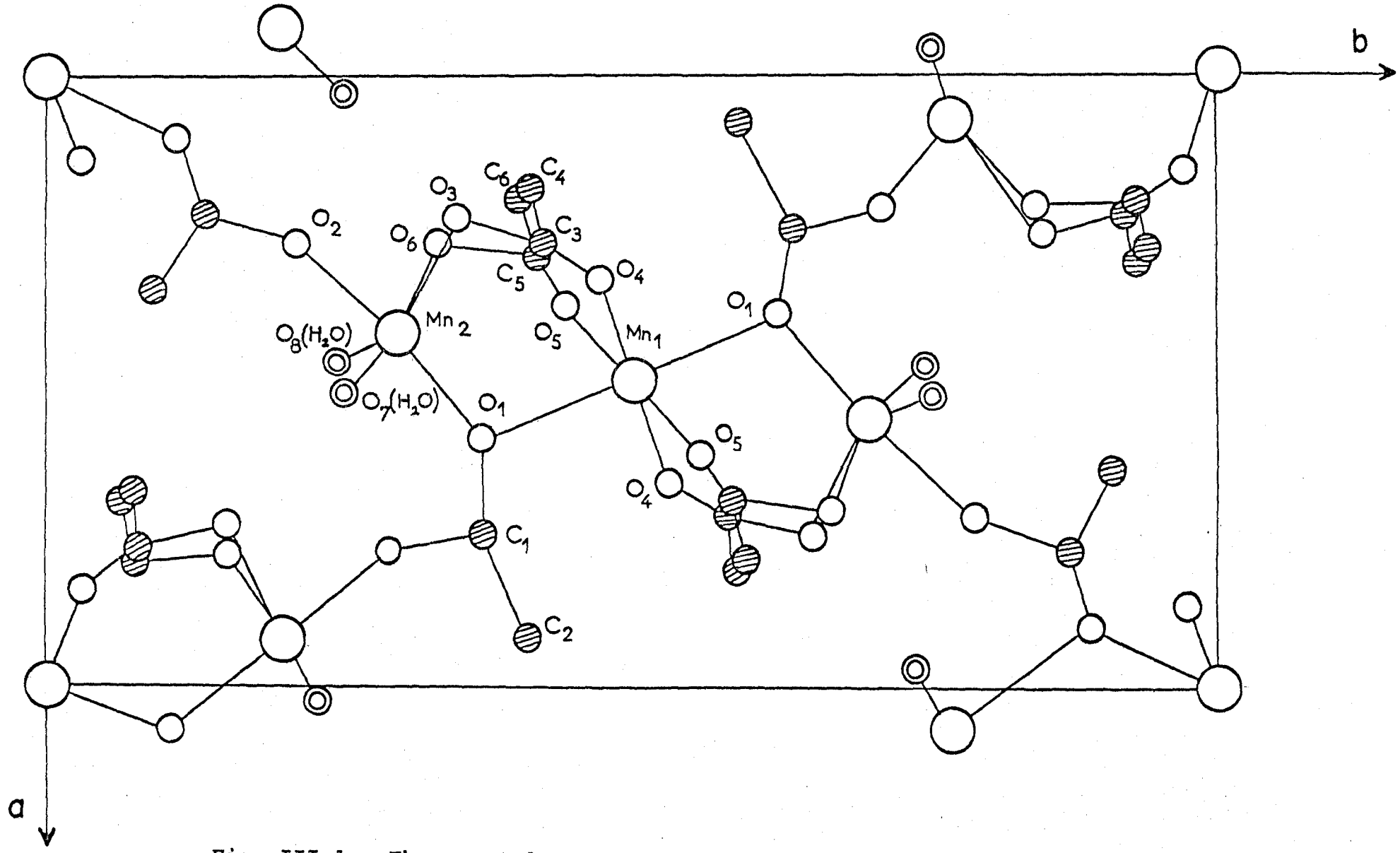

Fig. III-1. The crystal structure of $Mn(CH_3COO)_2 \cdot 4H_2O$, projected on the a-b plane which is the layer of the cleavage.

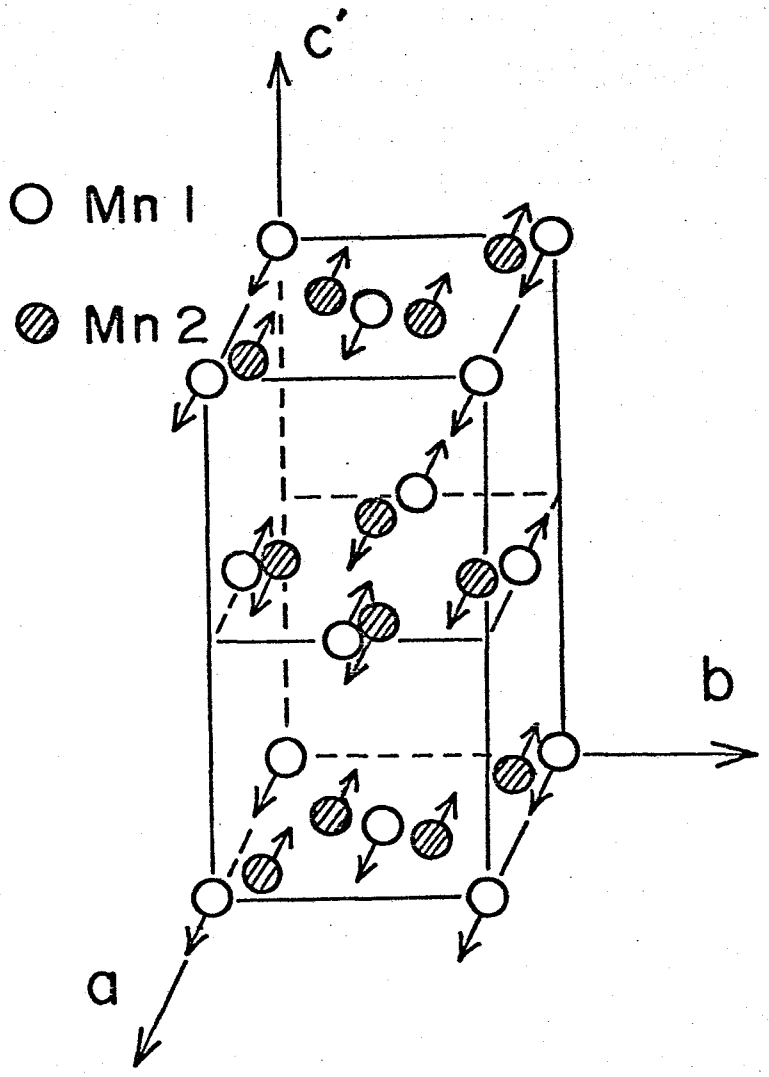

Fig. III-2. Spin alignment of $Mn(CH_3COO)_2 \cdot 4H_2O$ obtained by the neutron diffraction.[3)]

ferromagnetic interlayer interaction. The second easy axis is c' axis which is perpendicular to a and b axis, and b is the hard axis. χ_c, exhibits a less pronounced peak at T_N, but χ_b is almost flat near T_N. The anisotropy fields are estimated as $H_{c'}^A \sim 1350$ Oe and $H_b^A \sim 8600$ Oe.[6] There has been no explanation where this large anisotropy comes from in Mn^{2+} ions. This salt is approximated to 2-d planar ferromagnetic model and might be suited for the experiment mentioned in chapter I among others.

§III-2. Static susceptibility

The static susceptibility was measured in a wide temperature range from 1.2 K to 80 K in order to re-examine the character of this salt mentioned in §III-1. Figure III-3 shows inverse susceptibility of the powdered specimen. In a high temperature region χ_m obeys the Curie-Weiss law, giving the Curie constant C=5.0 (emu deg./mol.) and the Curie Weiss constant Θ=-48 K, which indicates a fairly strong antiferromagnetic interaction. This is consistent with the formation of the antiferromagnetically coupled trimer groups. Below 30 K the curvature of χ_m^{-1} begins to bend downwards as if Θ being positive. This is due to the ferromagnetic interaction among the trimer groups within a layer. The similar behavior of χ_m^{-1}-T is also observed in some manganese alkanoates.[7, 8]

In order to study the mechanism of the dynamic behavior, we examine the temperature dependence of the Onsager's kinetic coefficient L which would give some information about the torque mechanism. We measured the static susceptibility along the easy axis near T_N in detail. It is plotted in Fig. III-4. Figure III-5

is a log-log plot of the susceptibility above and below T_N, corrected for the demagnetization effect. The sample was shaped ellipsoidal; the longer axis is 10.4 mm and the shorter 1.0 mm. Measurement was done at 1 kHz which can be regarded as static, because there is no appreciable frequency dependence between 100 Hz and 100 kHz even near T_N. Measuring field was kept below 1.5 Oe. From the slope in Fig. III-5 the critical exponent in the paramagnetic region is obtained as $\gamma=1.53\pm0.03$ for $0.06<\varepsilon<1$ ($\varepsilon=T/T_N-1$). It should be noted that the antiferromagnetic interlayer interaction becomes important for $\varepsilon<0.06$, which prevents the susceptibility from diverging. Below T_N the exponent $\gamma'=1.53\pm0.03$ for $0.01<\varepsilon<0.1$. The ratio of the amplitude above T_N to that below T_N for the same ε is about 11. Renard et al. gave almost the same value of γ as ours in their static susceptibility measurement.[9] The value of 1.53 is very suggestive of the two dimensional XY model for which Betts gave $\gamma=1.5$ for $S=1/2$ by the high temperature expansion.[10]

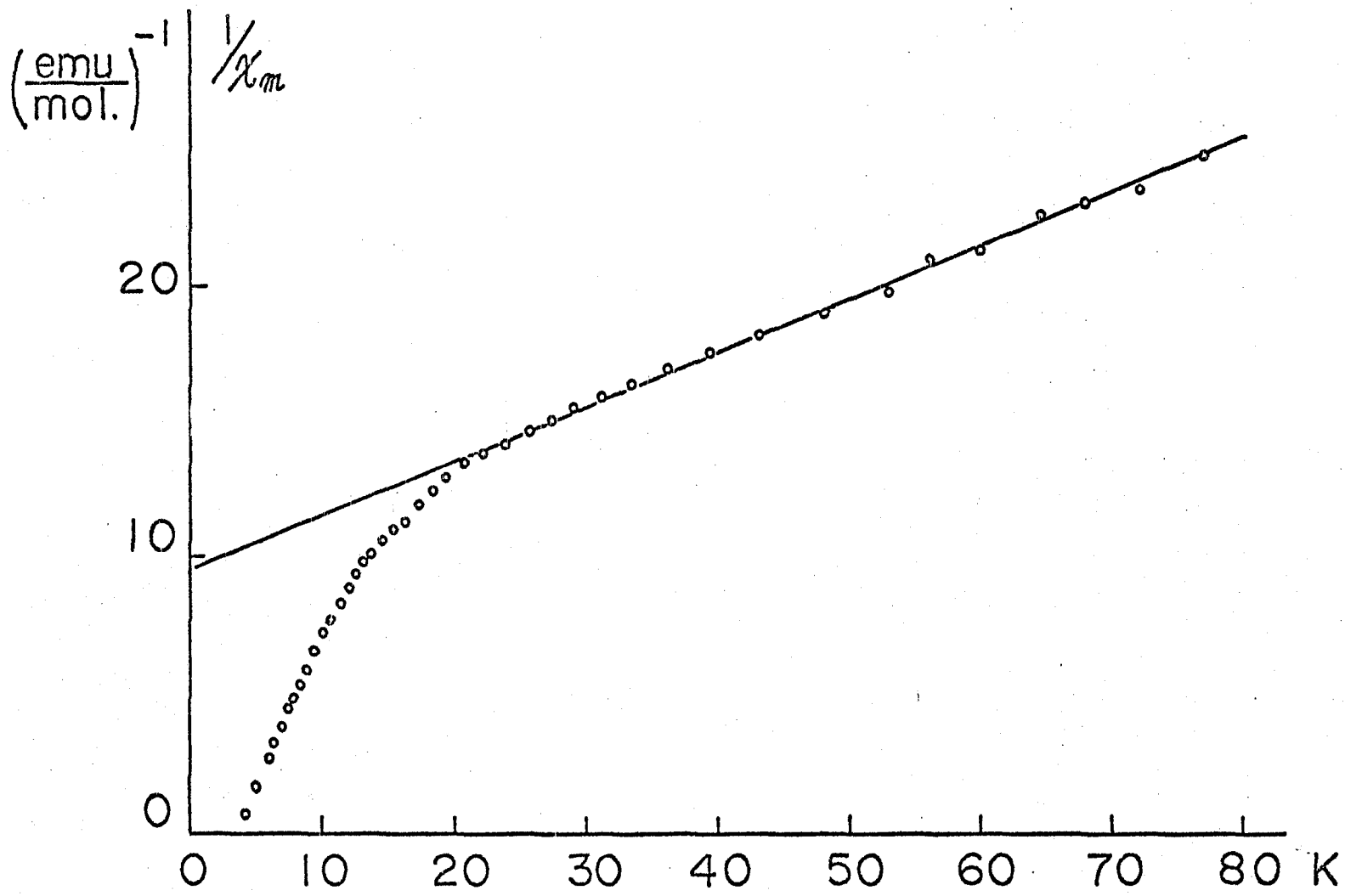

Fig. III-3. Inverse susceptibility of the powdered specimen of $Mn(CH_3COO)_2 \cdot 4H_2O$.

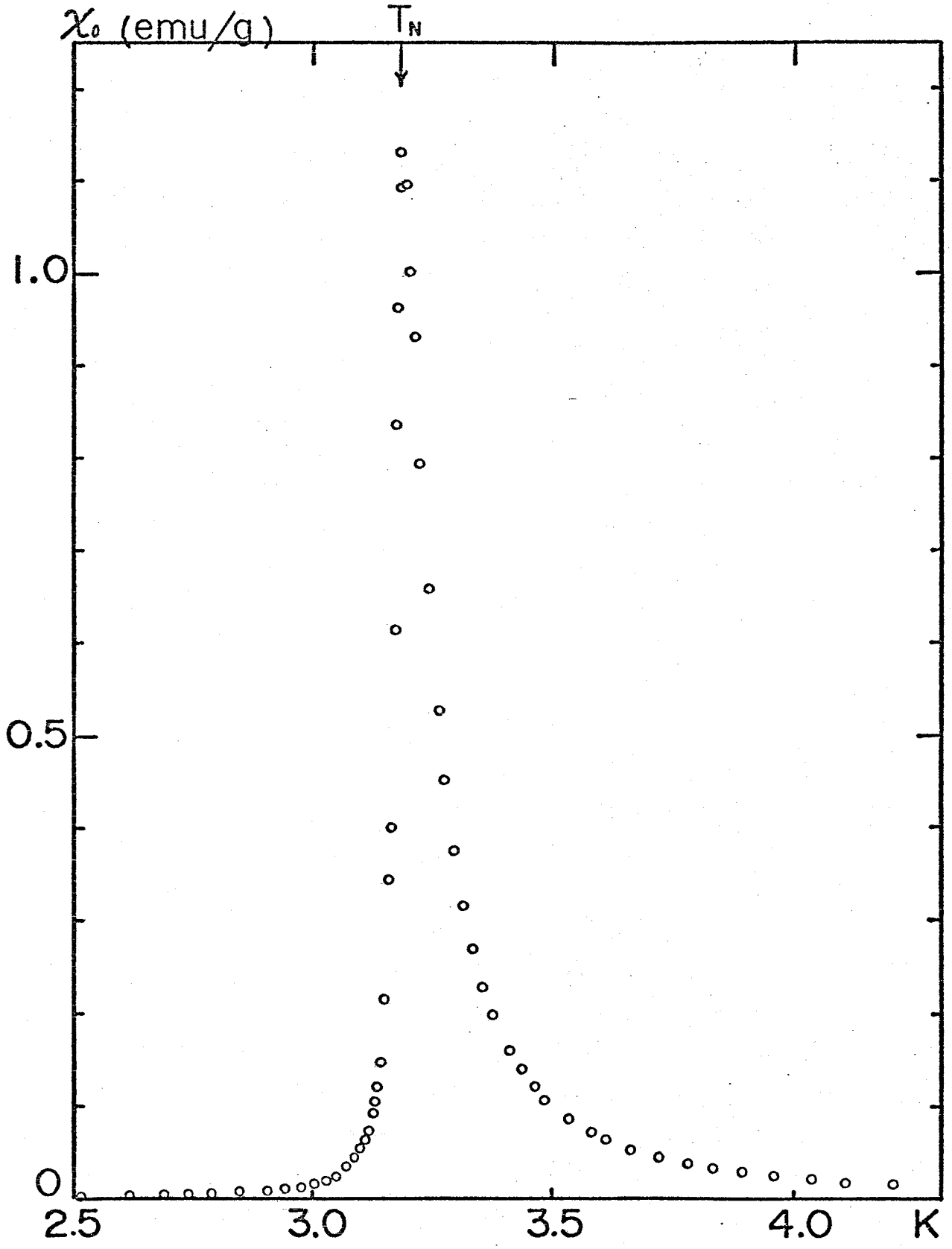

Fig. III-4. The static susceptibility along the easy axis (a-axis) near T_N of $Mn(CH_3COO)_2 \cdot 4H_2O$. The measuring frequency is 1 kHz which can be regarded as static.

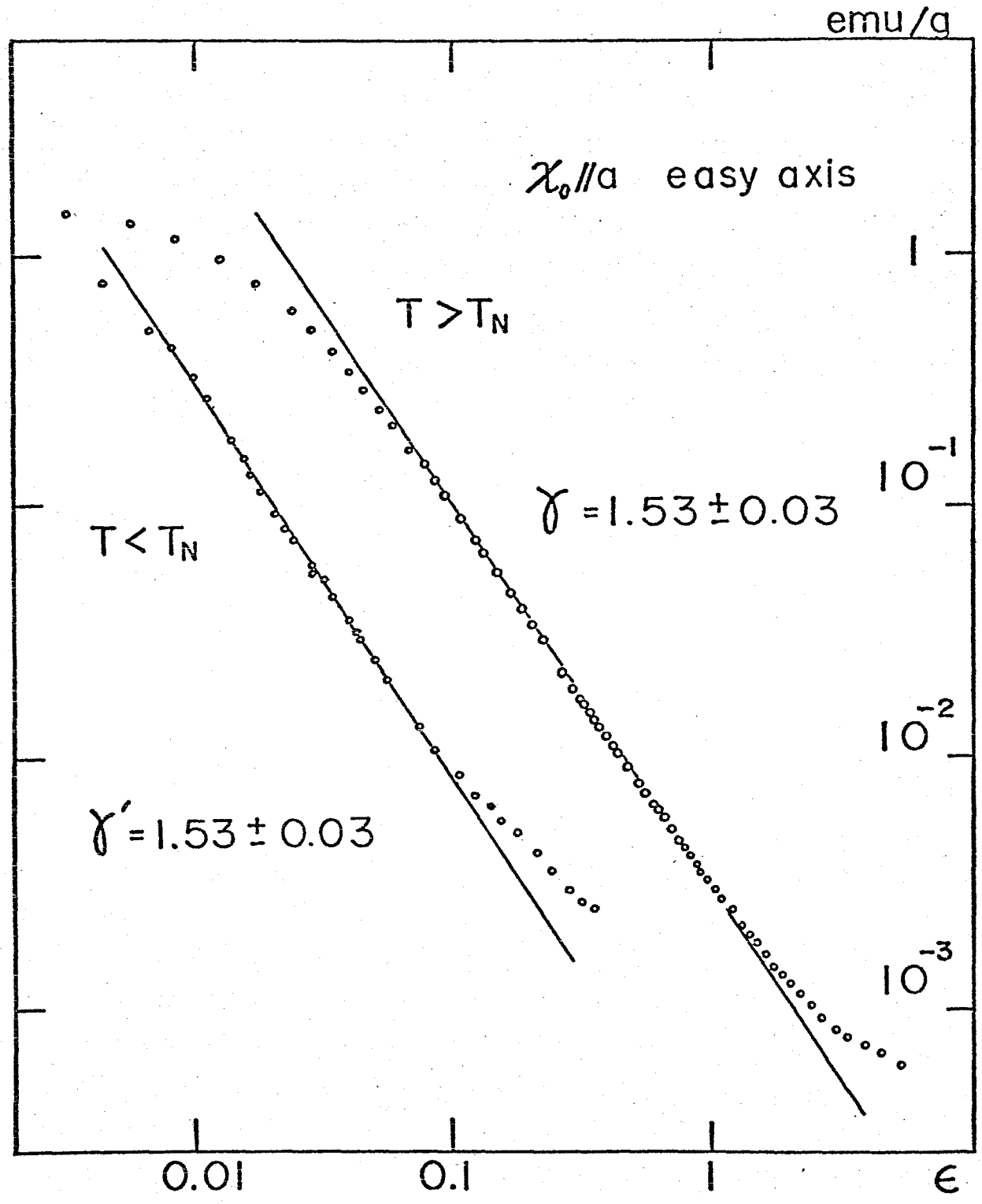

Fig. III-5. Log-log plot of the susceptibility of $Mn(CH_3COO)_2 \cdot 4H_2O$ along the easy axis vs. ε. Correction for the demagnetization effect is done.

§III-3. Dynamic susceptibility

Based on a simple model,[11] a relaxation process is described by an exponential decay and the frequency dependent susceptibility is given by the following formula.

$$\chi'(\omega) - \chi_\infty = \frac{\chi_0 - \chi_\infty}{1+(\omega\tau)^2} , \qquad (3\text{-}1)$$

where χ_0 and χ_∞ stand for the static and the high frequency limit susceptibility, and τ is the relaxation time. Now we introduce the temperature dependence of χ_0 and τ, which corresponds to the critical slowing down. If the exponent of τ is larger than a half of the exponent of χ_0, and χ_∞ is neglected, then

$$\lim_{T\to T_c} \chi'(\omega) = 0. \qquad (3\text{-}2)$$

There must be a dip in $\chi'(\omega)$ just at T_c. Even if the relaxation is not described exactly by (3-1), a small dip will appear so long as the temperature dependence of χ_0 and τ fulfills the condition mentioned above, which will be discussed later in §III-4. A dip in $\chi'(\omega)$ just at T_c is a qualitative evidence of the critical slowing down. This phenomenon has been found in the high frequency dielectric constant in some ferroelectrics, such as $Ca_2Sr(C_2H_5COO)_6$.[12] But there has been no report on this phenomenon in any magnetic system up to now.

Figure III-6 and III-7 show the frequency dependent susceptibility near the critical point for various frequencies. For lower frequencies (<10 MHz) $\chi'(\omega)$ is almost the same as the static one except a slight deviation near T_N. As frequency increases, the

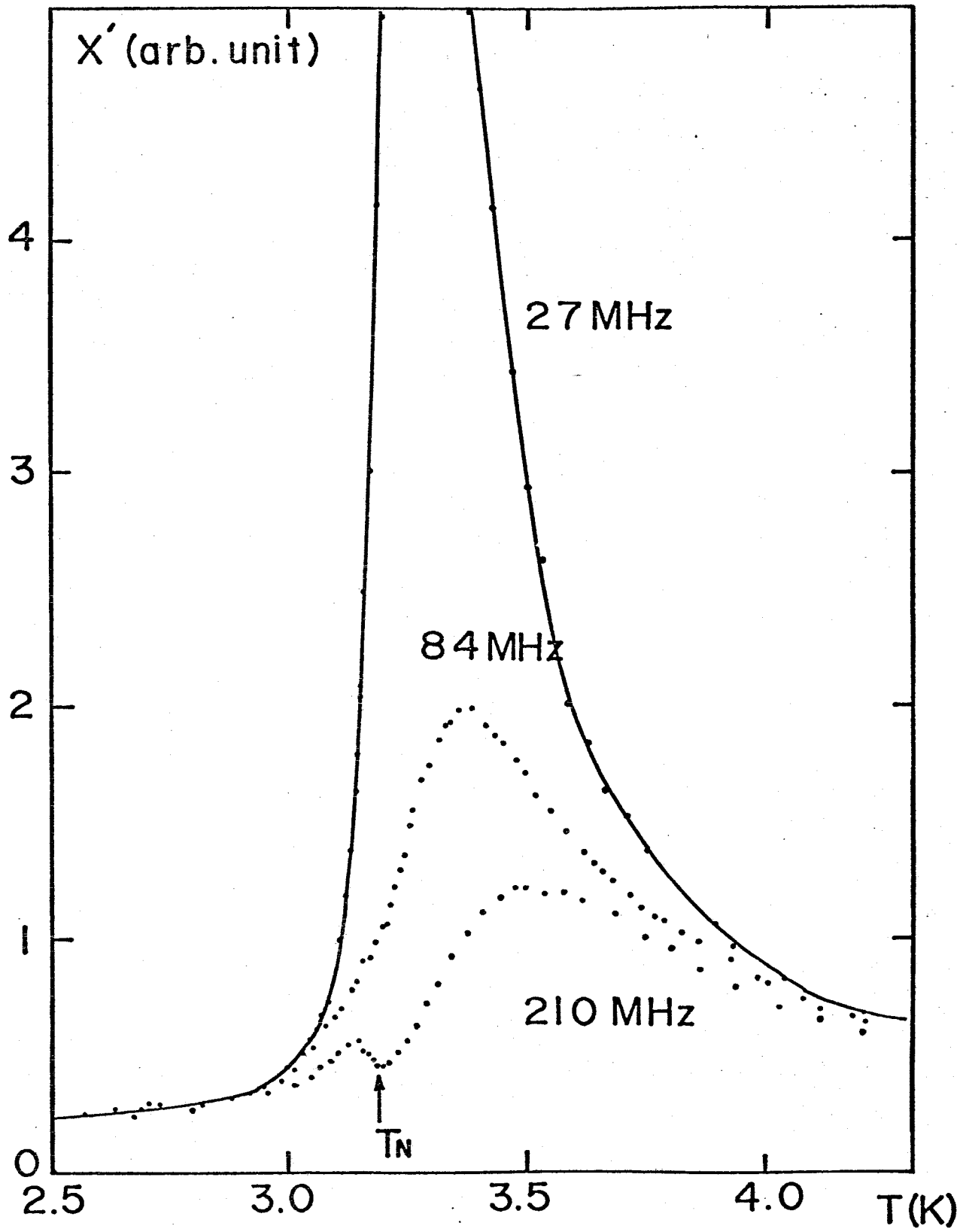

Fig. III-6. Real part of the dynamic susceptibility of $Mn(CH_3COO)_2 \cdot 4H_2O$ along the easy axis.

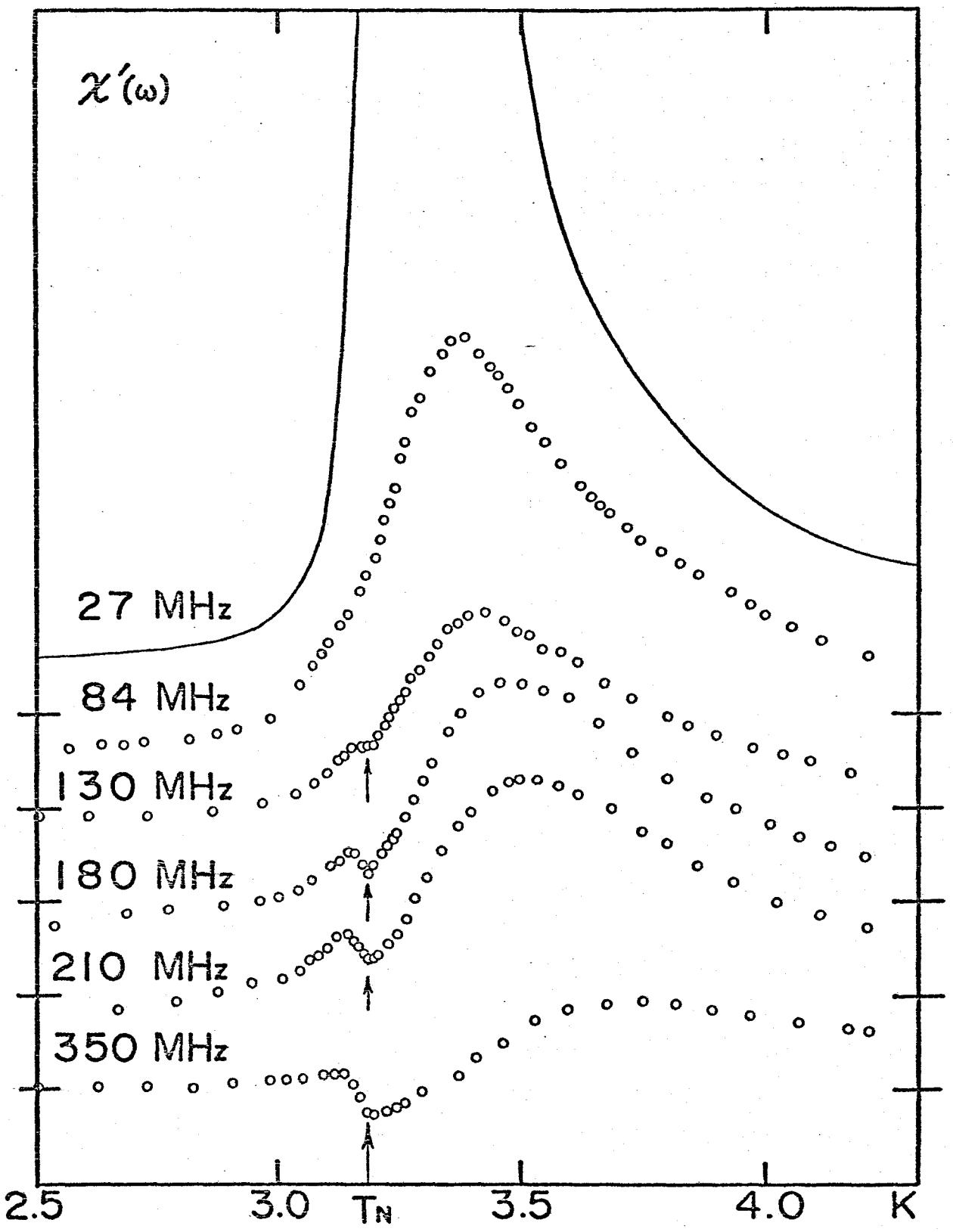

Fig. III-7. $\chi'(\omega)$-T for various frequencies ranging up to 450 MHz. The vertical axis is shifted for each frequency in order to make the view easy.

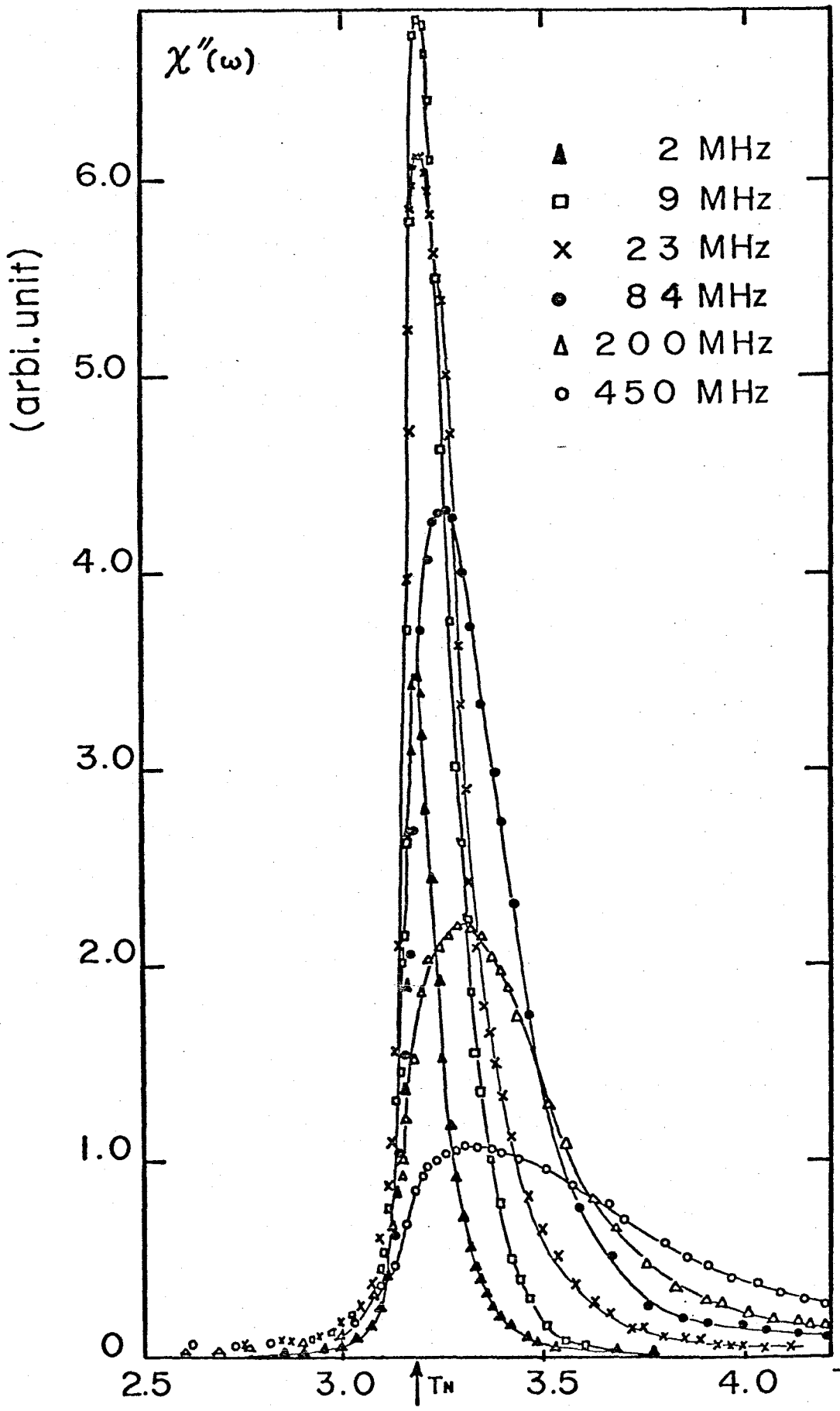

Fig. III-8. Imaginary part of the dynamic susceptibility of $Mn(CH_3COO)_2 \cdot 4H_2O$ along the easy axis for various frequencies.

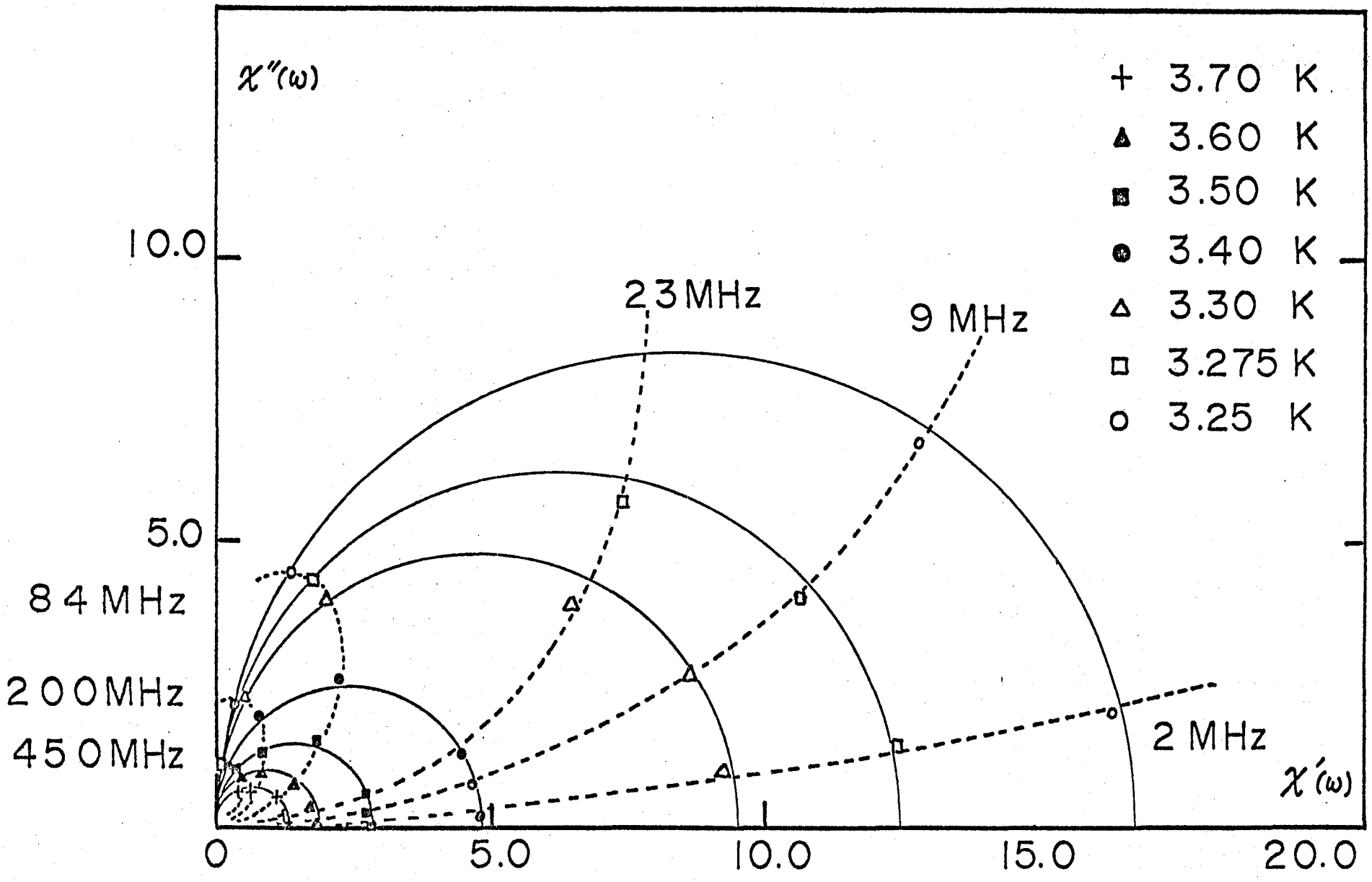

Fig. III-9. Cole-Cole plot of $Mn(CH_3COO)_2 \cdot 4H_2O$ in the paramagnetic region T>3.25 K.

peak height of $\chi'(\omega)$ near T_N begins to decrease and the maximum of $\chi'(\omega)$-T shifts to higher temperature. At 180 MHz a small dip is observed just at T_N Increasing the frequency up to 210 MHz, 350 MHz and 450 MHz, this dip becomes deeper and the distance between the two peaks on both sides of T_N becomes larger. At 350 MHz the maximum above T_N shifts by about 500 mK to higher temperature. This dip is a clear evidence of the critical slowing down as mentioned above. This is the first experiment on this phenomenon in the magnetic system. $\chi''(\omega)$ is plotted in Fig. III-8.

In order to examine the dispersion extensively, the Cole=Cole plot in the paramagnetic region is shown in Fig. III-9. Experimental points fall on a semi-circle, suggesting a simple Debye-type relaxation. The relaxation time can be obtained from (3-1). As the temperature approaches T_N in the temperature region below 3.25 K, the Cole-Cole semi-circle becomes a little flatter, suggesting a polydispersive relaxation process. To examine the width of a distribution of the relaxation time and to get the relaxation time in the polydispersive system, we used the empirical formula of the Cole-Cole arc introduced in analyzing the ferroelectric relaxation. The formula[13] is

$$\chi^*(\omega)-\chi_\infty = \frac{\chi_0-\chi_\infty}{1+(i\omega\tau)^\beta} , \qquad (3-3)$$

where $\chi^*(\omega)$ is the frequency dependent complex susceptibility, and β is a parameter which indicates the width of the distribution of the relaxation time. If $\beta=1$, the relaxation is reduced to the familiar Debye-type dispersion. When $\beta<1$, the dispersion is

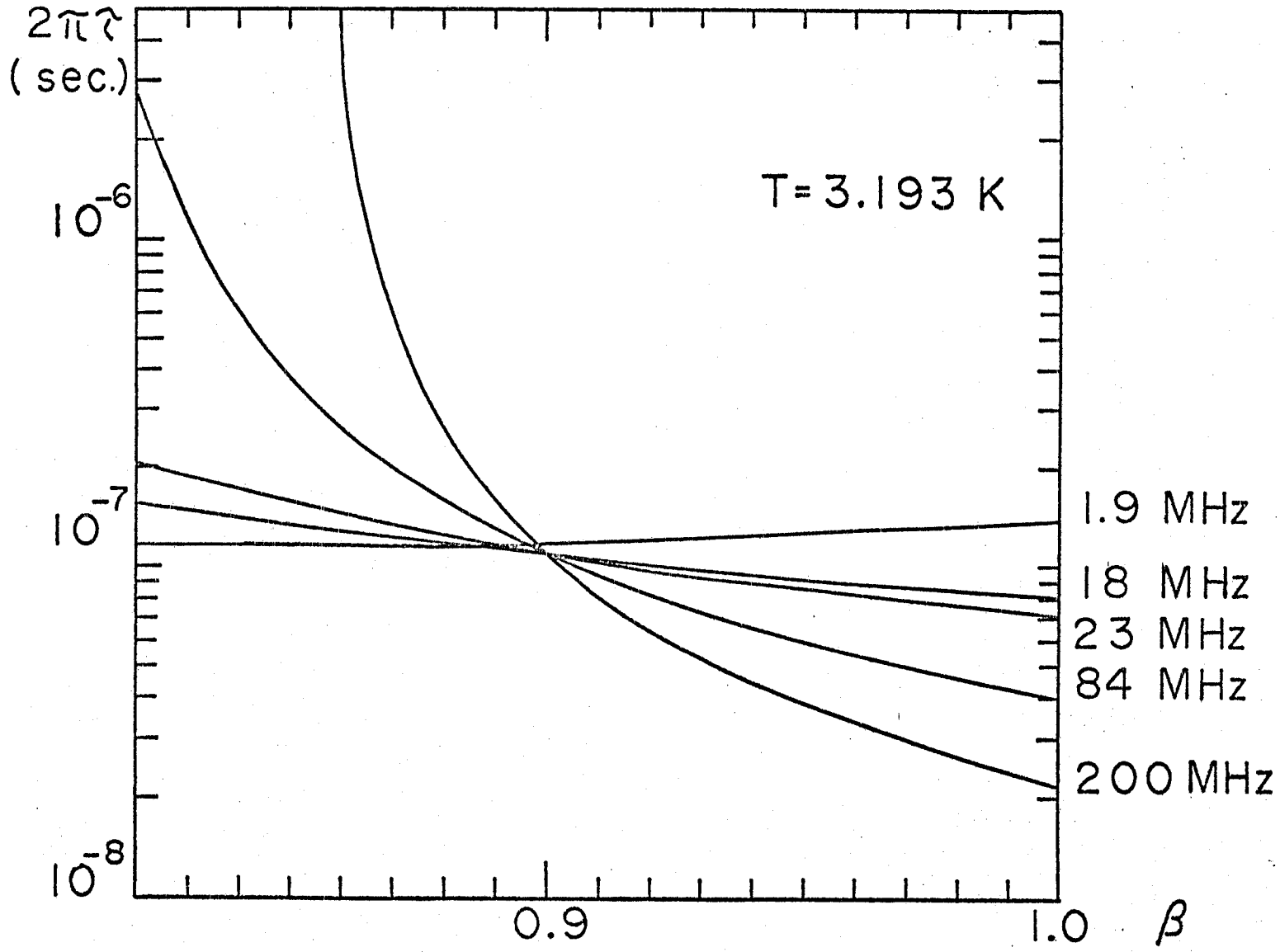

Fig. III-10. An example of the equation (3-4), as a function of β. The points at β=1 are experimental f_ω's for various frequencies where $f_\omega=\chi''(\omega)/\omega\chi'(\omega)$.

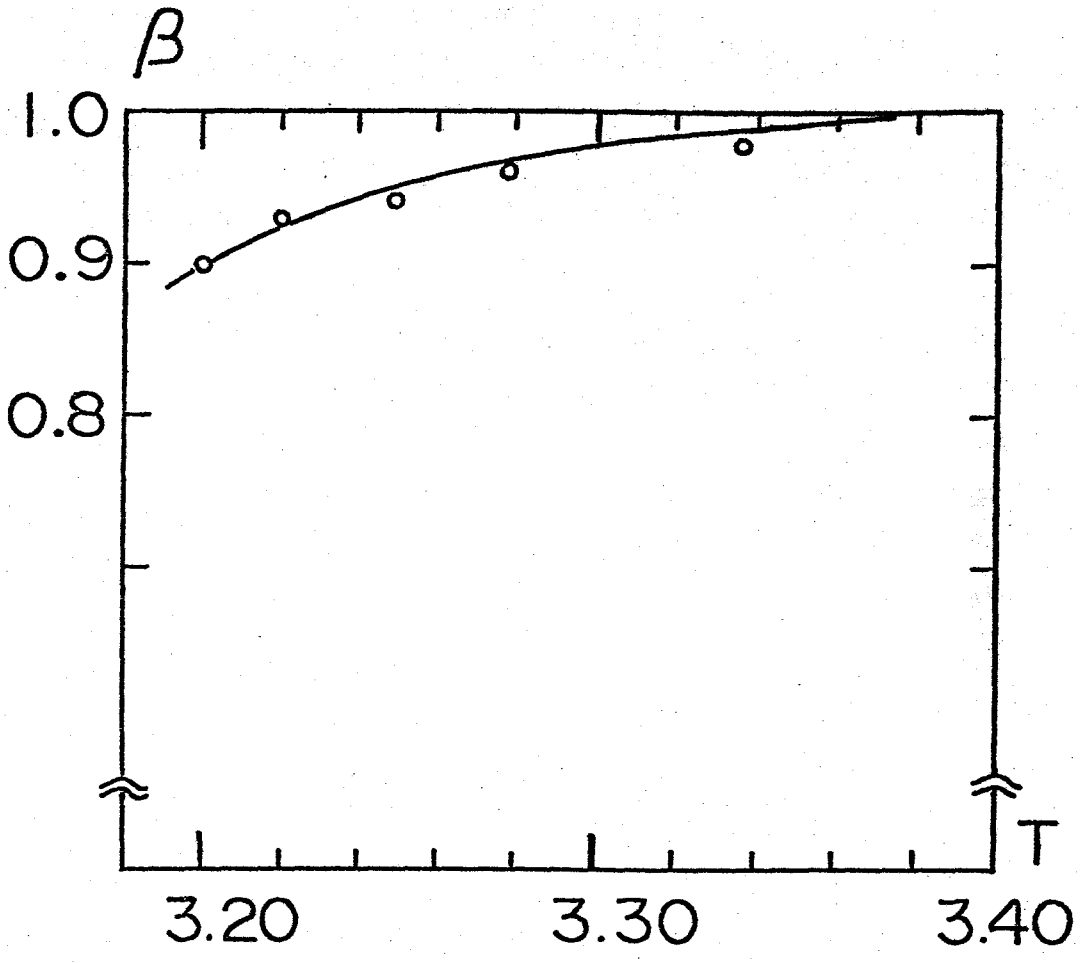

Fig. III-11. β vs. T of $Mn(CH_3COO)_2 \cdot 4H_2O$ in the paramagnetic region.

not monodispersive but polydispersive; the smaller β is, the wider the distribution of the relaxation time is. It should be kept in mind that the formula (3-3) is only a phenomenological one and that there is no reason that it holds for the critical magnetic relaxation. But it will help to understand the behavior phenomenologically. τ can be easily derived from (3-3) as

$$\tau = \left[\frac{f_\omega \cdot \omega^{1-\beta}}{\sin(\beta\pi/2) - f_\omega \omega \cos(\beta\pi/2)}\right]^{1/\beta}, \qquad (3\text{-}4)$$

where f_ω is $\chi''(\omega)/\omega\chi'(\omega)$. χ_∞ is neglected here. If $\beta=1$, f_ω is independent of ω and is just the relaxation time. If $\beta<1$, f_ω depends on ω. The relaxation time should be obtained by the relation (3-4). It is necessary to determine β in order to get the relaxation time. β is so determined that τ in (3-4) is independent of ω, putting the experimental $\chi'(\omega)$ and $\chi''(\omega)$ into f_ω for various frequencies. In Fig. III-10 is shown an example of $\tau(\omega,\beta)$, the relation of (3-4) as a function of β for T=3.193 K. The relaxation time and β are obtained simultaneously from (3-4). In Fig. III-11 is given the temperature dependence of β obtained by this procedure. As T approaches T_N, β decreases down to 0.9. Figure III-12 gives the relaxation time in the log-log scale. The critical slowing down is manifested, giving the exponent $\Delta=1.30\pm0.03$ for $3\times10^{-2}<\varepsilon<1$ (almost the same range of ε as the static susceptibility). This exponent is smaller than that of the static susceptibility. This indicates that the Onsager's kinetic coefficient L has a definite temperature dependence, though it is rather weak compared with χ_0 and τ. L behaves as if it weakly diverges in this ε region as

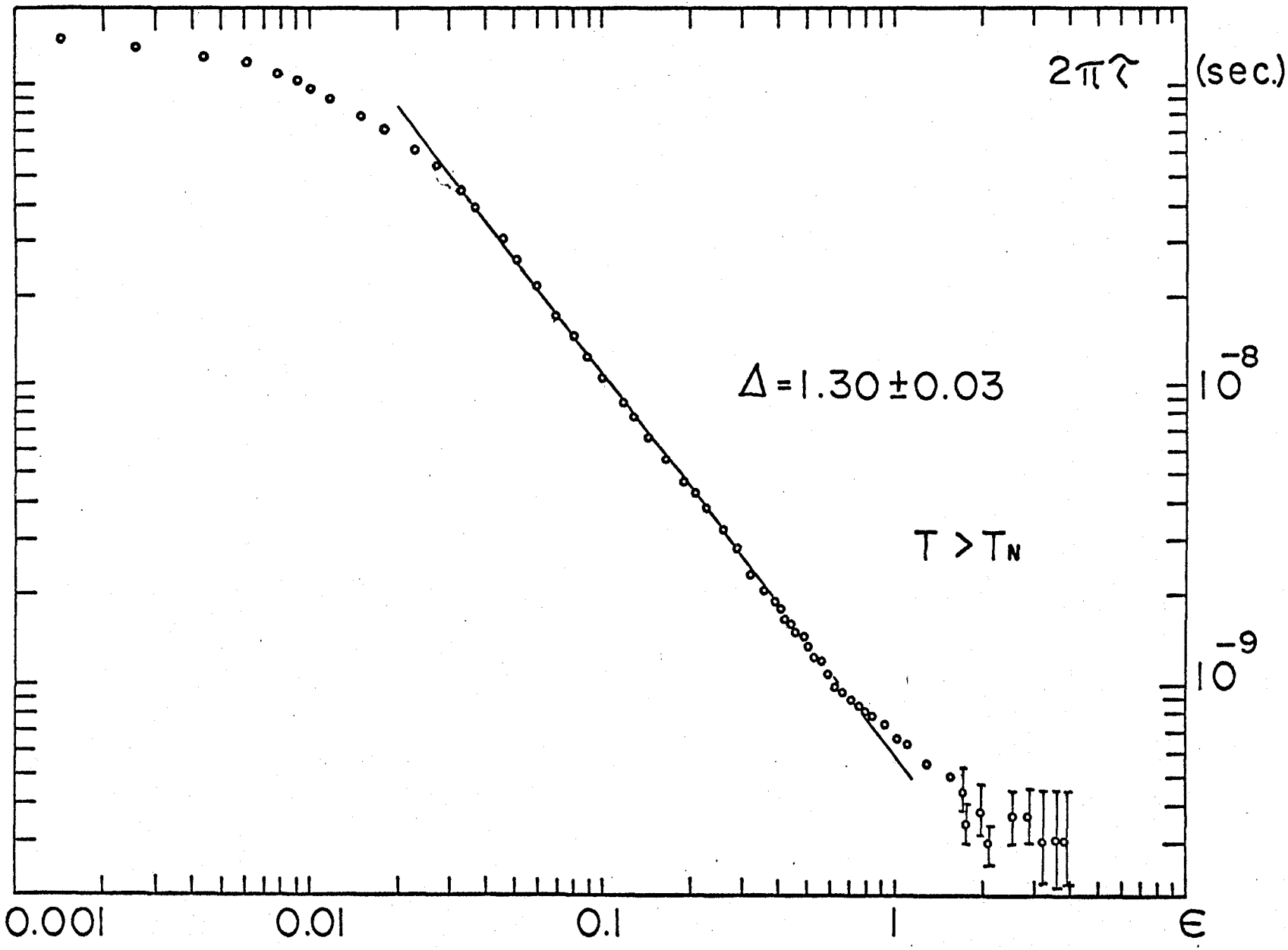

Fig. III-12. Log-log plot of the relaxation time of $Mn(CH_3COO)_2 \cdot 4H_2O$ along the easy axis in the paramagnetic region.

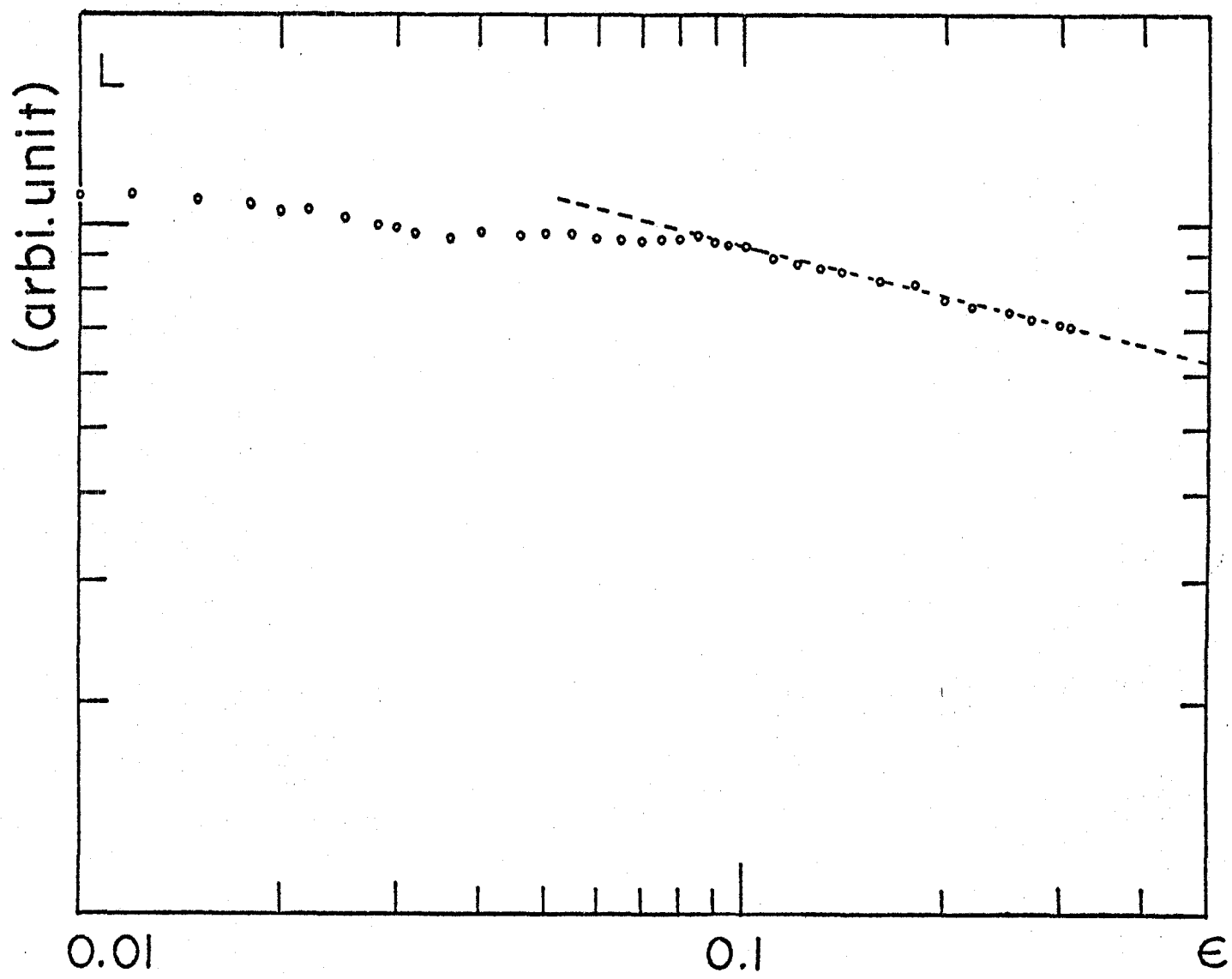

Fig. III-13. Log-log plot of the Onsager's kinetic coefficient L. L is calculated by the relation $L=\chi_0/\tau$.

the temperature approaches T_N. The temperature dependence of L is shown in Fig. III-13 in the paramagnetic region.

§III-4. Discussion

We shall confine ourselves here to the dynamic character of $Mn(CH_3COO)_2 \cdot 4H_2O$. As mentioned in the previous section, the critical slowing down is observed as a dip in $\chi'(\omega)$. But $\chi'(\omega)$ for high frequency does not drop to zero value at the critical point. According to Yoshimitsu and Matsubara[13] who have discussed the formula (3-3), there must appear a dip at T_c in $\chi'(\omega)$ so long as β is larger than 0.5. But $\chi'(\omega)$ does not vanish at T_c unless β is equal to 1. In $Mn(CH_3COO)_2 \cdot 4H_2O$ β actually gets to about 0.9 at T_N. It is reasonable from the formula of (3-3) that $\chi'(\omega)$ in Mn·acetate does not vanish at T_N. After the formula of (3-3), the change of β from 1 to 0.9 is understood as the change of the relaxation from the monodispersive to the polydispersive relaxation.

Owing to the final three dimensional antiferromagnetic ordering, both the static susceptibility and the relaxation time are prevented from diverging, but they are still increasing as the temperature approaches T_N, since the interlayer antiferromagnetic interaction is very weak (see Fig. III-5 and Fig. III-12). This roundening effect will also make the dip obscure. Whether a dip at T_N appears or not depends which of χ_0 and τ exceeds near T_N, even though there is a roundening effect in both χ_0 and τ.

The critical exponents of χ_0 and τ are obtained as $\gamma=1.53$ and $\Delta=1.30$ except for the immediate vicinity of T_N ($6\times10^{-2}<\varepsilon<1$). $\gamma-\Delta=0.23$ is the temperature dependence of the Onsager's kinetic

coefficient L. L behaves as if it diverges weakly in this ε region as the temperature approaches T_N. The weak but definite temperature dependence of L indicates that there develops a correlation of the random torque which acts on the uniform mode as T approaches T_N. Hatta studied[14] the dielectric relaxation in $NaNO_2$ and found that the exponent of the static dielectric constant is smaller than that of the relaxation time in contrast with the present work. In the dynamics of the Heisenberg spin system, the effect of xy components may play an important role to correlate the random torque. This effect will be reflected in the temperature dependence of L.

A change over from the monodispersive to the polydispersive near T_N is found by fitting the experimental data to the formula (3-3), though it is very slight ($\beta \sim 0.9$). After the phenomenological theory,[15] the time dependent motion of the uniform mode M is given by the next equation.

$$\tau_c \frac{dM}{dt} = -\lambda M - \eta M^3 + \cdots \quad . \tag{3-5}$$

The coefficient of the first order of M corresponds to χ_0^{-1} which vanishes at T_c. The theory says that the dispersion is monodispersive if the linear term is dominant and it becomes polydispersive if the second term becomes effective. But we cannot step into more microscopic detail by the phenomenological treatment. The discussion on the phenomenological formula of (3-3) and on the non-linear equation of (3-5) is done in chapter IV and in the appendix.

References

1) E. F. Bertaut, Tran Qui Duc, P. Burlet, P. Burlet, M. Thomas and J. M. Moreau: Acta Cryst. B 30 (1974) 2234.

2) V. A. Schmidt and S. A. Friedberg: Phys. Rev. 188 (1969) 809.

3) P. Burlet: Thèse de Doctarat d'Etat, Grenoble, 1973.

4) P. Beauvillain and J. P. Renard: Physica 86-88B (1977) 667.

5) P. Burlet, P. Burlet and E. F. Bertaut: Solid State Commun. 14 (1974) 665.

6) J. A. Cowen, G. T. Johnston and H. Van Till: J. Chem. Phys. 45 (1966) 644.

7) D. M. Aranaz and T. R. Lomer: J. Phys. C 2 (1969) 2431.

8) T. Haseda, H. Yamakawa, M. Ishizuka, Y. Okuda, T. Kubota, M. Hata and K. Amaya: Solid State Commun. 24 (1977) 599.

9) P. Beauvillain and J. P. Renard: Physica 86-88B (1977) 667.

10) D. D. Betts: *Phase Transitions and Critical Phenomena*, ed. C. Domb and M. S. Green (Academic Press, London, 1974) Vol. 3.

11) W. P. Mason: Phys. Rev. 72 (1965) 854.

12) E. Nakamura and M. Hosoya: J. Phys. Soc. Japan 23 (1967) 844.

13) K. Yoshimitsu and T. Matsubara: Progr. theor. Phys. Suppl. Extra Number (1968) 109.

14) I. Hatta: J. Phys. Soc. Japan 28 (1970) 1266.

15) M. Suzuki and R. Kubo: J. Phys. Soc. Japan 24 (1968) 51.

IV. Critical slowing down in $(CH_3NH_3)_2CuCl_4$

§IV-1. Introduction

In the previous chapter, we have discussed the experimental data obtained from the dispersion and absorption technique in a quasi two dimensional ferrimagnet Mn·acetate. The dip in $\chi'(\omega)$ just at T_N was observed for the first time in the magnetic system for the frequency higher than 180 MHz.[1, 2] The exponent of the critical slowing down was $\Delta=1.30\pm0.03$. The Onsager's kinetic coefficient L was revealed to increase as T_N was approached, though the temperature dependence was very weak. Another important result was a definite deviation of the Cole-Cole plot from the semi-circle to the Cole-Cole arc near T_c; β was about 0.9, in the notation of the formula of Yoshimitsu and Matsubara (YM).[3] As Mn·acetate, however, ultimately sets into the three dimensional antiferromagnetic ordering, the uniform susceptibility does not diverge to infinity at T_N, due to the weak interlayer antiferromagnetic interaction. There appears, indeed, a roundening in the log-log plot of χ_0 vs. ε for $\varepsilon<0.06$ and the relaxation time has a likewise roundening for the same epsilon. This roundening will smear the critical behavior of the uniform magnetization.

The dip for $\chi'(\omega)$ at T_N did not actually fall to zero even in the highest frequency measured, which seemed to imply that there remained fairly high frequency relaxation modes. This might be partly ascribed to the roundening effect and partly to the essential feature of the critical slowing down. In order to make sure that those dynamical properties are essential and

general in the dynamics of the quasi two dimensional ferromagnet and not peculiar to Mn·acetate, we will try to perform the same experiment on other samples, especially on a purely ferromagnetic material.

Does the dip appear in $\chi'(\omega)$ at T_c and does it reach to the bottom at T_c in the system whose χ_0 diverges with a definite critical exponent? Does the decay function also deviate from the Debye type exponential in the immediate vicinity of T_c in the same way as Mn·acetate?

$(CH_3NH_3)_2CuCl_4$ is a n=1 compound of a series $(C_nH_{2n+1}NH_3)_2CuX_4$ (n=1,2,···10; X=Cl, Br) which was studied by de Jongh and Miedema.[4] The compounds are well approximated to the two dimensional Heisenberg ferromagnet with the weak XY anisotropy. A weak interlayer interaction is ferromagnetic or antiferromagnetic depending on the value of n. In the present case (n=1), the interlayer coupling is ferromagnetic. The compound sets into the three dimensional ferromagnetic ordering at 8.90 K. The critical exponent of the static susceptibility was 1.75 for $0.05<\varepsilon<0.2$ and 1.25 for $0.003<\varepsilon<0.05$, which was reported as a crossover phenomenon from two dimensional Ising system to three dimensional Ising system for the first time by de Jongh and Stanley.[5] The intralayer exchange interaction was estimated to be $H_E=530\times10^3$ Oe, the interlayer interaction $H_E'=60$ Oe, the anisotropies within and perpendicular to the ferromagnetic layer have been obtained as $H_A^{in}=72$ Oe and $H_A^{out}=1720$ Oe, respectively.[6] Ferromagnetic spin alignment within a layer is similar as the case of Mn·acetate as is depicted in Fig. IV-1. The experiment on this compound will give the answer

to the problems which were observed in Mn·acetate and remained to be checked in a pure ferromagnet.

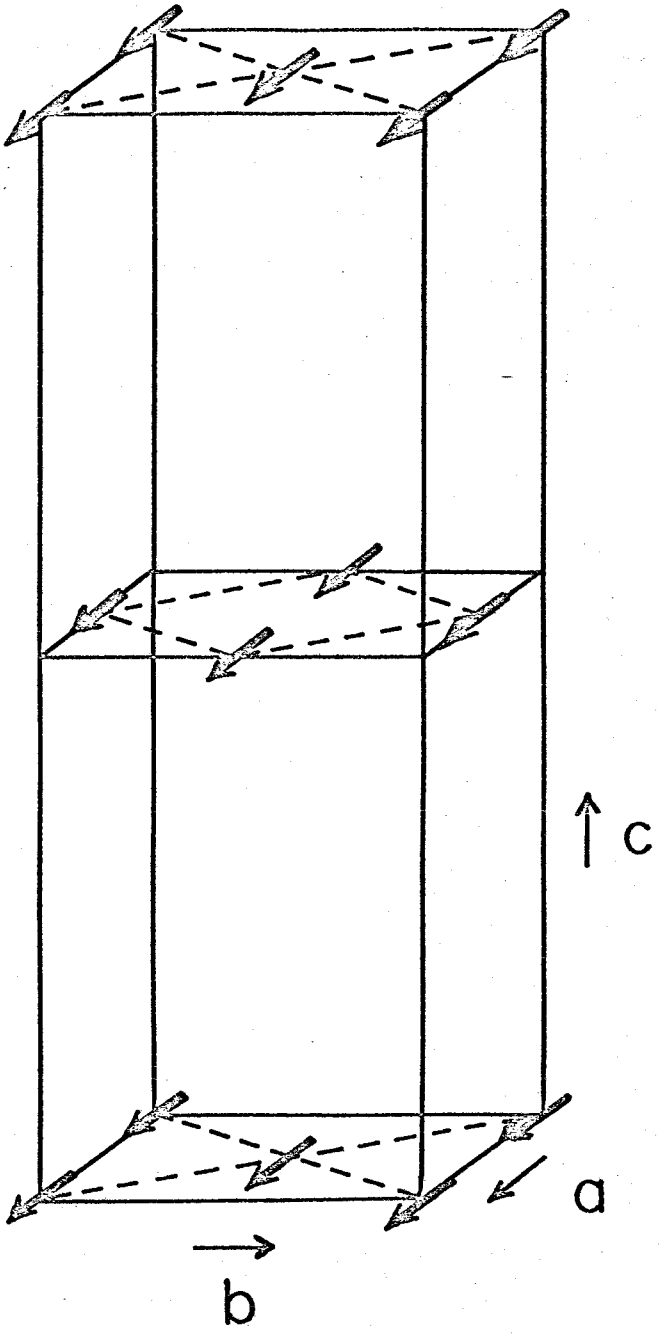

Fig. IV-1. Sketch of the spin structure of $(CH_3NH_3)_2CuCl_4$.

§IV-2. Static susceptibility

The static susceptibility along the easy axis was obtained by the measurement at 50 Hz which can be regarded as a static measurement in this case, because there is no appreciable frequency dependence of the susceptibility between 50 Hz and 50 kHz in the paramagnetic region. In the ordered state there exists a low frequency relaxation which might be a domain wall motion or something else often observed in ferromagnetic materials.[7] Figure IV-2 presents the static susceptibility thus obtained. Below T_c the susceptibility is constant of which value is consistent with the demagnetization factor N which is calculated for the ellipsoidal shape of the sample. So we took the experimental value as the demagnetization factor for all samples including not well shaped ones. Transition point T_c was determined from the point of intersection of N^{-1} line and the extrapolated line of the experimental data in the paramagnetic region. It is 8.89 ±0.01 K. The detailed measurement of the static susceptibility near T_c is indispensable to obtain the temperature dependence of the Onsager's kinetic coefficient L and to make sure the purity of the samples. In Fig. IV-3 is shown χ_0 vs. ε in the log-log scale. χ_0 is corrected for the demagnetization effect. The critical exponent γ is found to be 1.73 ± 0.03 for $0.05<\varepsilon<0.3$ and 1.20 ± 0.03 for $0.004<\varepsilon<0.05$. This is consistent with the data by de Jongh et al.[8]

The straight line in the log-log plot of χ_0 vs. ε is extended to smaller ε region ($\sim$0.004) than the case of Mn·acetate. This result is very important. In the case of Mn·acetate β which

is the measure of the deviation from the Cole-Cole semi-circle to the Cole-Cole arc begins to get smaller from 1 for ε where χ_0 begins to deviate from the straight line in the log-log plot of χ_0 vs. ε. So it was not concluded whether this deviation from the Debye type relaxation is surely an intrinsic feature of the critical behavior in the immediate vicinity of T_c. In the present case of $(CH_3NH_3)_2CuCl_4$, it is sure the deviation, if any, has nothing to do with the roundening of χ_0, as the straight line of χ_0 vs. ε is extended enough.

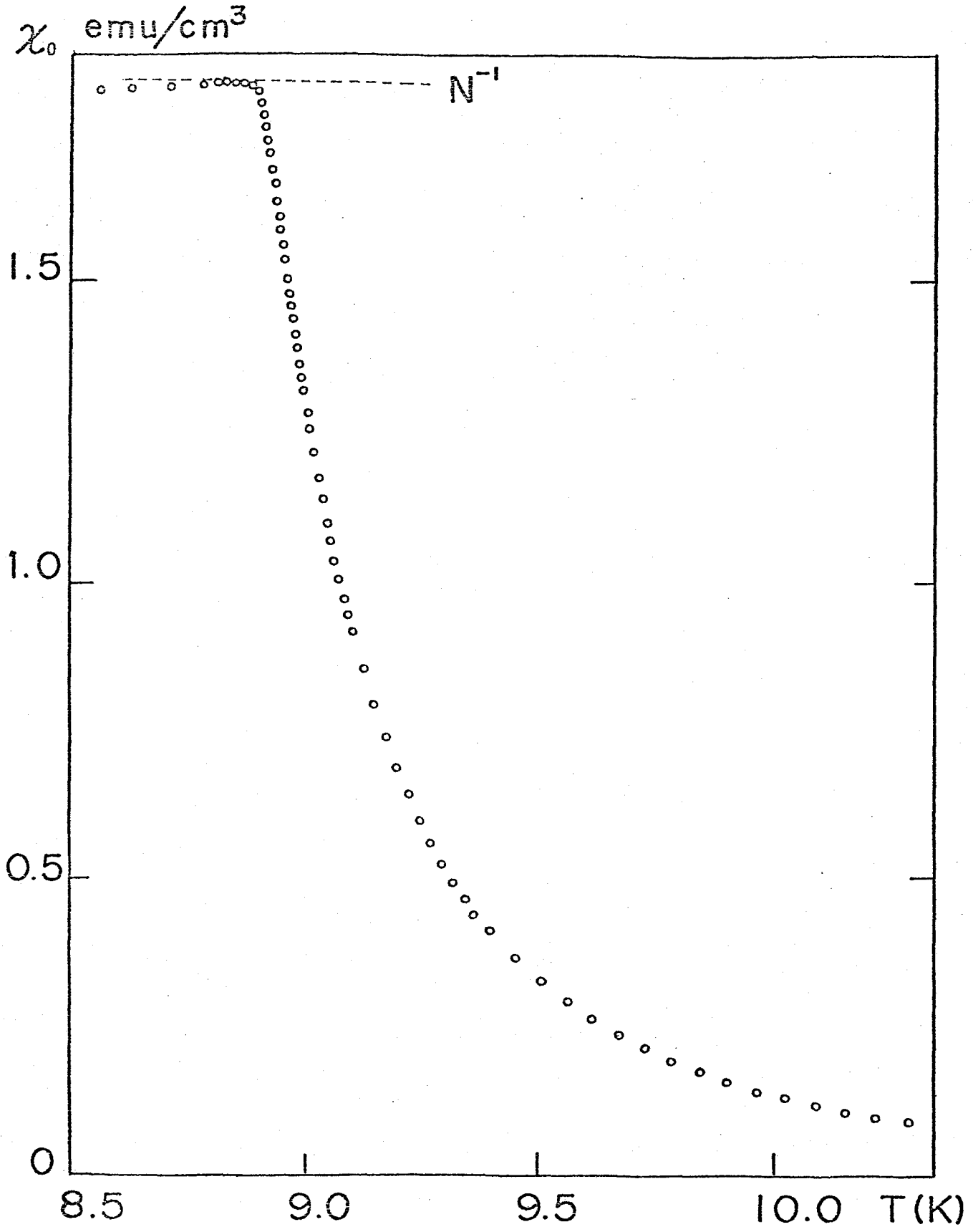

Fig. IV-2. The static susceptibility of $(CH_3NH_3)_2CuCl_4$ along the easy axis. N is the demagnetization factor which is calculated from the ellipsoidal shape of the sample. The measuring frequency is 50 Hz which can be regarded as static in this compound in the paramagnetic region.

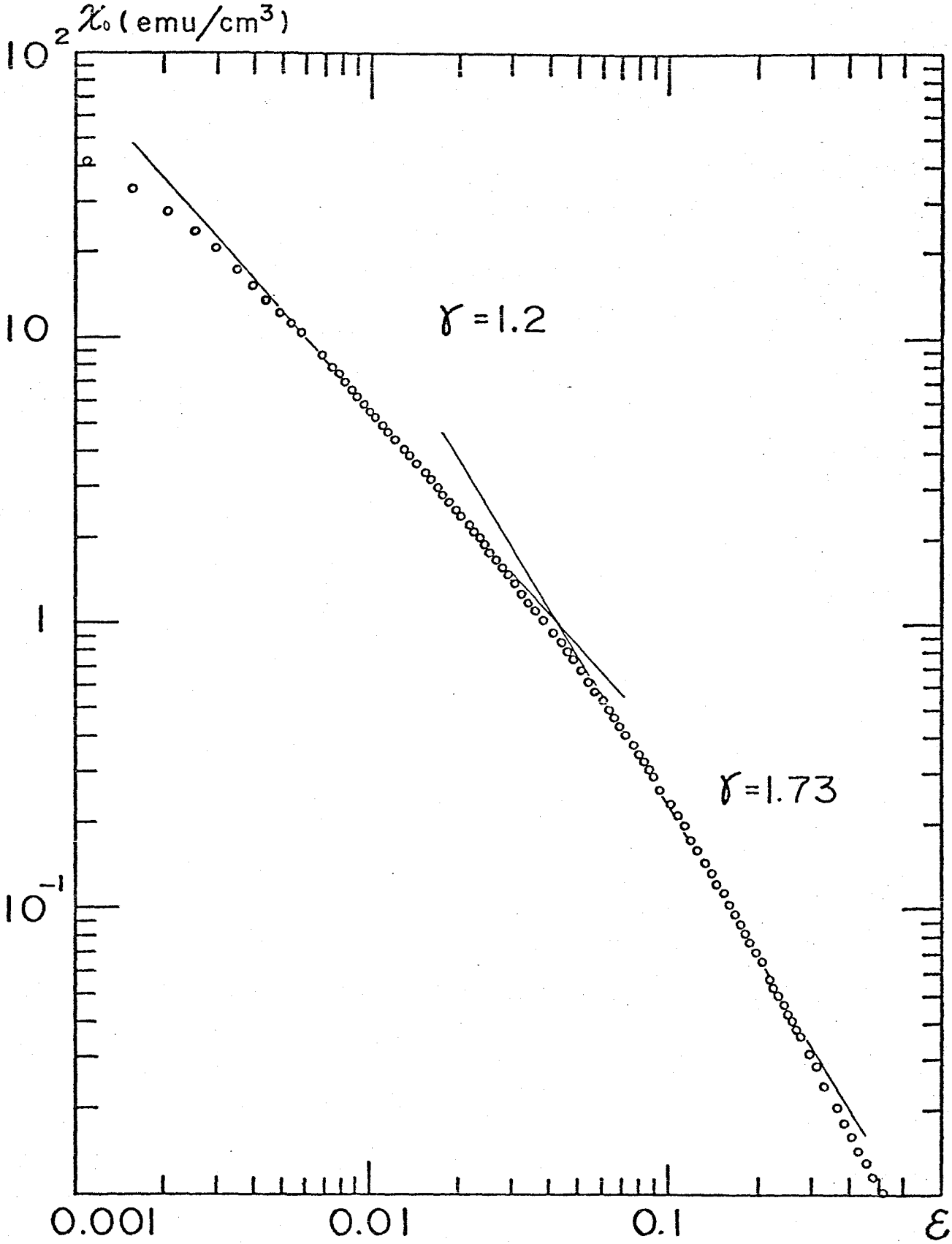

Fig. IV-3. Log-log plot of the static susceptibility of $(CH_3NH_3)_2CuCl_4$ in the paramagnetic region. The data are corrected for the demagnetization effect.

§IV-3. Dynamic susceptibility

The frequency dependent susceptibility along the easy axis from 1.2 MHz to 62 MHz is displayed in Fig. IV-4. The demagnetization correction was made using the relation (4) in chapter II. There appears a dip just at T_c for the frequency higher than 9.8 MHz. This is again a clear evidence of the critical slowing down for the uniform mode in the purely ferromagnetic substance. The dip seems to be deeper than that of Mn•acetate. The dip does not reach to zero value, which indicates that there remain fairly high frequency relaxation modes even at T_c in spite of the full divergence of the static susceptibility up to N^{-1}.

Figure IV-5 is the Cole-Cole plot of $\chi'(\omega)$ and $\chi''(\omega)$ for various temperatures in the paramagnetic region. The temperature is given by the reduced temperature ε. The experimental points fall on a semi-circle for ε larger than 0.01, to indicate a well-known Debye type single relaxation. As the temperature approaches T_c more closely, there occurs a small but definite deviation from the semi-circle to the Cole-Cole arc. In this temperature region there does not occur a roundening in the static susceptibility in the log-log plot as is clearly seen from Fig. IV-3. So this deviation can be assumed not to be attributed to the impurity effect or something else. The similar deviation found in the case of Mn•acetate will be also considered to be a same intrinsic phenomenon in the dynamics near the transition point, apart from the roundening due to the antiferromagnetic interlayer coupling. The black points below the abscissa ($\chi'(\omega)$-axis) in Fig. IV-5 are centers of the Cole-Cole arcs.

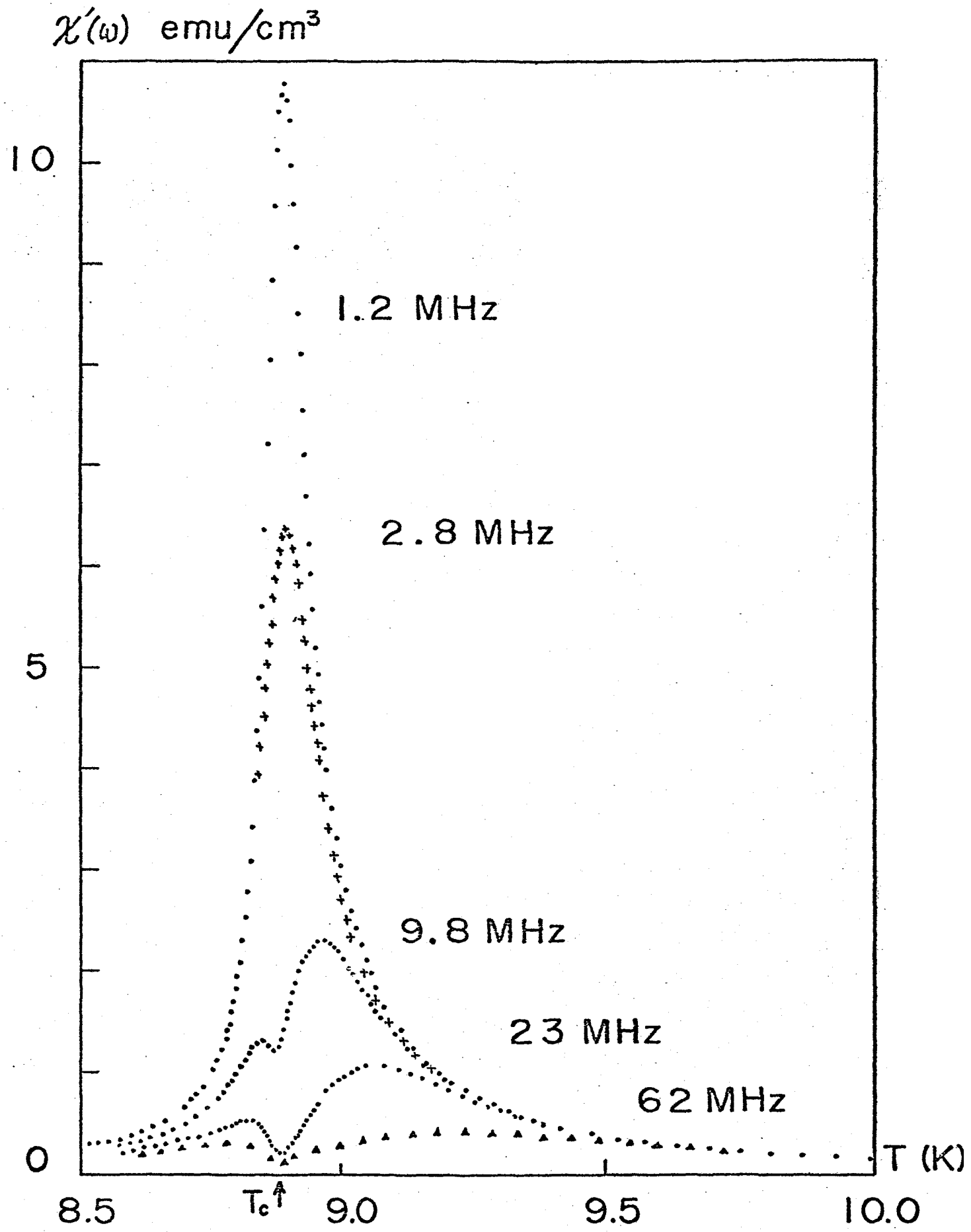

Fig. IV-4. Real part of the complex susceptibility of $(CH_3NH_3)_2CuCl_4$ for various frequencies. The data are corrected for the demagnetization effect.

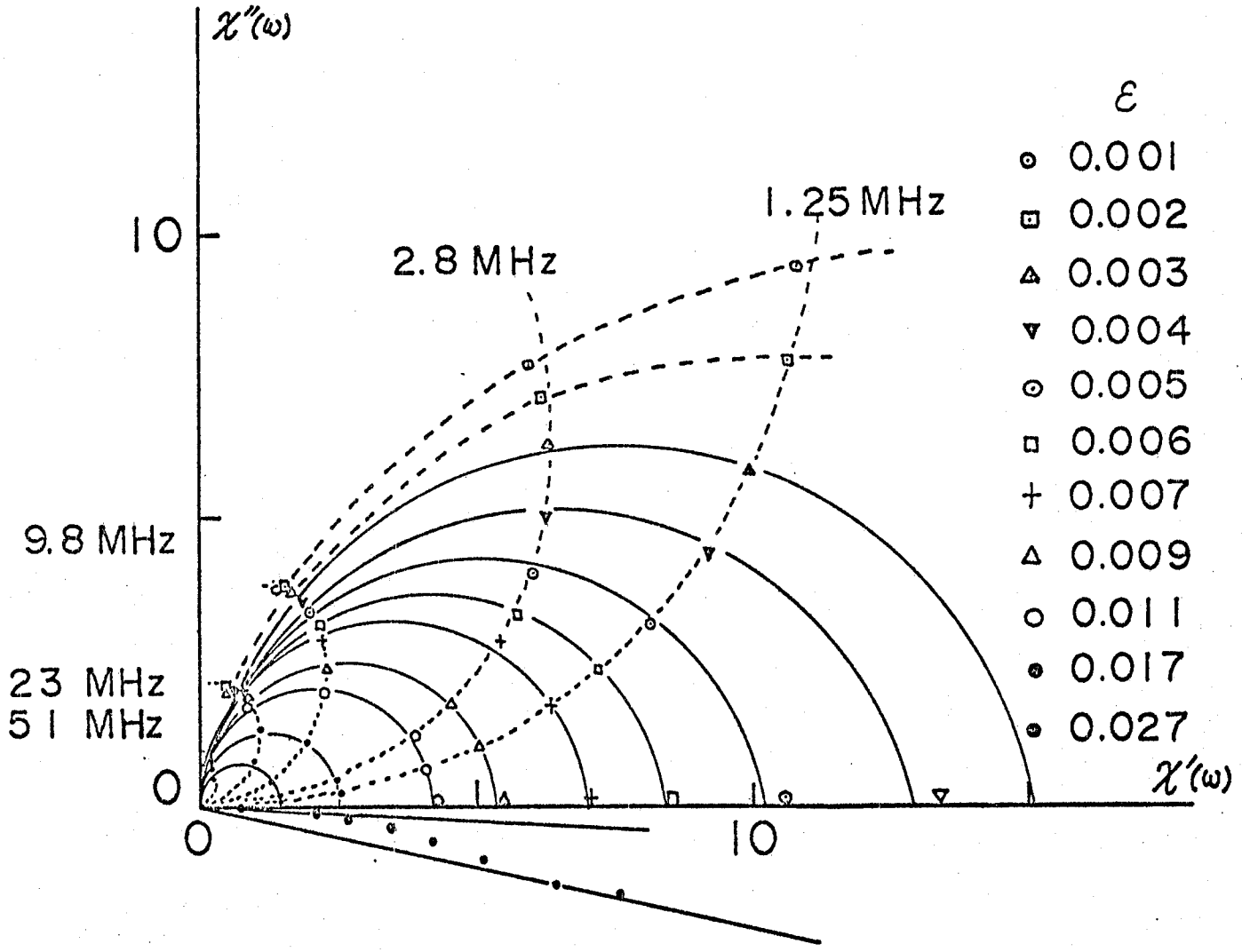

Fig. IV-5. Cole-Cole plot of $(CH_3NH_3)_2CuCl_4$ for $T>T_c$. The dots below the abscissa ($\chi'(\omega)$-axis) denote the centers of the Cole-Cole arcs.

The deviation from the semi-circle to the Cole-Cole arc is measured by the angle α between the abscissa and the straight line which passes through the origin and the center of the Cole-Cole arc for each ε. As the temperature approaches T_c, the angle gets larger. Using the notation, β, in the formula of YM, the angle α is equal to $\frac{\pi}{2}(1-\beta)$. For ε larger than 0.01, β is approximated to 1. As ε becomes smaller, β starts to get smaller from 1 and reaches to about 0.9 near T_c. Figure IV-6 presents β vs. ΔT plot in the paramagnetic region. The relaxation time can be obtained from the frequency which gives the maximum of $\chi''(\omega)$ for each temperature so long as the relaxation is of the Debye-type. In this case, $\chi''(\omega)/\omega\chi'(\omega)$ is independent of ω and is equal to the relaxation time τ. In the case of the depressed semi-circle of the Cole-Cole plot, the relaxation time was calculated as was performed in the case of Mn·acetate in chapter III from the formula of YM, provided that the experimental data could be represented by this formula.

The formula of YM is given as

$$\chi^*(\omega)-\chi_\infty = \frac{\chi_0-\chi_\infty}{1+(i\omega\tau_0)^\beta} \quad , \tag{4-1}$$

where χ_∞ stands for the high frequency limit susceptibility and it will be neglected hereafter. τ_0 is a function of T and exhibits the critical slowing down. This formula is re-written as

$$\frac{\chi_0}{1+(i\omega\tau_0)^\beta} = \int_0^\infty \frac{G(\tau)}{1+i\omega\tau} d\tau \quad . \tag{4-2}$$

$G(\tau)$ is the distribution function of τ and can be obtained as[9)]

$$G(\tau) = \frac{\sin\beta\pi}{\pi\tau\{(\tau/\tau_0)^{\beta}+(\tau/\tau_0)^{-\beta}+2\cos\beta\pi\}} \quad . \qquad (4\text{-}3)$$

If β is 1, $G(\tau)$ is given as the δ-function, which indicates the single relaxation process (Debye type). If $\beta<1$, $G(\tau)$ distributes around τ_0 as is seen in Fig. IV-7. The relaxation time in this case should be defined as

$$\begin{aligned}\bar{\tau} &= \int_0^{\infty} \tau G(\tau) d\tau \\ &= \tau_0 f(\beta) \\ &= \tau_0 \cdot \frac{\sin\beta\pi}{\beta\sin(-\pi/\beta)} \qquad (0.5<\beta<1) \quad . \end{aligned} \qquad (4\text{-}4)$$

$f(\beta)$ is given in Fig. IV-8. As is easily seen from Fig. IV-8, $f(\beta)$ is almost equal to 1 so long as β is larger than 0.8. So the relaxation time $\bar{\tau}$ in the case of the polydispersive relaxation is well approximated by τ_0 in (4-1). Therefore for $\varepsilon<0.01$, the relaxation time $\bar{\tau}$ $(=\tau_0)$ can be calculated by fitting the experimental data to the formula of MY. The relaxation time obtained by this procedure is plotted in the log-log scale in Fig. IV-9. The critical slowing down manifested itself in this figure. The experimental points fall on the straight line for ε between 0.003 and 0.1, giving the critical exponent $\Delta=1.05\pm0.05$ for this ε region in the paramagnetic state. This value differs from that of Mn·acetate. The exponent γ of the static susceptibility has two values; 1.73 for $0.05<\varepsilon<0.3$ and 1.2 for $0.004<\varepsilon<0.05$. On the other hand, the exponent of the relaxation time Δ has one value in the whole range of this ε region. In other words, there does not occur a crossover phenomenon in the dynamics.

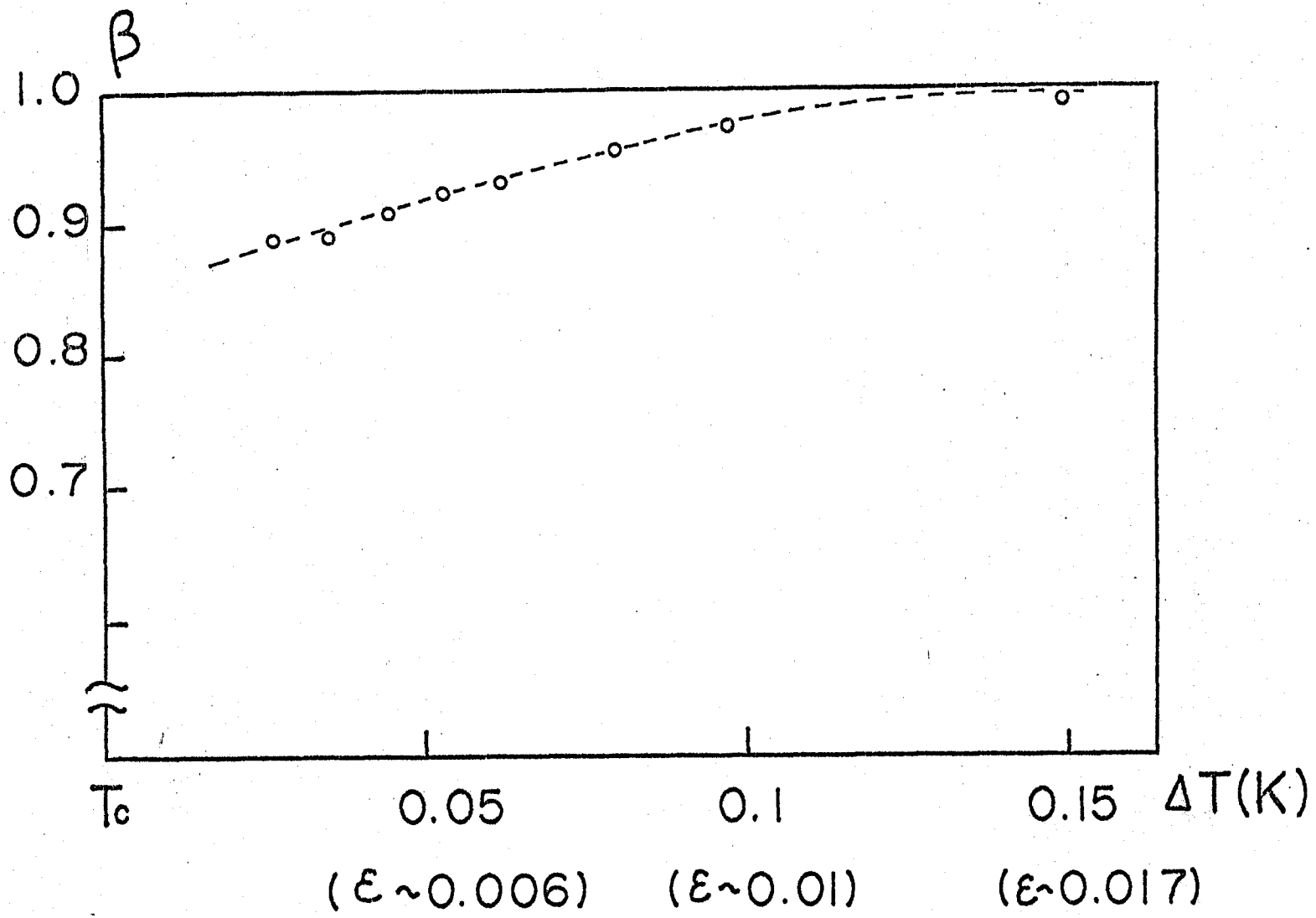

Fig. IV-6. β vs. ΔT of $(CH_3NH_3)_2CuCl_4$ in the paramagnetic region.

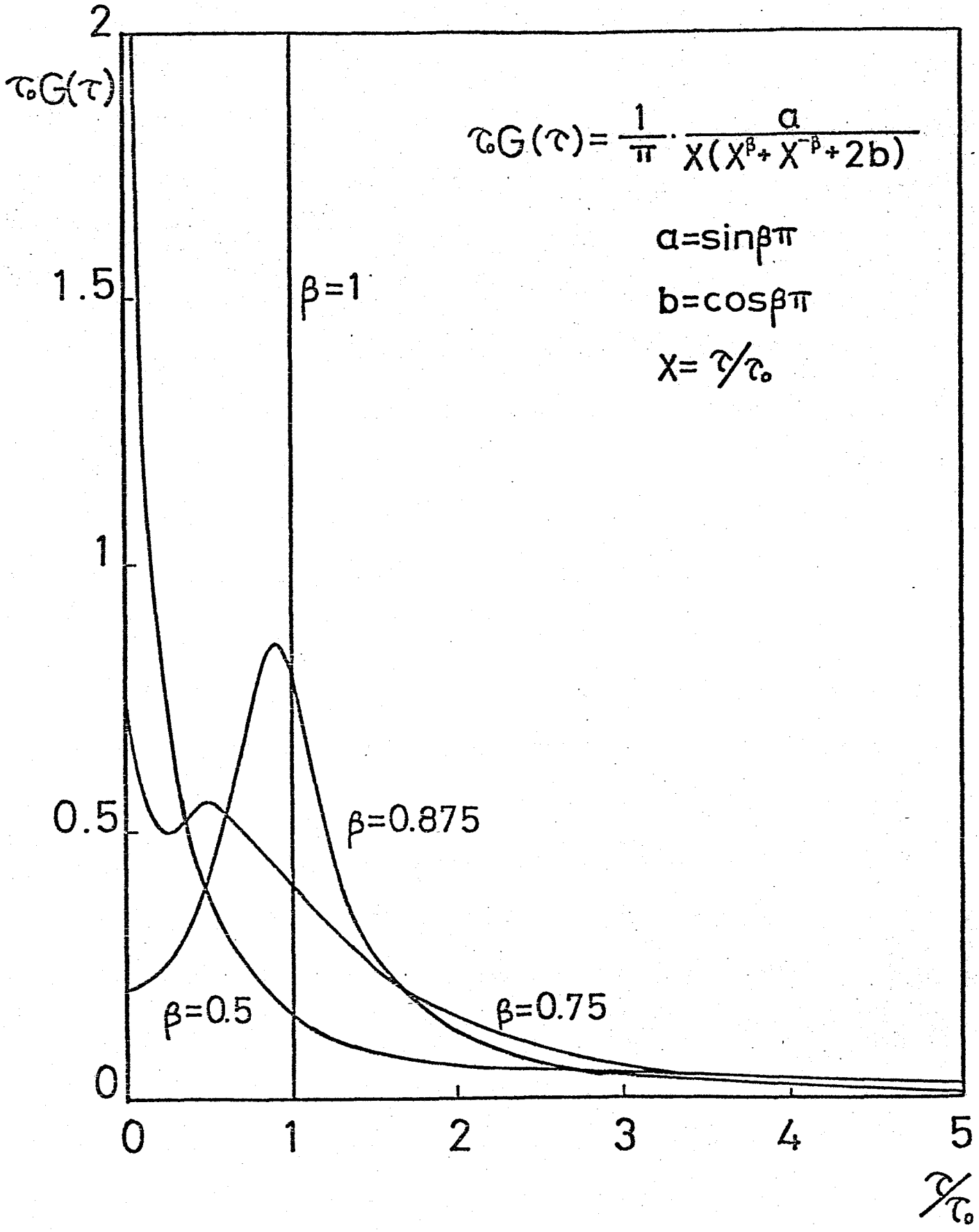

Fig. IV-7. The distribution function of the formula of YM.

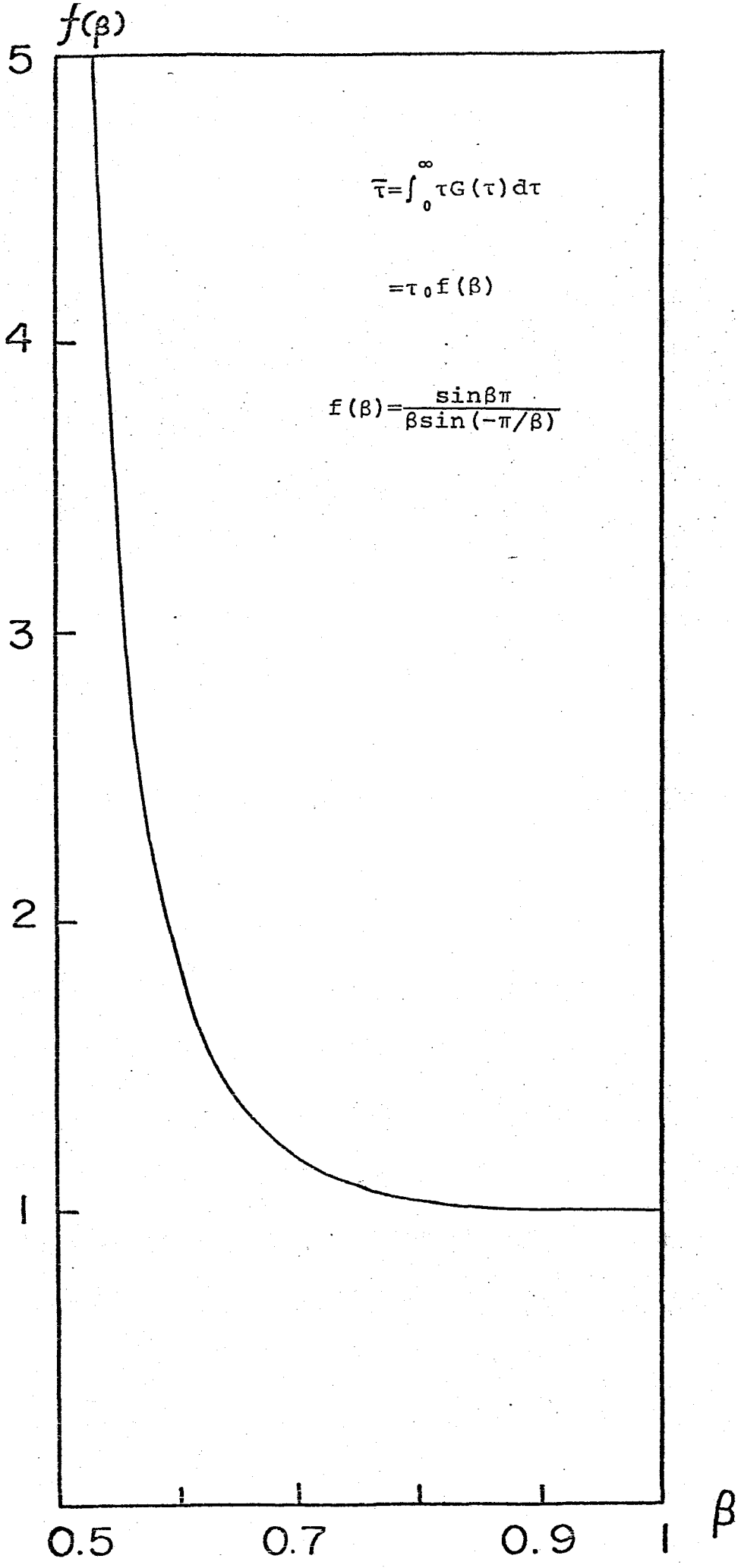

Fig. IV-8. f(β) vs. β.

The value of Δ=1.05 is much smaller than γ=1.73 of the exponent of the static susceptibility. This indicates that the Onsager's kinetic coefficient L increases as the temperature approaches T_c. The difference of the two exponents, γ and Δ, is the exponent of L; 1.73-1.05=0.68 for $0.05<\varepsilon<0.3$ and 1.20-1.05=0.15 for $0.003<\varepsilon<0.05$ (Fig. IV-10). L diverges more strongly in this case than the case of Mn·acetate. Hatta studied the dielectric relaxation[10] in $NaNO_2$ which can be approximated to the Ising model and found that the exponent of the static dielectric constant is smaller than that of the relaxation time. This means that L decreases as the transition point is approached. The importance of the xy components for the temperature dependence of L in the spin system will be noticed by this comparison.

In the static sense $(CH_3NH_3)_2CuCl_4$ is included to the two dimensional Ising model for $0.05<\varepsilon<0.3$ as the exponent of the static susceptibility for this temperature region is 1.75. According to the two dimensional kinetic Ising model,[11] Δ is equal to 2 which is about twice of the present experimental data. Dynamic scaling law[12] predicts that Δ for the three dimensional Heisenberg ferromagnet is 1.33 which does not agree with the present result, but is closer than the value of the two dimensional kinetic Ising model. So long as the exponent of the dynamic quantity is concerned, this compound could not be approximated to the two dimensional Ising system. Isotropic character or the xy components of the interaction will play an important role in the dynamics.

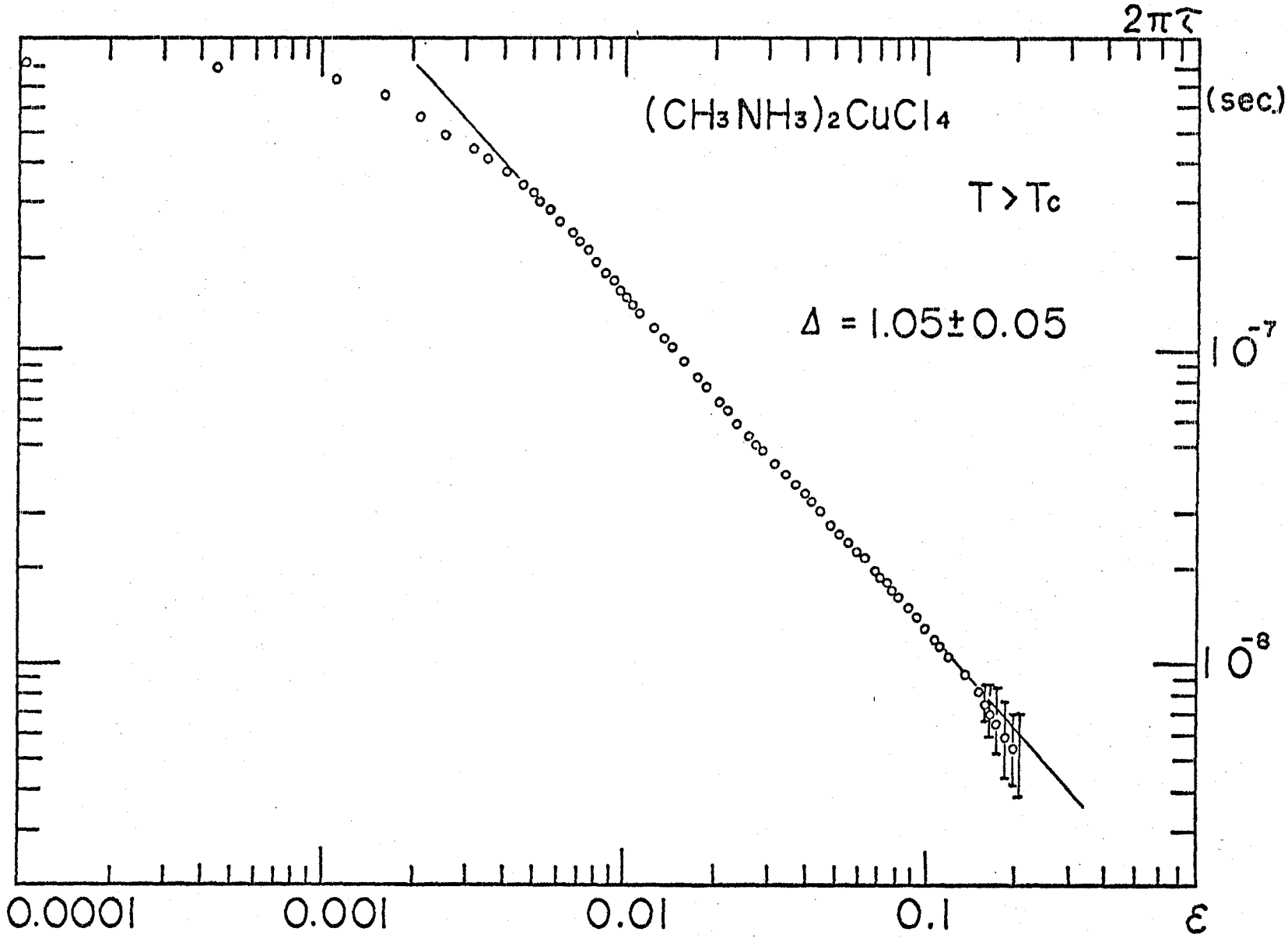

Fig. IV-9. Log-log plot of the relaxation time of $(CH_3NH_3)_2CuCl_4$ in the paramagnetic region.

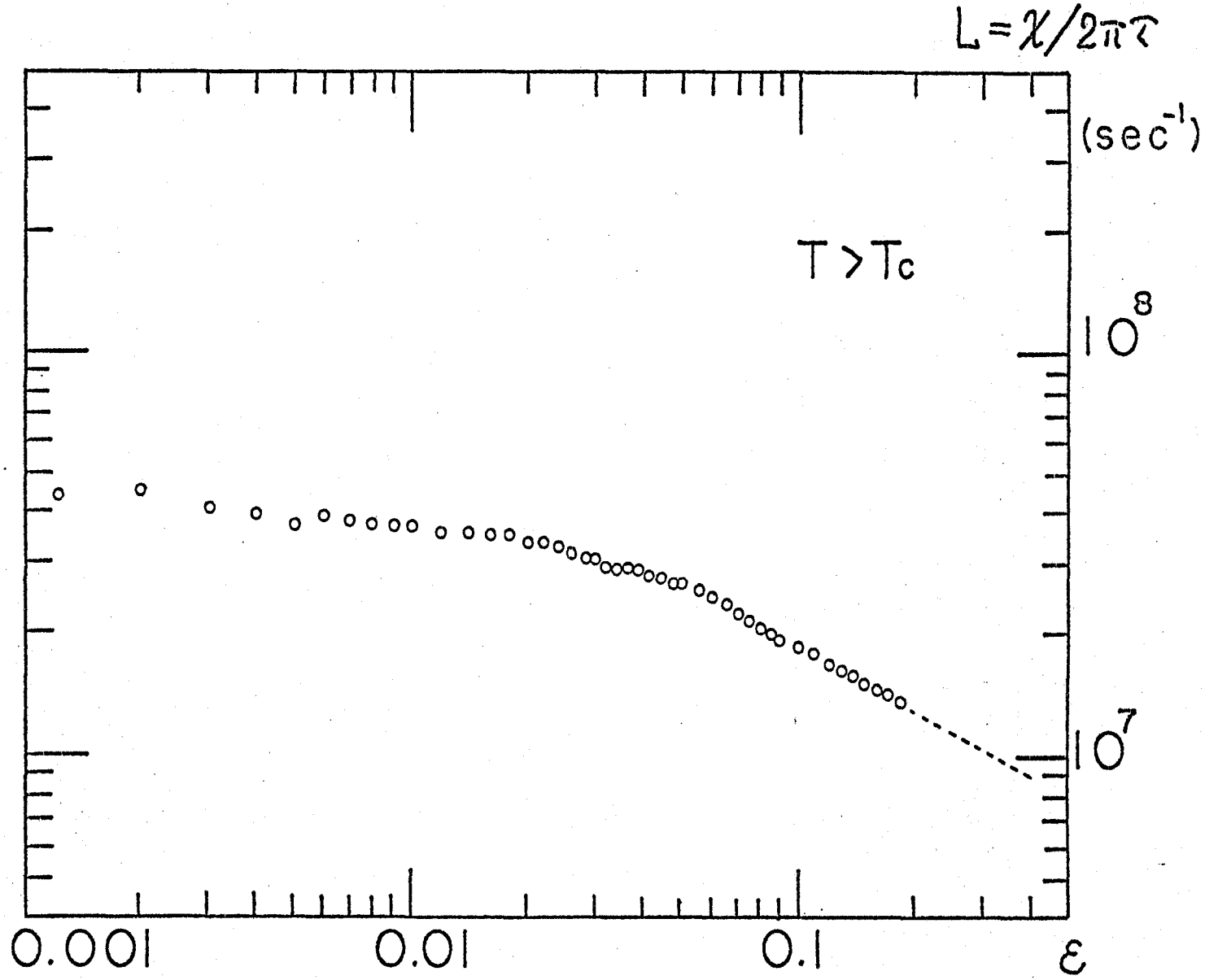

Fig. IV-10. Log-log plot of the Onsager's kinetic coefficient L of $(CH_3NH_3)_2CuCl_4$ in the paramagnetic region. L is calculated from $L=\chi_0/\tau$.

§IV-4. Analysis and discussion of the polydispersive relaxation

In both cases of $Mn(CH_3COO)_2 \cdot 4H_2O$ and $(CH_3NH_3)_2CuCl_4$, there is a small but definite deviation from the Cole-Cole semi-circle to the Cole-Cole arc near T_c. This small deviation can be interpreted as the deviation of the relaxation from the Debye type exponential decay. The symmetrically depressed semi-circle is given by the formula of YM. The fact that the experimental results are well approximated by this formula implys there must exist some reasons or some physical meanings in this formula. Now, let's consider what physical meaning this formula has.

The relaxation function $\Psi_\beta(t)$ which gives $\chi^*(\omega)$ of (4-1) is obtained as follows.

$$\Psi_\beta(t) = \int_0^\infty e^{-t/\tau} G(\tau)\, d\tau$$

$$= \int_0^\infty e^{-t/\tau} \frac{\sin\beta\pi}{\pi\tau\{(\tau/\tau_0)^\beta + (\tau/\tau_0)^{-\beta} + 2\cos\beta\pi\}}\, d\tau. \quad (4\text{-}5)$$

The calculated value of this integral by the computer is given in Fig. IV-11.

It is the long time behavior that is important in the dynamics near the phase transition point. So let us look at the low frequency behavior in the following. As is seen from Fig.IV-11 the time variation of $\Psi_\beta(t)$ for t larger than τ_0 is slower than that of the usual exponential type. This corresponds to a long tail of $G(\tau)$ for $\tau >> \tau_0$ (see Fig. IV-7). This tendency becomes stronger as β becomes smaller. It is also reflected in the Cole-Cole plot. Right half of the depressed semi-circle corres-

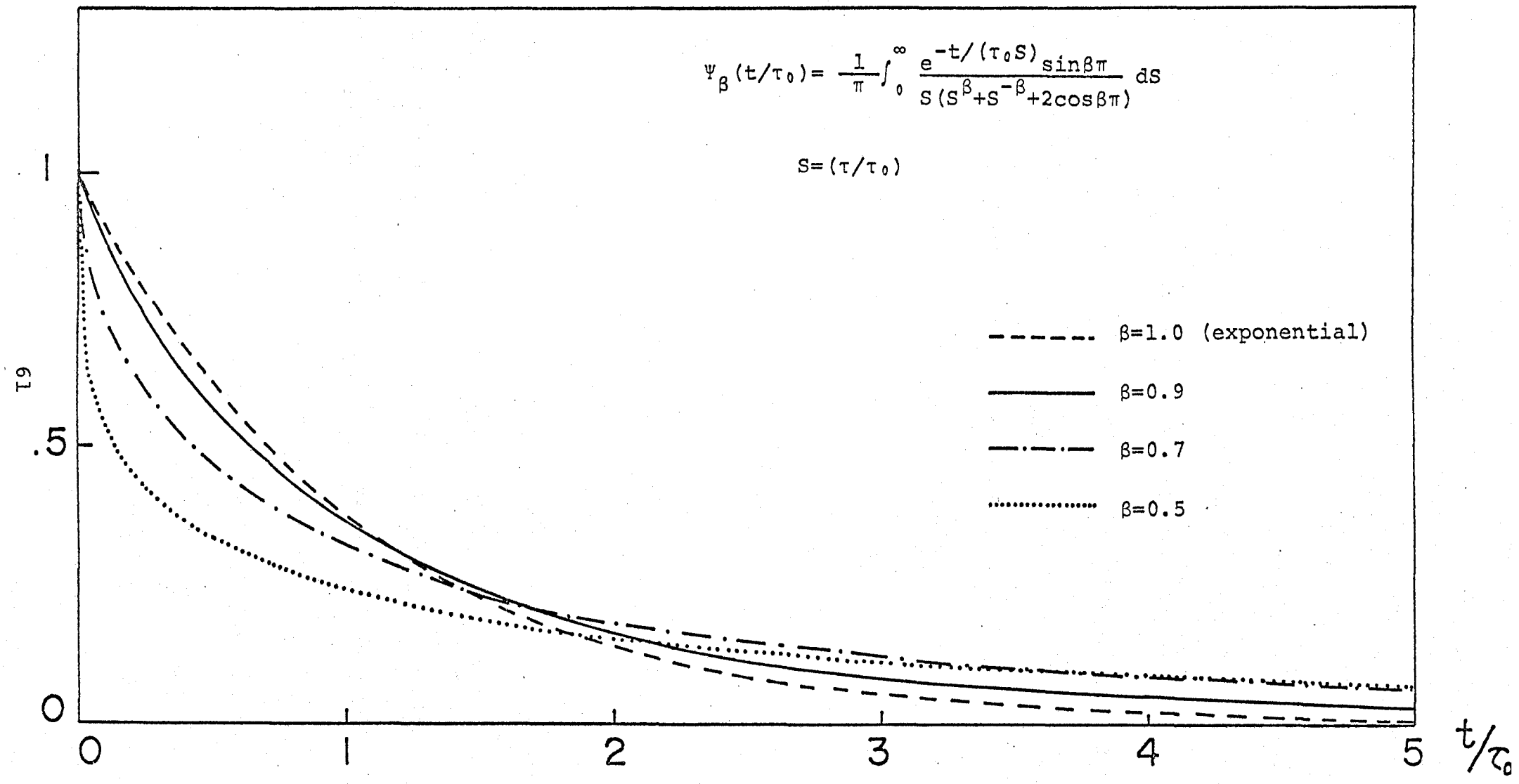

Fig. IV-11. $\Psi_\beta(t/\tau_0)$ calculated for several β's.

ponds to this slower variation of $\Psi_\beta(t)$ for large t.

The asymptotic behavior of $\Psi_\beta(t)$ is

$$\Psi_\beta(t) \sim \frac{1}{t^\beta} \qquad \text{for } t\to\infty \quad (\ \beta<1\ ). \tag{4-6}$$

If the angle between the abscissa and the tangent at $\omega=0$ is α, the asymptotic behavior of the relaxation function is $t^{-2\alpha/\pi}$. If $\alpha=\pi/4$, the long time tail of $t^{-1/2}$ will be realized.* The asymptotic behavior for large t of the experimental results at T_c is approximately $t^{-0.9}$, provided that the formula of YM can be applied for large t.

The power spectrum $I(\omega)=\chi''(\omega)/\omega$ has an anomaly at $\omega=0$ if $\beta<1$. The divergence of $I(\omega)$ at $\omega=0$ is confined within a narrow area near $\omega=0$ so long as β is very close to 1. As β becomes smaller from 1, the region where $I(\omega)$ increases divergently becomes wider around $\omega=0$. The divergence of $I(\omega)$ at $\omega=0$ is attributed to an extremely slow decay of $\Psi_\beta(t)$ for $t>>\tau_0$, or in other words, to a long tail of $G(\tau)$ for $\tau>>\tau_0$.

Thus, the power spectrum near $\omega=0$, the relaxation function for $t>>\tau_0$ and the Cole-Cole figure near $\omega=0$ represent the same phenomena of the long time. Considering the characteristic frequency measured near the transition point, the Cole-Cole analysis is the best method in the present case.

In the formula of YM, τ_0 is the characteristic time and

---

* Note that (4-6) cannot be applied in the case of $\beta=1$. $G(\tau)$ is not continuously reduced to the δ-function.

exhibits the critical slowing down. The experimental results tell that as the transition point is approached the relaxation time τ_0 diverges accompanying a deviation from the Debye type relaxation. Near T_c where the relaxation time gets slow down sufficiently, the decay becomes slower than the exponential for large t. $G(\tau)$ is no longer the δ-function. There is a finite probability of arbitrary relaxation time τ. This can be called polydispersive in this sense phenomenologically. This polydispersive relaxation does not indicate immediately that there come out many microscopic relaxation mechanisms near the critical point. It might be thought as follows. The polydispersive nature might be connected with the various sizes of cluster which is formed near the transition point due to the short range ordering. The fast relaxation time would correspond to the small cluster and the slow relaxation time to the large cluster.

Now let's examine the short time behavior for $t<\tau_0$. $\Psi_\beta(t)$, in this case, decays faster than the exponential decay. This faster decay corresponds to $G(\tau)$ near $\tau=0$ (see Fig. IV-7). If $\beta<1$, $\chi'(\omega)$ of (4-1) does not vanish at T_c, even if τ_0 diverges to infinity. The experimental result that the dip of $\chi'(\omega)$ did not reach to zero for the highest frequency measured might be consistent with this character, considering $\beta=0.9$ at T_c. The depression of the semi-circle in the left half (for higher frequency) implys this fast multi-relaxation times.

References

1) Y. Okuda, M. Matsuura and T. Haseda: J. Phys. Soc. Japan 42 (1977) 341.

2) Y. Okuda, M. Matsuura and T. Haseda: J. Phys. Soc. Japan 44 (1978) 371.

3) T. Matsubara and K. Yoshimitsu: Progr. theor. Phys. 37 (1967) 634.

4) L. J. de Jongh, A. C. Botterman, F. R. de Boer and A. R. Miedema: J. appl. Phys. 40 (1969) 1363.

P. Bloembergen, K. G. Tan, F. H. J. Lefèvre and A. H. M. Bleyendaal: Proc. Int. Conf. Magn., Grenoble 1970. J. Phys., suppl. no. 2-3, Tome 32 (1971) 879.

L. J. de Jongh and W. D. van Amstel: Proc. Int. Conf. Magn. Grenoble 1970. J. Phys., suppl. no. 2-3, Tome 32 (1971) 880.

A. R. Miedema: Proc. Int. Conf. Magn., Grenoble 1970. J. Phys., suppl. no. 2-3, Tome 32 (1971) 305.

5) L. J. de Jongh and H. E. Stanley: Phys. Rev. Letters 36 (1976) 817.

6) L. J. de Jongh and A. R. Miedema: Advances in Phys. 23 (1970) 1.

7) L. J. de Jongh and A. R. Miedema: Physica 46 (1970) 44.

8) L. J. de Jongh: Physica 82B (1976) 247.

9) E. C. Titchmarsh: *Theory of Fourier Integrals* (Clarendon Press, 1949), p.92.

10) I. Hatta: J. Phys. Soc. Japan 28 (1970) 1266.

11) H. Yahata and M. Suzuki: J. Phys. Soc. Japan 27 (1969) 1421.

12) B. I. Halperin and P. C. Hohenberg: Phys. Rev. 177 (1969) 952.

V. Dynamics in a randomly diluted ferromagnetic system $(CH_3NH_3)_2Cu_{1-x}Cd_xCl_4$

§V-1. Introduction

The experimental results in $Mn(CH_3COO)_2 \cdot 4H_2O$ and $(CH_3NH_3)_2CuCl_4$ revealed a clear evidence of the non-Debye relaxation near the transition point which will imply the polydispersive relaxation. The non-linear interactions will introduce the polydispersive relaxation. The non-linear interactions couple $q=0$ mode to the other $q\neq 0$ modes. So the uniform mode may be decomposed into various q modes with various relaxation times, resulting in the polydispersive relaxation. This tendency is most dominant at T_c because the critical slowing down leads to the enhancement of the non-linear couplings. But we have not yet reached the clear understanding of this polydispersive relaxation.

In this chapter we try to take the effect of randomness into consideration positively. By the introduction of the spatially random substitution by the non-magnetic ions, there could be an enhancement of the polydispersive relaxation near T_c in the relaxation of the uniform mode.

According to the recent theoretical work on the dynamics of the spin glass,[1)] the relaxation of the uniform mode in the spin glass is single dispersive at high temperature, but it becomes anomalously polydispersive near the transition point. It is understood as follows. At high temperature the relaxation of a spin at a given site is equal for each site because the corre-

lation among the spins is of microscopic-scale and it has only a weak effect on the spin dynamics. On the other hand near T_c, the relaxation of a given spin must be determined by the correlation of its local environment. If the local environment varies from site to site, it is reasonable that the relaxation becomes polydispersive. The similar picture might be speculated in the random diluted ferromagnet. The random distribution of the non-magnetic ions might bring the distribution of the interaction.

So we performed the experiment of the dynamics of the random diluted ferromagnet $(CH_3NH_3)_2Cu_{1-x}Cd_xCl_4$. The main interest is in the randomness effect on the Cole-Cole plot. How the Cole-Cole plots are deformed from the semi-circle at T_c, especially near $\omega=0$? This experiment will give an instructive image of the polydispersive relaxation found in the preceding chapters (III, IV) in the purely regular system at T_c.

§V-2. Experimental results

Samples prepared for this experiment were $(CH_3NH_3)_2Cu_{1-x}Cd_xCl_4$ where x=0.08 and 0.11,which were prepared from the stoichiometric mixture of CH_3NH_3Cl, $CuCl_2$ and $CdCl_2$. It is known that $(CH_3NH_3)_2CdCl_4$ is the isomorph of $(CH_3NH_3)_2CuCl_4$. The atomic percentage of Cd was determined by the chemical analysis. As the divergence of the susceptibility turns out to be a broad maximum in these diluted ferromagnets, it is difficult to determine the transition temperature T_c accurately. We took as T_c the temperature at which the static susceptibility took its maximum.† In Fig. V-1 is shown $T_c(x)$ vs. x. The experimental results seem to hold the next relation near x=0.

$$\left[\frac{d}{dx} T_c(x)/T_c(0)\right]_{x=0} = 1. \qquad (5\text{-}1)$$

This is consistent with the theoretical result of the three dimensional Ising model.[2)]

In Fig. V-2 is given the Cole-Cole plot of the dynamical susceptibility $\chi'(\omega)$ and $\chi''(\omega)$ for the frequency from 1.2 MHz to 173 MHz in the system of x=0.08. Temperature is given by the reduced temperature ε. As is seen from the figure, the frequency which gives the maximum of $\chi''(\omega)$ at each temperature becomes lower gradually as T_c is approached. For ε larger than

---

† As in the discussion below is not treated the divergent quantities which are expressed by some power of ε, the ambiguity of determining T_c has little effect on the discussion of the experimental results.

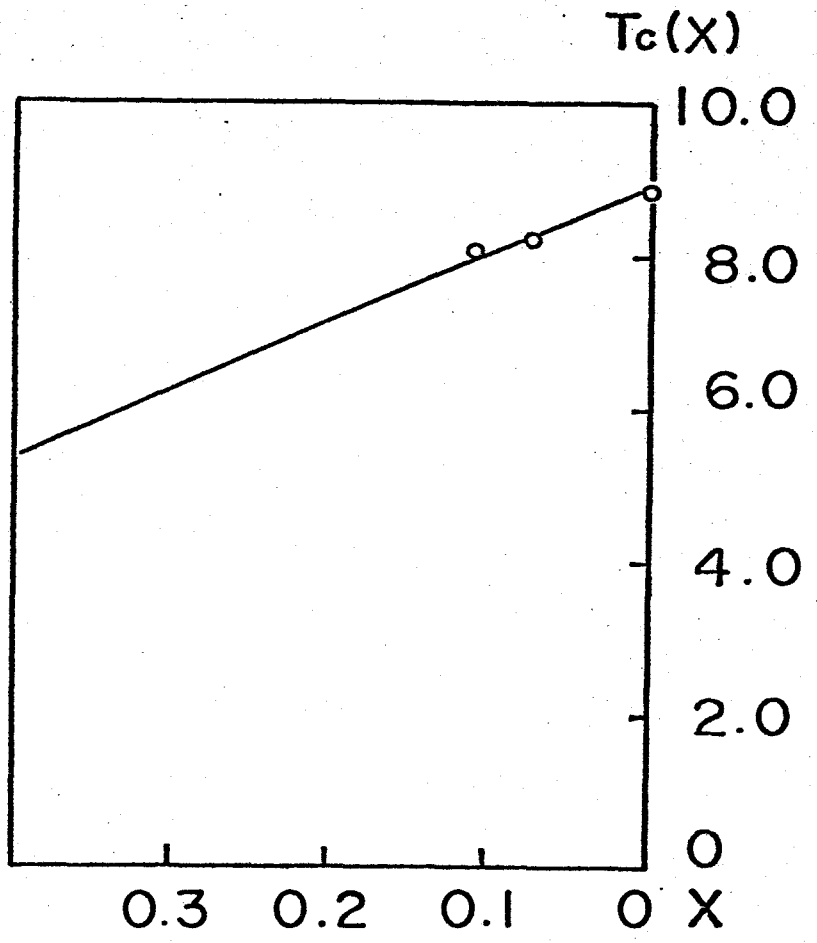

Fig. V-1. $T_c(x)$ vs. x of the system $(CH_3NH_3)_2Cu_{1-x}Cd_xCl_4$.

0.05, the Cole-Cole figure is well approximated by the semi-circle or the slightly depressed Cole-Cole arc. For ε smaller than 0.05, however, the figure is not approximated by the symmetric Cole-Cole arc unlike the case of the pure system. The outstanding feature of the plot is the extremely depressed form in the low frequency region. The tangent at $\omega=0$ is approximately $\pi/4$ which corresponds to $t^{-1/2}$ of the asymptotic behavior of the decay function. $t^{-1/2}$ dependence was predicted by Kinzel and Fischer for the decay of the uniform mode in the spin glass. The comparison of the experimental results with their theory will be made in the next section.

Figure V-3 is the Cole-Cole plot for the ordered state of the same x sample. The Cole-Cole figure is also depressed one as that of the paramagnetic region near T_c. For ε larger than 0.05, there appears a new hump in the low frequency region which might be due to something like the domain wall motions. The experimental data in the system of x=0.11 is shown in Fig. V-4 for the paramagnetic region. The overall character of the Cole-Cole plot is the same as the one with x=0.08. The characteristic frequency which gives the maximum of $\chi''(\omega)$ for a same ε is higher in this case than the case of x=0.08. For example, for ε=0.03 it is about 60 MHz in the case of x=0.08 whereas it is about 80 MHz in the case of x=0.11.

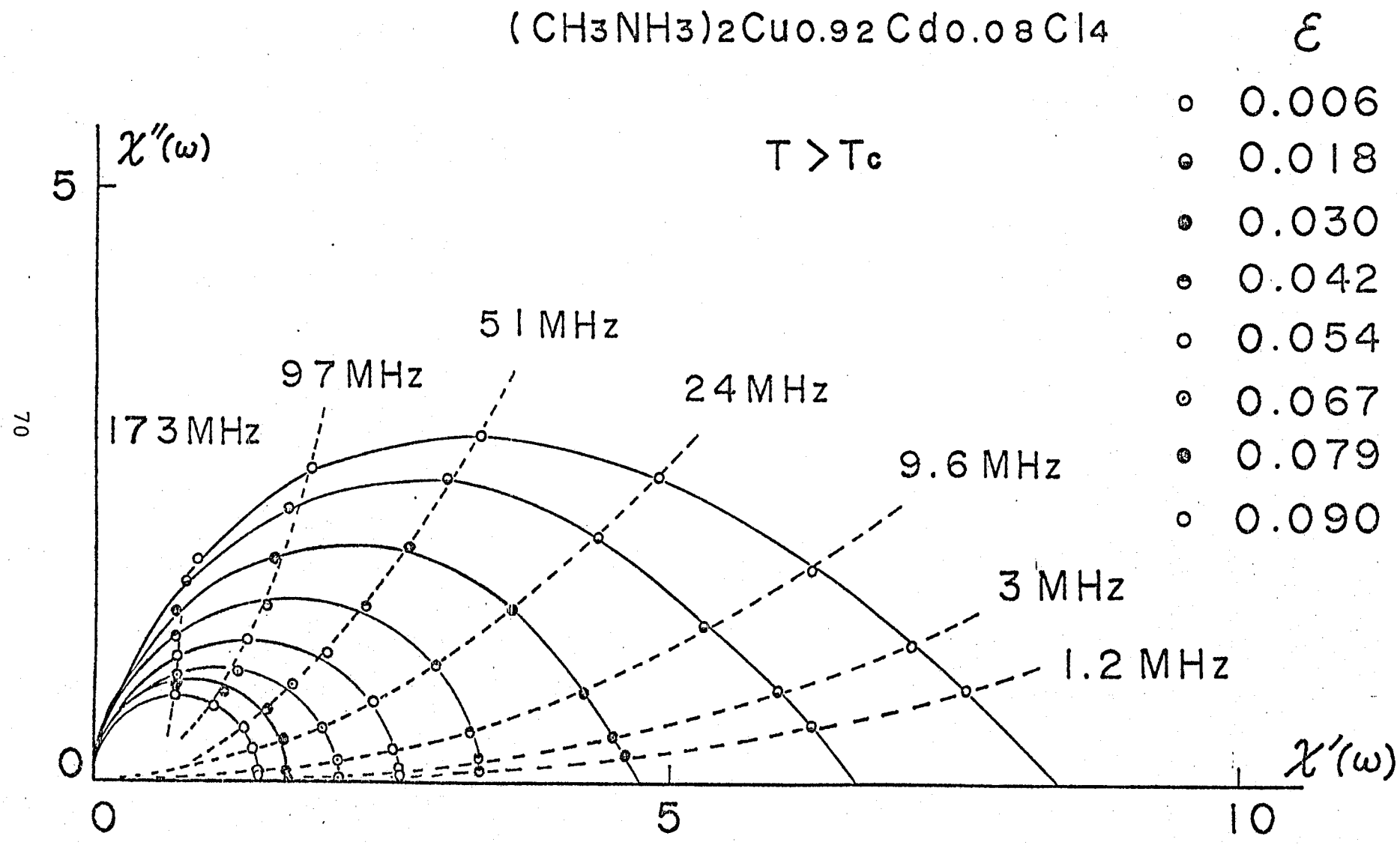

Fig. V-2. Cole-Cole plot of the uniform mode of $(CH_3NH_3)_2Cu_{0.92}Cd_{0.08}Cl_4$ in the paramagnetic region.

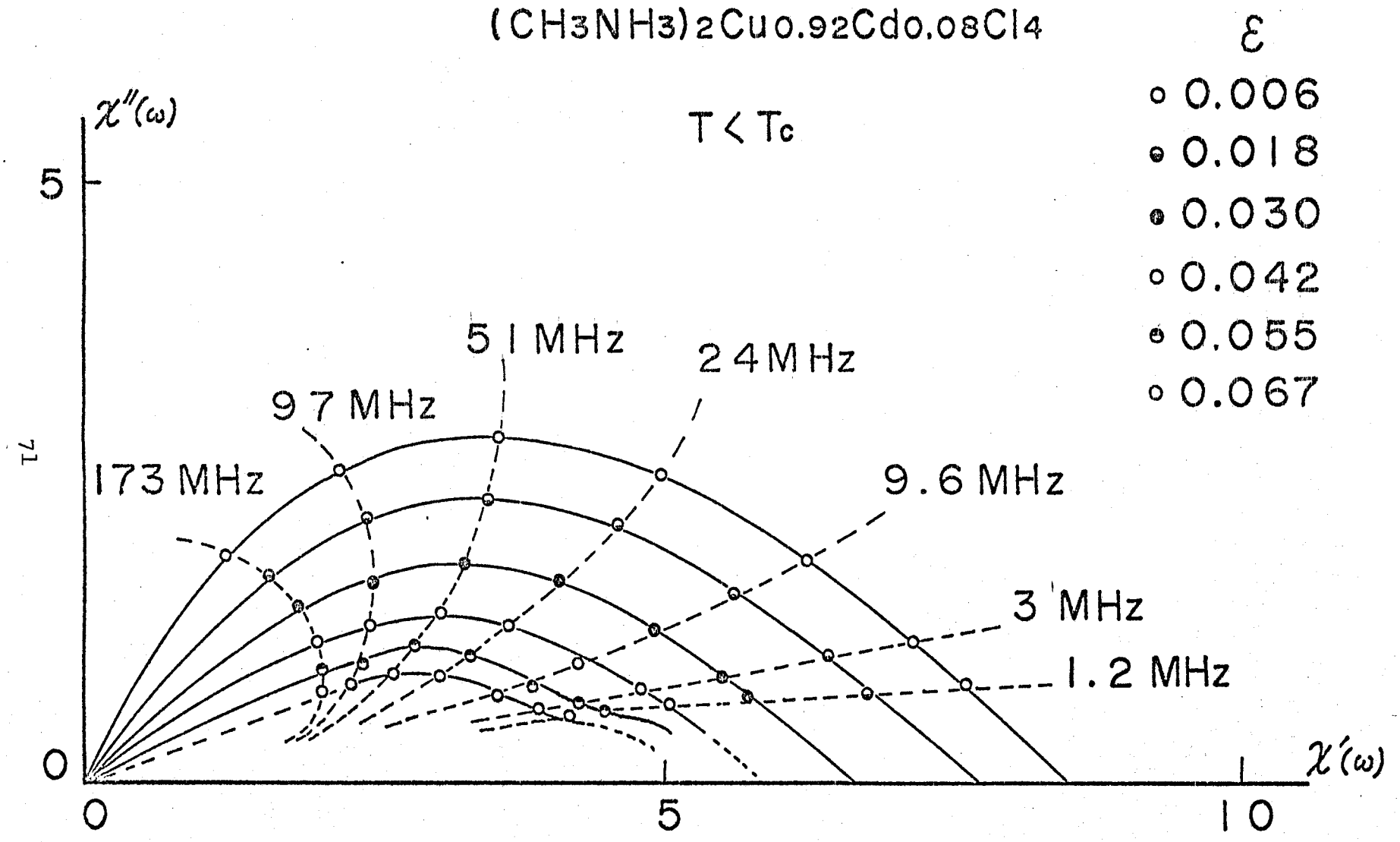

Fig. V-3. Cole-Cole plot of $(CH_3NH_3)_2Cu_{0.92}Cd_{0.08}Cl_4$ below T_c.

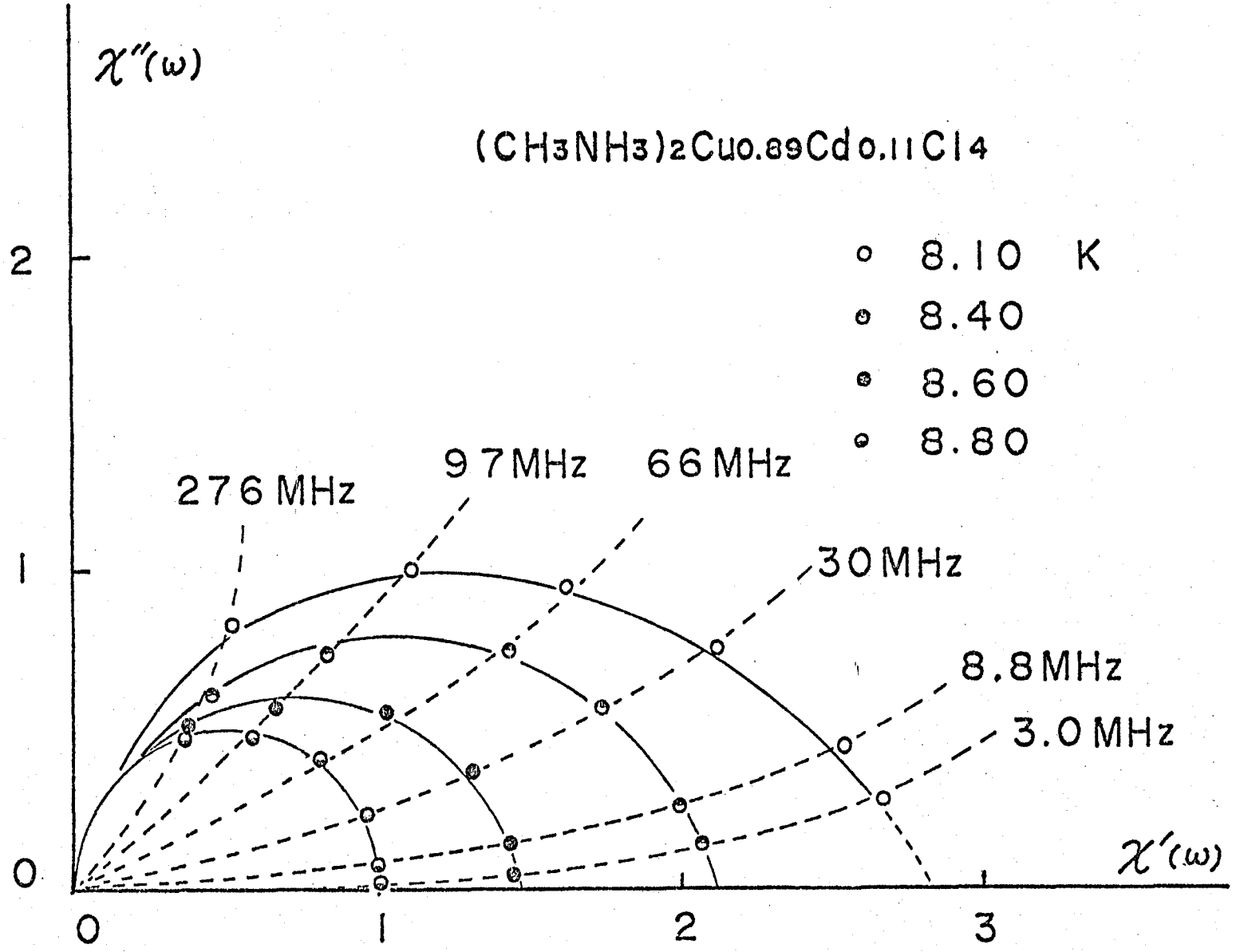

Fig. V-4. Cole-Cole plot of $(CH_3NH_3)_2Cu_{0.89}Cd_{0.11}Cl_4$ above T_c.

§V-3. Comparison with the theory of the spin glass

Kinzel and Fischer[1] calculated the dynamic uniform susceptibility $\chi^*(\omega)$ of the spin glass. Their calculation is based on the random distribution of the exchange interaction which is the symmetric gaussian distribution. The model is the kinetic Ising model and the molecular field approximation was used. The dynamic susceptibility was derived as this.

$$\chi^*(\omega) = \frac{2}{k_B T}(T/T_f)^2 [1+i\omega\tau_0-\{(1+i\omega\tau_0)^2-(T_f/T)^2\}^{1/2}] , \quad (5-2)$$

where T_f is the freezing point of the spin glass and τ_0 is the elementary relaxation time. The Cole-Cole plot of this non-Debye susceptibility is depicted in Fig. V-5. In the figure at T_f, the tangent at $\omega=0$ has the angle $\pi/4$ against the abscissa. The similarity with the experimental results in the random diluted ferromagnet is noteworthy.

Here we try to look into the polydispersive relaxation of the spin glass. It might be helpful to understand the polydispersive nature of the present experimental results because the Cole-Cole plot is very resembling in both cases. The susceptibility of (5-2) can be expressed as

$$\chi^*(\omega) = \int_0^\infty \frac{G(\tau)}{1+i\omega\tau} d\tau , \quad (5-3)$$

where $G(\tau)$ is the distribution function of the polydispersive relaxation. By putting (5-2) into the left hand side of (5-3), $G(\tau)$ can be obtained as[3],

$$G(\tau) = \frac{2}{k_B T}(T/T_f)^2 \cdot \frac{1}{\pi \tau}\sqrt{2(\tau_0/\tau)-(\tau_0/\tau)^2-1+(T_f/T)^2} \quad . \qquad (5\text{-}4)$$

$G(\tau)$ is drawn for various α's ($=T_f/T$) in Fig. V-6. As the transition point T_f is approached, the breadth of the distribution becomes broader and the tail of $G(\tau)$ for large τ extends to infinity at T_f. This long tail of $G(\tau)$ corresponds to the slow decay of $t^{-1/2}$.

In the spin glass the polydispersive character comes from the distribution of the exchange interaction as mentioned in the introduction. Though the distribution of the exchange interaction is independent of the temperature, the distribution of the relaxation time crucially depends on the temperature owing to the critical slowing down of the mode with respect to the configuration which is realized in the spin glass state. So the breadth of the distribution diverges at T_f.

The fact that the experimental results (Cole-Cole plot) are very resembling to this theory indicates that the analogous behavior of the distribution $G(\tau)$ would be realized in this random diluted ferromagnet, though the microscopic detail might be quite different.

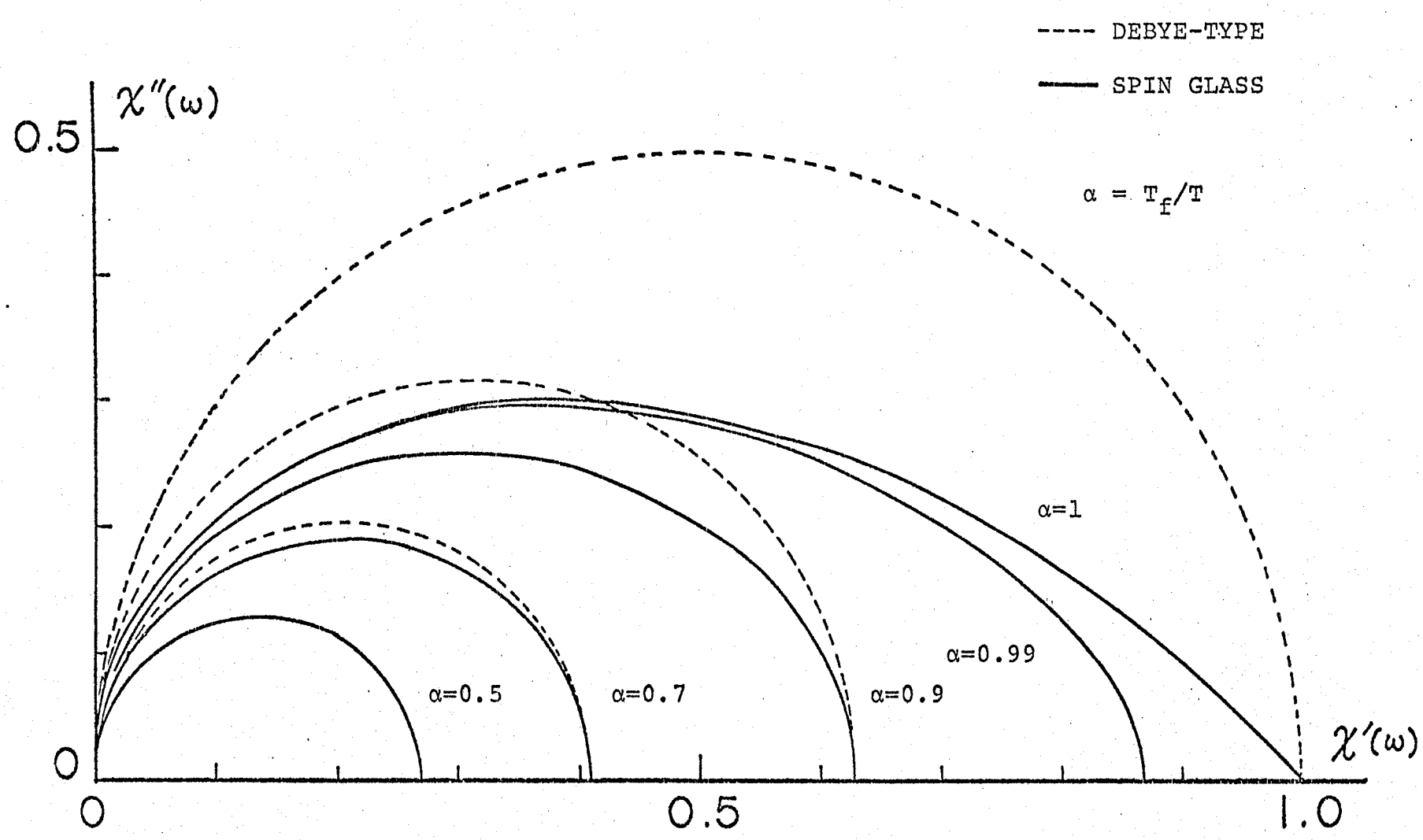

Fig. V-5. Cole-Cole plot of the theoretical result by Kinzel and Fischer for the uniform susceptibility of the spin glass.

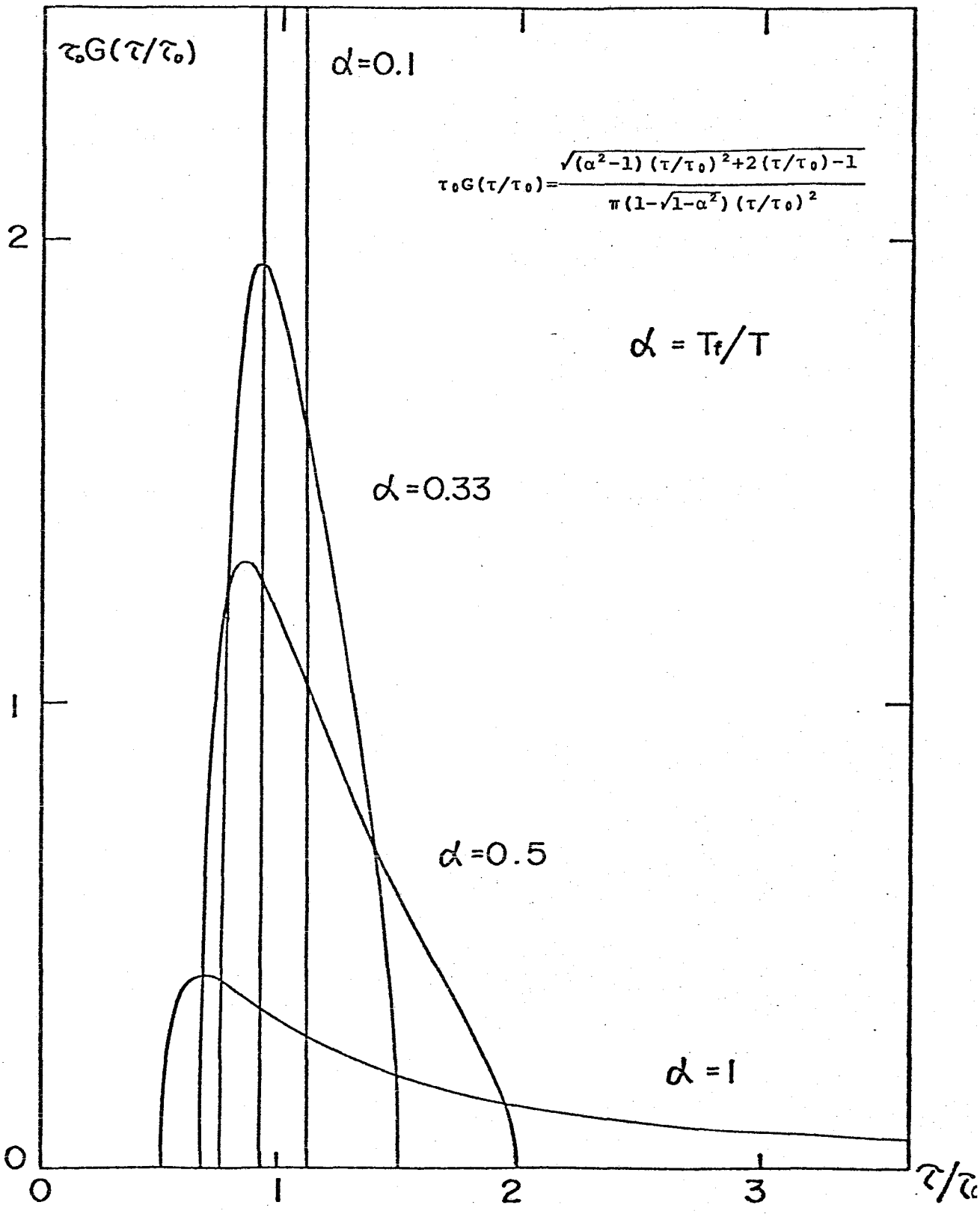

Fig. V-6. The distribution function of the polydispersive relaxation of the uniform mode which is calculated from the result of Kinzel and Fischer.

References

1) W. Kinzel and K. H. Fischer: Solid State Commun. 23 (1977) 687.

2) G. S. Rushbrooke and D. J. Morgan: Molecular Phys. 4 (1961) 1.
D. J. Morgan and G. S. Rushbrooke: Molecular Phys. 4 (1961) 291.

3) E. C. Titchmarsh: *Theory of Fourier Integrals* (Clarendon Press, Oxford, 1949), p.92.

VI. Relaxation time near T_c under external field

§VI-1. Introduction

In the case of an ideal isotropic Heisenberg ferromagnet, the uniform magnetization M_z is a constant of motion, and there will be no damping of M_z. But the Hamiltonian of the real system always contains some anisotropy which comes from the dipole-dipole interaction, antisymmetric exchange interaction, spin lattice interaction and so on. In that case the uniform magnetization is no longer a constant of motion and there is a decay rate associated with those interactions. The relaxation measurement in the present study is to inspect the uniform relaxation via such interactions that do not conserve the total magnetization.

Let the relaxation function of M_z be $(M_z(t),M_z(0))$. As is shown by Mori and Kawasaki,[1] when the decay rate of $(\dot{M}_z(t),\dot{M}(0))$ is much faster than the decay rate of $(M_z(t),M_z(0))$, then $(M_z(t),M_z(0))$ can be approximated by $(M_z(0),M_z(0))\exp[-\Gamma t]$ where

$$\Gamma = 1/\tau = \frac{1}{(M_z(0),M_z(0))} \int_0^\infty (\dot{M}_z(t),\dot{M}_z(0))dt \ . \qquad (6\text{-}1)$$

$\dot{M}_z(t)$ is given as

$$\dot{M}_z(t) = (i\hbar)^{-1}[M_z(t),H_{tot}] \ . \qquad (6\text{-}2)$$

H_{tot} is the total Hamiltonian which consists of the isotropic and the anisotropic interaction. The relaxation time of the uniform magnetization can be factorized into two parts. The denominator

of the above relation (6-1) is nothing but the uniform susceptibility. Then the time integral of $(\dot{M}_z(t),\dot{M}_z(0))$ is what is called the Onsager's kinetic coefficient L for the uniform mode. If there exists no correlation between $\dot{M}_z(t)$ and $\dot{M}_z(0)$, that is to say, if $\dot{M}_z(t)$ can be looked upon as a white noise acting on $M_z(t)$, the integral gives the temperature independent constant L and the relation is reduced to that of the conventional theory.[2] If there comes in the correlation of $\dot{M}_z(t)$ as T_c is approached, the temperature dependence of τ is determined by a competing process between χ_0, the denominator of (6-1), and L, the numerator of (6-1). If the divergence of χ_0 is stronger than that of L, the critical slowing down will be realized, though it will be weaker than the case of the conventional theory. If the divergence of L is stronger than that of χ_0, the critical slowing down will be replaced by the critical speeding up.

The critical speeding up is in fact reported in some antiferromagnets such as $CuCl_2 \cdot 2H_2O$ and $LiCuCl_3 \cdot 2H_2O$ by the relaxation measurement[3] and MnF_2 by ESR line width measurement.[4] The phenomena are interpreted as the divergence of L, since the uniform susceptibility does not show any singular behavior. Divergence of L is understood as follows.[5] The anisotropy couples the fluctuation of the uniform mode to the fluctuations with non zero q by the relation (6-2). Near T_N the fluctuations near K_0, which is the wave vector characterizing the antiferromagnetic ordering, becomes enormously large. So the coupling between q=0 and $q \neq 0$ via the anisotropy is dominated by the coupling between q=0 and $q=K_0$, resulting into an anomalous increase of L as is seen

from (6-1) and (6-2).

On the other hand in the ferromagnetic case, χ_0, the denominator of (6-1) exhibits a strong divergence at T_c. The contribution to the numerator of (6-1) comes from the coupling between q=0 mode and q≠0 modes near q=0 via the anisotropy. As the q≠0 fluctuations near q=0 becomes large in the ferromagnetic case, the numerator of (6-1) also can exhibit anomalous increase. So the temperature dependence of τ —— which of the critical slowing down and the critical speeding up is realized —— is very delicate.

In the experiment of ESR line width on a ferromagnet $CdCr_2Se_4$ Koetzler et al.[6] have found the similar line broadening with that of antiferromagnets and attributed it as an indication of the critical speeding up. In the ESR experiment the line broadening measures the decay of the uniform mode perpendicular to the external field. As is pointed out by Tomita,[7] both the transverse and the longitudinal magnetization may exert torque on the transverse component. There exists a definite damping in the transverse magnetization which will lead to the increase of the numerator of (6-1). Moreover, the external field inherent to the magnetic resonance will depress the static susceptibility, the denominator of (6-1). This will help to speed up the relaxation time.

However, in our experiment on the non-resonant relaxation of the longitudinal magnetization M_z under zero external field on a ferromagnetic crystal $(CH_3NH_3)_2CuCl_4$ (chapter IV), not the critical speeding up but the critical slowing down was observed.

It is interesting to study by the non-resonant experiment

how the external field as a weak perturbation modulates the relaxation of the longitudinal magnetization M_z and to compare it with the result of ESR. As the external field perpendicular to the easy axis gives the additional relaxation mechanism of M_z as mentioned above, the field $H_\perp$ will give a drastic effect on the relaxation of M_z in the non-resonant relaxation measurement. The result of the relaxation under $H_\perp$ will be compared with the case of $H_{//}$ which does not give the additional relaxation mechanism.

§VI-2. Experimental results

In order to study the fluctuation along the easy axis under the external fields of various directions, the high frequency susceptibility measurement was carried out always along the easy axis.

The high frequency susceptibility of $Mn(CH_3COO)_2 \cdot 4H_2O$, $\chi_a'(\omega)$, at 28 MHz under the external field $H_{c'}$, is given in Fig. VI-1. The field was applied along c' axis which is the second easy axis. In high temperature region (T>3.45 K), the high frequency susceptibility gradually decreases as $H_{c'}$ increases. When T_N is approached (T<3.45 K), there appears a hump in $\chi_a'(\omega)$-$H_{c'}$. The susceptibility at first increases and then decreases as the applied external field is increased. The hump in $\chi_a'(\omega)$-$H_{c'}$ becomes larger and shifts to higher field as T_N is approached. Figure VI-2 gives the schematic view of this phenomenon. The dotted line in the figure is the static susceptibility χ_a under zero external field. The dip in $\chi_a'(\omega)$-$H_{c'}$ at $H_{c'}$=0 near T_N is the result of the critical slowing down under zero external field. For a finite $H_{c'}$, the relaxation time makes a quick recovery to the fast relaxation time, whereas χ_a gradually decreases as is shown in Fig. VI-5. So there appears a hump in $\chi_a'(\omega)$-$H_{c'}$. The relaxation time vs. $H_{c'}$ is plotted in Fig. VI-3 for several temperatures near T_N. The quick speeding up is manifested for $H_{c'}$ less than 500 Oe.

As there is no anomaly in $\chi_a''(\omega)$ for $H_{c'}$ at which the hump of $\chi_a'(\omega)$ appears, the possibility of the magnetic resonance was excluded. The relaxation time was obtained from $\chi_a'(\omega)$ and $\chi_a''(\omega)$ for 28 MHz, provided that the relaxation is single dispersive.

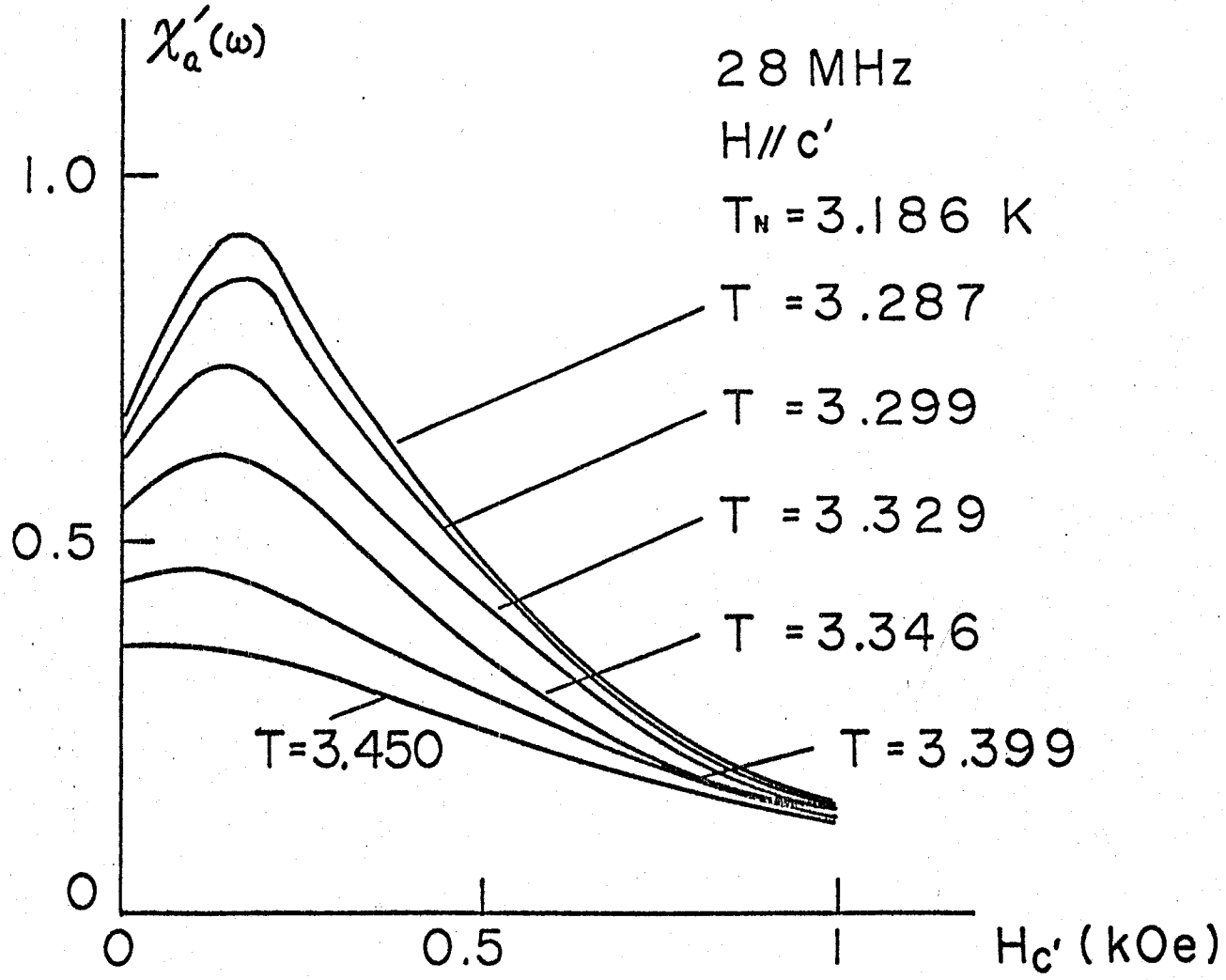

Fig. VI-1. Real part of the complex susceptibility at 28 MHz of $Mn(CH_3COO)_2 \cdot 4H_2O$ under the external field which is applied along the second easy axis, c' axis.

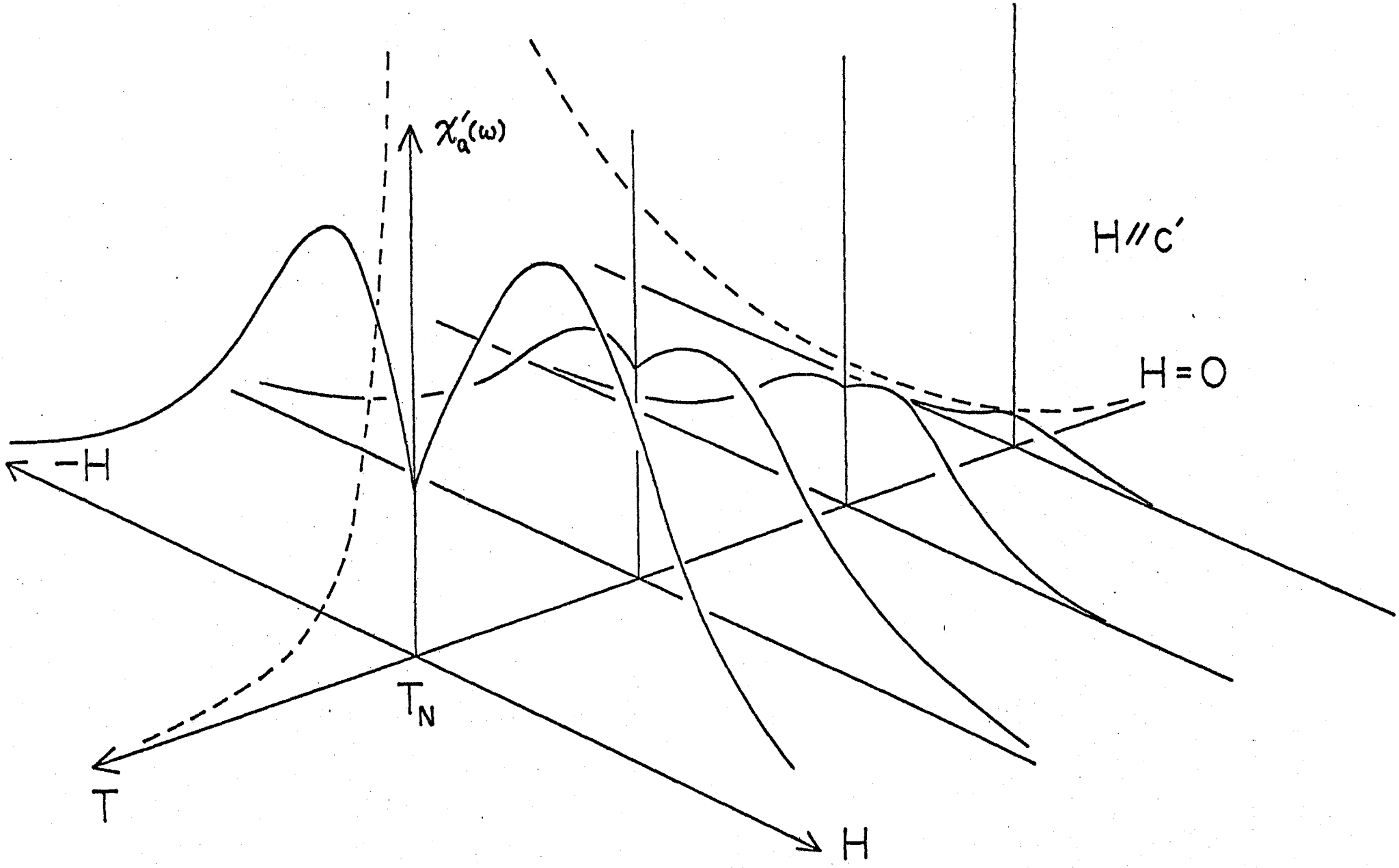

Fig. VI-2. Schematic view of $\chi_a'(\omega)$-T-$H_{c'}$ of $Mn(CH_3COO)\cdot 4H_2O$. The dotted line denotes the static susceptibility under zero external field. The field is applied along c' axis, which is the second easy axis.

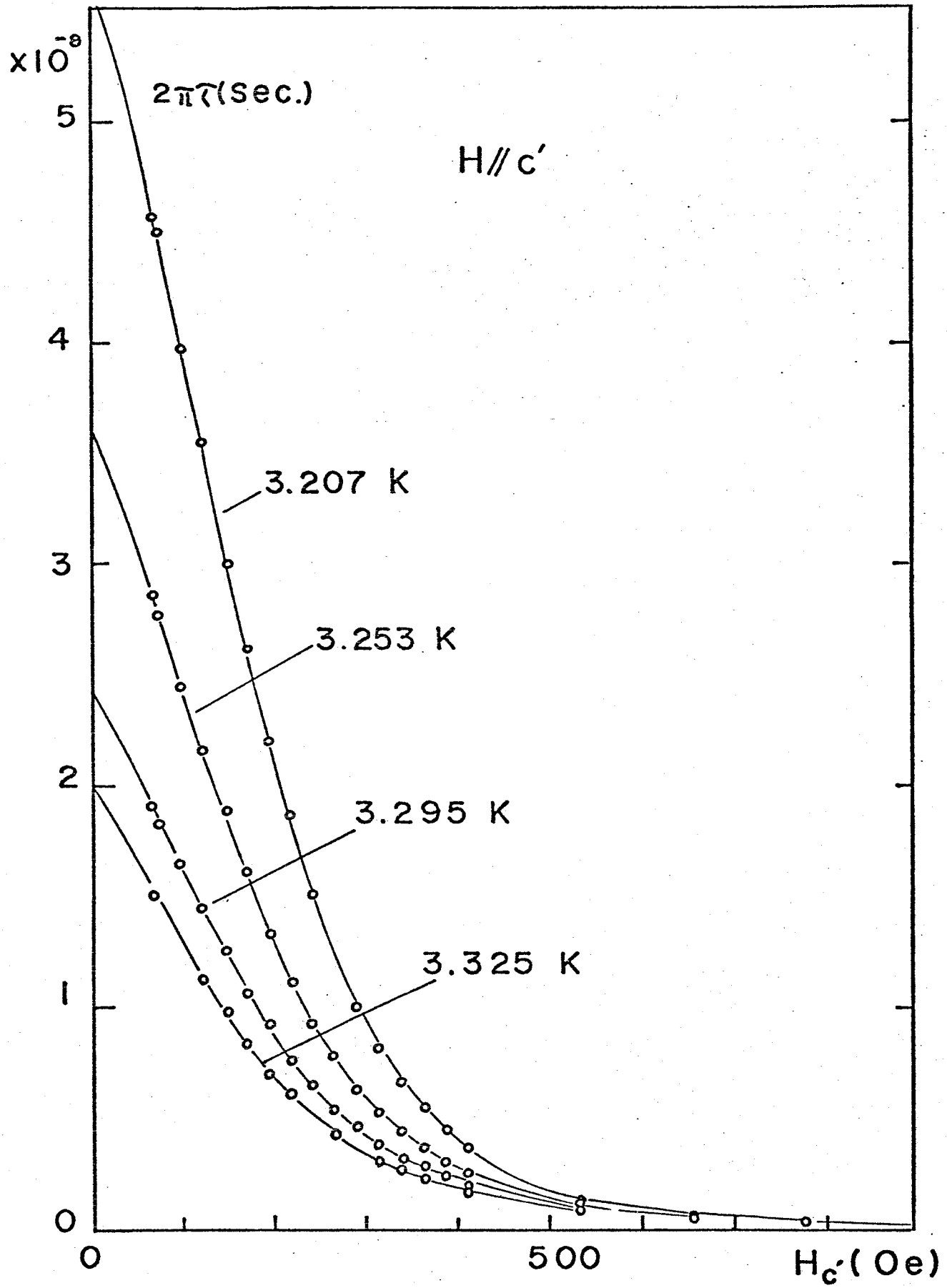

Fig. VI-3. The relaxation time of $Mn(CH_3COO)_2 \cdot 4H_2O$ under the external field which is applied along c' axis.

This assumption was justified only for $H_{c'}=0$, except for near T_N. But so long as the qualitative character of τ vs. $H_{c'}$ is concerned, this assumption will be permitted.

The temperature dependence of the relaxation time under the external field $H_{c'}$ is displayed in Fig. VI-4. When $H_{c'}$ is applied, the critical slowing down is crucially supressed. At $H_{c'}=650$ Oe, the relaxation time is almost constant for $\varepsilon<0.03$ and the constant value is 10^{-3} times as small as that of the case of $H_{c'}=0$ at T_N. But the critical speeding up was not observed.

The field dependence of the Onsager's kinetic coefficient L was obtained from the relation $L(H_{c'})=\chi_a(H_{c'})/\tau(H_{c'})$. As is shown in Fig. VI-5, the $H_{c'}$ dependence of χ_a is much weaker than that of τ, which indicates the strong $H_{c'}$ dependence of L. $L(H_{c'})$ is plotted against $H_{c'}^2$, in Fig. VI-6. For the field lower than 400 Oe, the experimental data are well approximated by a straight line, which means $L(H_{c'})\propto H_{c'}^2$, for small $H_{c'}$. Figure VI-7 presents the temperature dependence of L under $H_{c'}$. As mentioned above, L increases as $H_{c'}$ increases, but the temperature dependence is almost the same for each $H_{c'}$.

When the field is applied along the easy axis (a axis), the external field will not have in principle any effect on the relaxation mechanism. Figure VI-8 and VI-9 are the results of χ_a and τ when H_a is applied along the same direction of the susceptibility (a axis). The hump in $\chi_a'(\omega)$ was not observed in this case. χ_a and τ drastically decrease for the field lower than the case of $H_{c'}$. For example, 50 Oe is enough to depress them. The decrease of χ_a is more rapid than that of τ in contrast with the

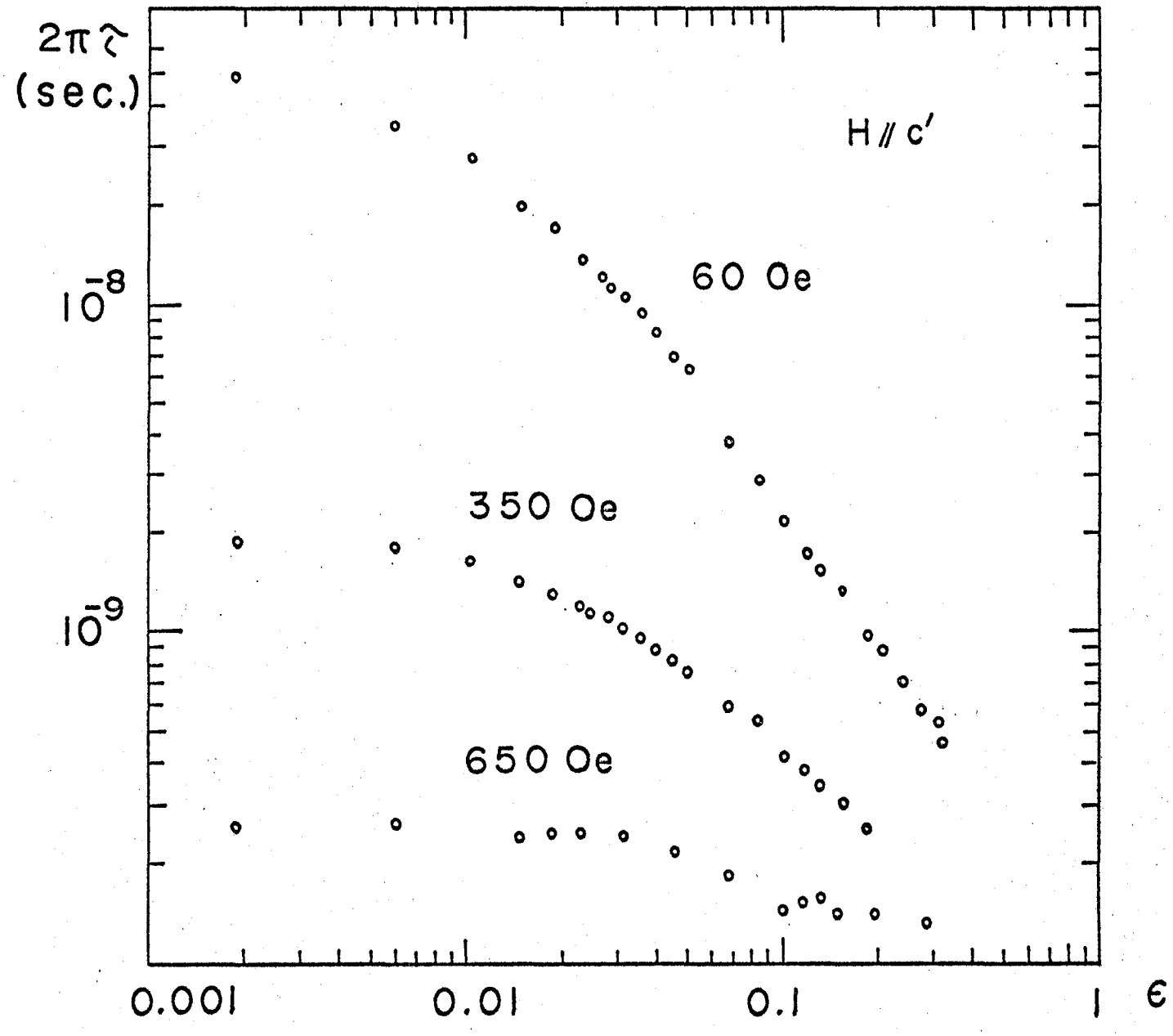

Fig. VI-4. The temperature dependence of the relaxation time of $Mn(CH_3COO)_2 \cdot 4H_2O$ under the external field which is applied along c' axis.

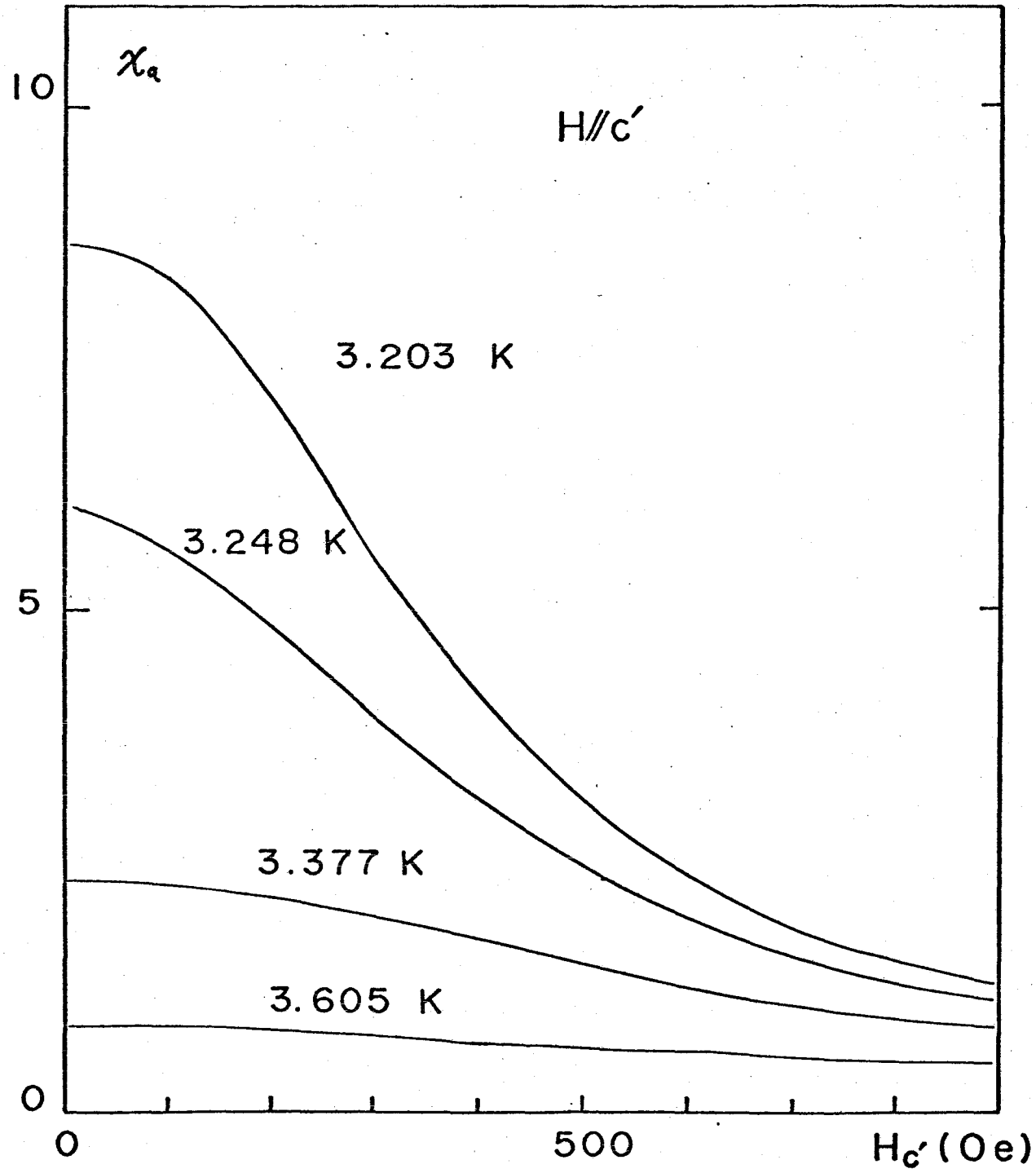

Fig. VI-5. The static susceptibility along the easy axis (a axis) of $Mn(CH_3COO)_2 \cdot 4H_2O$ under the external field which is applied along c' axis.

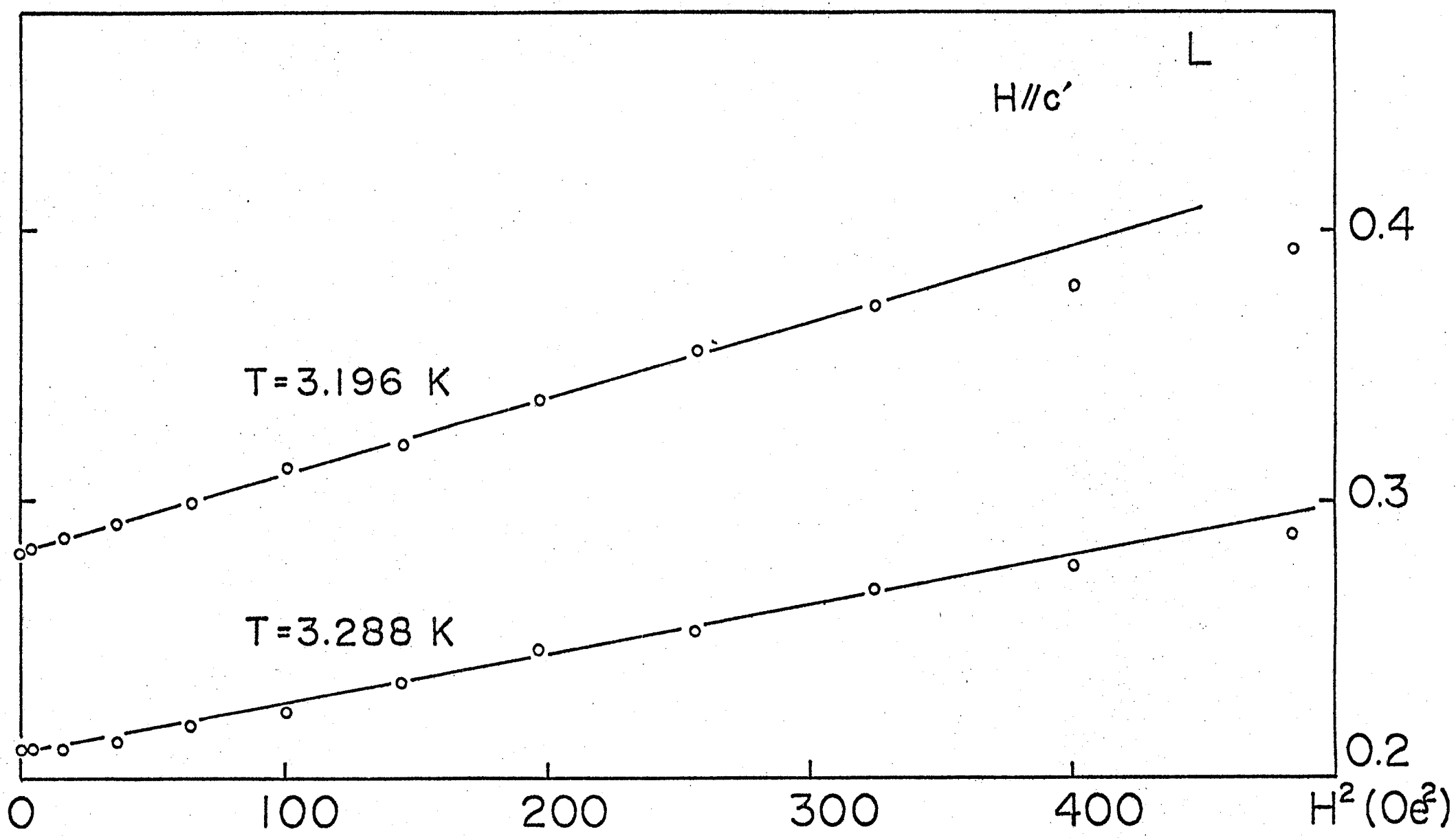

Fig. VI-6. The Onsager's kinetic coefficient L of $Mn(CH_3COO)_2 \cdot 4H_2O$ plotted against $H_{c'}^2$. The field $H_{c'}$ is applied along c' axis.

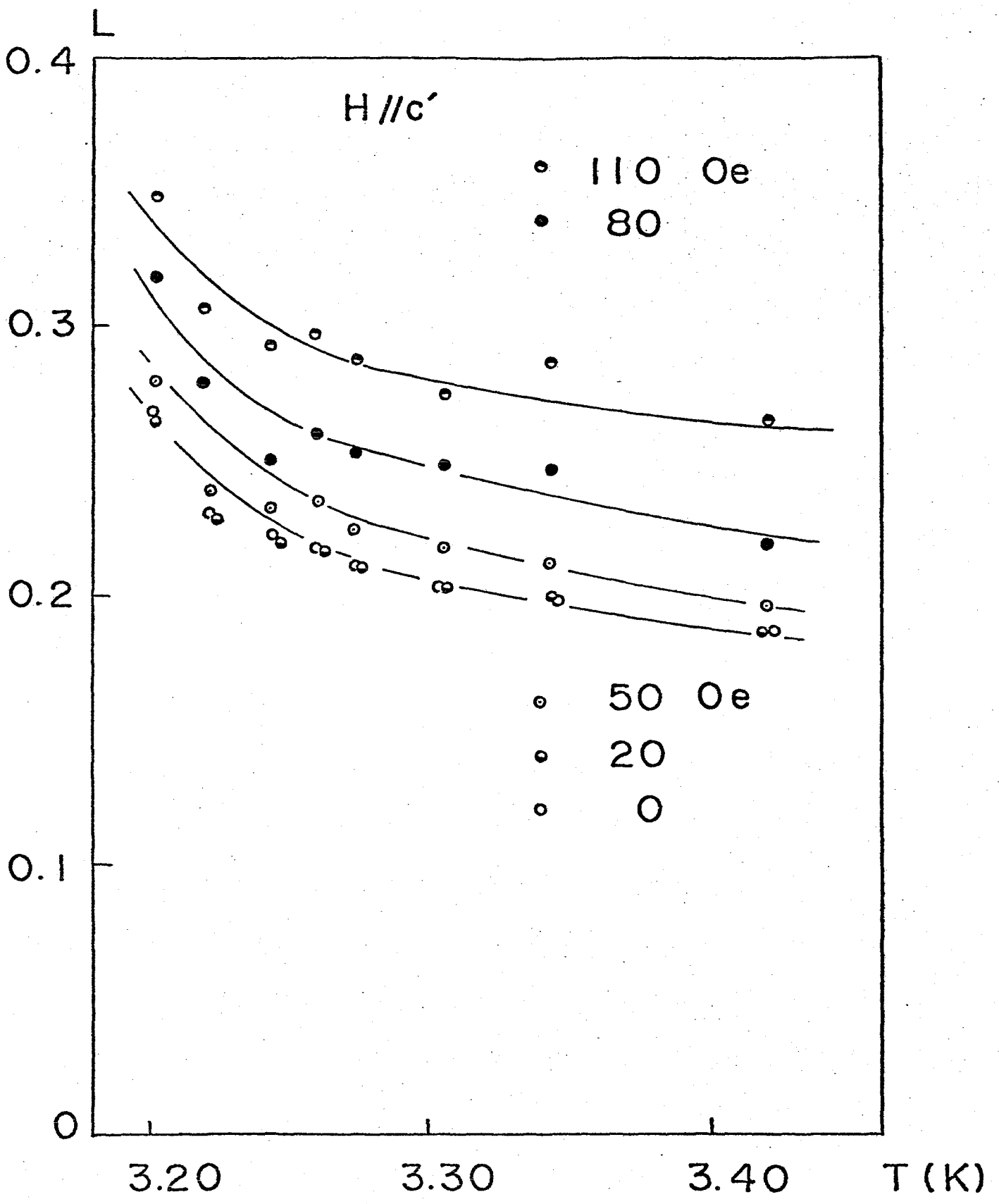

Fig. VI-7. The temperature dependence of the Onsager's kinetic coefficient L of $Mn(CH_3COO)_2 \cdot 4H_2O$ under various external fields which are applied along c' axis.

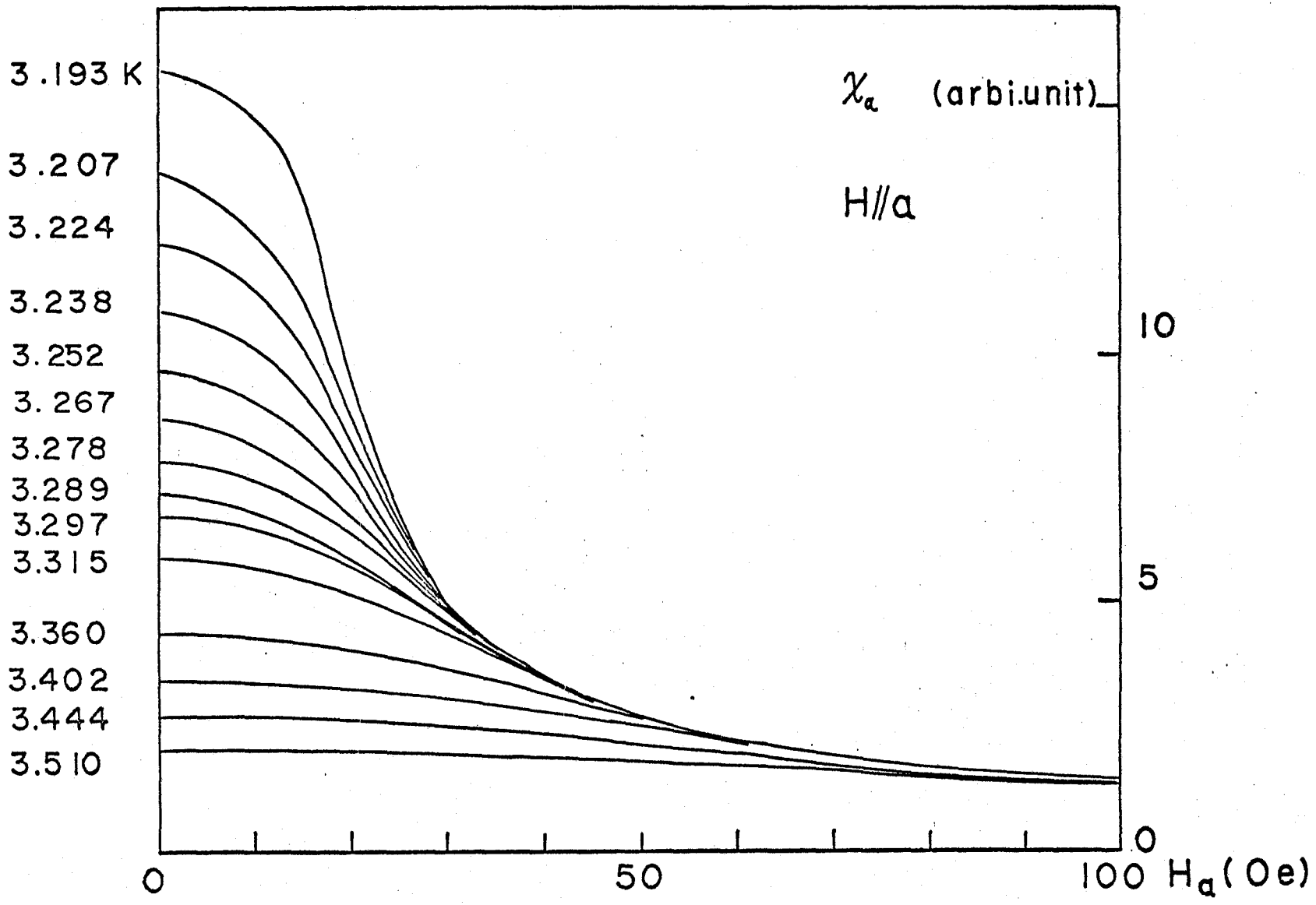

Fig. VI-8. The static susceptibility of $Mn(CH_3COO)_2 \cdot 4H_2O$ under the external field along the easy axis which is the same direction of the measurement of the susceptibility.

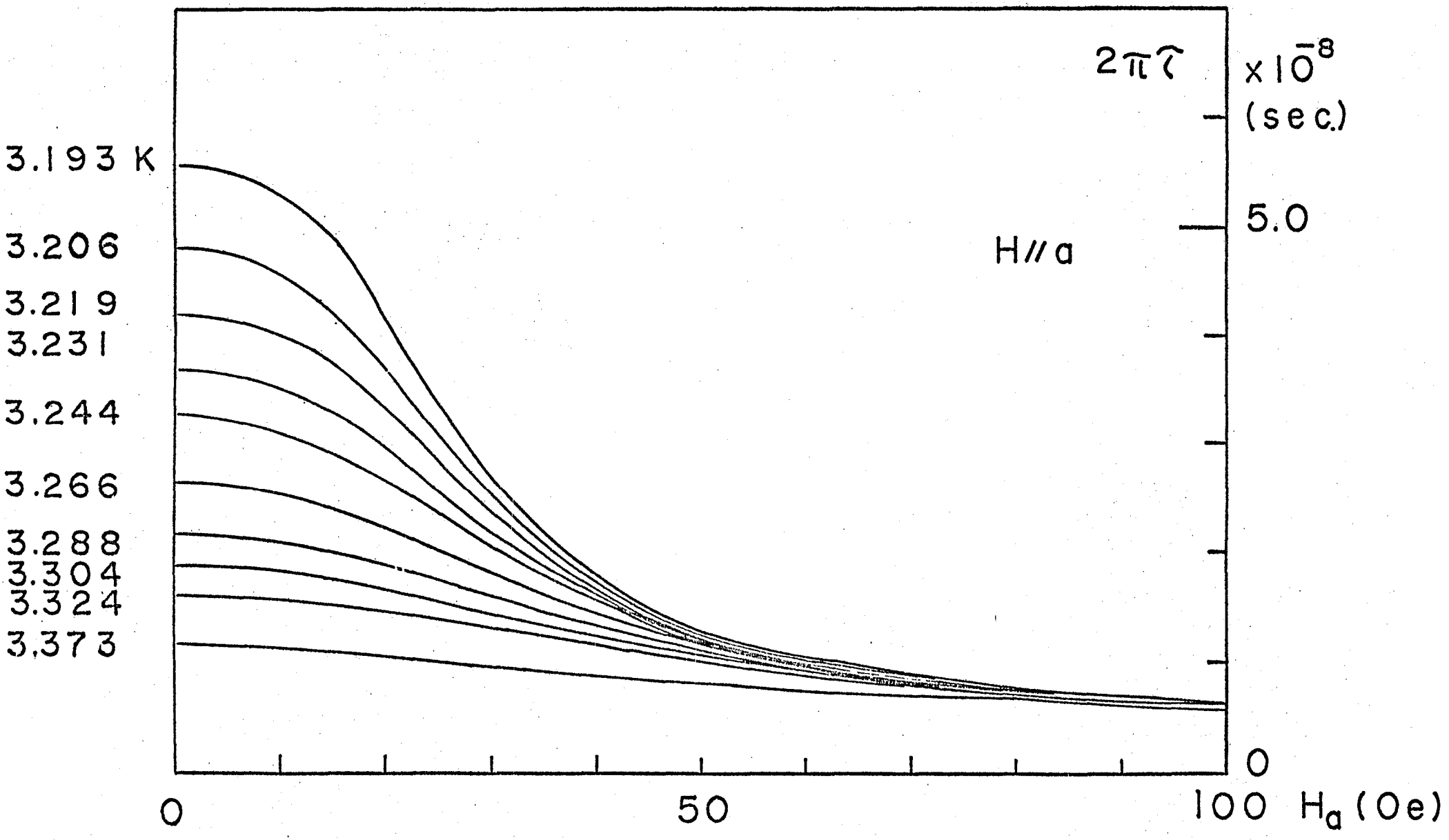

Fig. VI-9. The relaxation time of $Mn(CH_3COO)_2 \cdot 4H_2O$ under the external field which is applied along the easy axis (a axis).

case of $H_{c'}$. That is to say, L decreases when H_a is increased. This phenomenon implies that the external field supresses not only the correlation of the magnetization but also the correlation of the torque. The decrease of L might be attributed to the decrease of χ_a, though the relation is not so simple. The temperature dependence of L is plotted in Fig. VI-10, for several values of H_a. For H_a larger than 15 Oe, L decreases as T_N is approached.

The experimental results on $(CH_3NH_3)_2CuCl_4$ were similar with those of $Mn(CH_3COO)_2 \cdot 4H_2O$. Figure VI-11 is the temperature dependence of L for several H_a's which are applied along the same direction of the susceptibility measurement. Unlike the case of Mn·acetate, the susceptibility is very feasible against the parallel external field. Even the field 1 Oe brings a perceptible change of χ_a just at T_c. So the earth field could not be neglected there. The result shown in Fig. VI-11 is qualitatively the same as the case of Mn·acetate. Figure VI-12 is the result of L when H_b is applied along b axis which is the second easy axis. As the case of Mn·acetate, L increases suddenly under the increase of H_b from zero. In this case the value of the field which brings the same change of L is 10 times as large as the case of H_a. Note that the value of L when the field is applied along b axis becomes two or three times as large as the case of the parallel field. The temperature dependence of L when the field is applied along the second easy axis (b axis) is not the same as the case of Mn·acetate. For H_b larger than 10 Oe, L increases at first, then decreases as T_c is approached. The temperature which gives the maximum of L shifts to higher temperature as H_b increases. Figure VI-13 presents

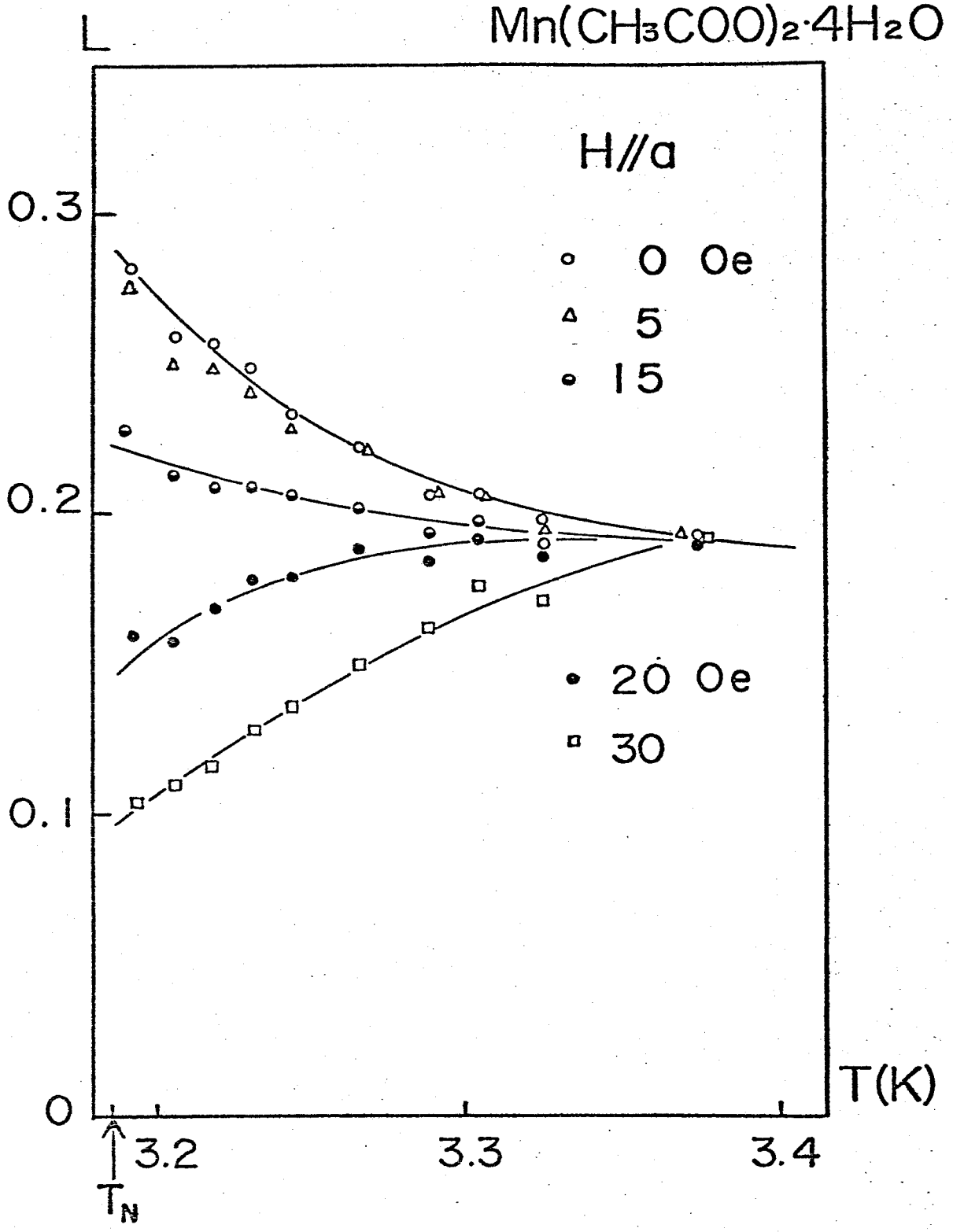

Fig. VI-10. The temperature dependence of the Onsager's kinetic coefficient L of $Mn(CH_3COO)_2 \cdot 4H_2O$ for various external fields which are applied along the easy axis (a axis).

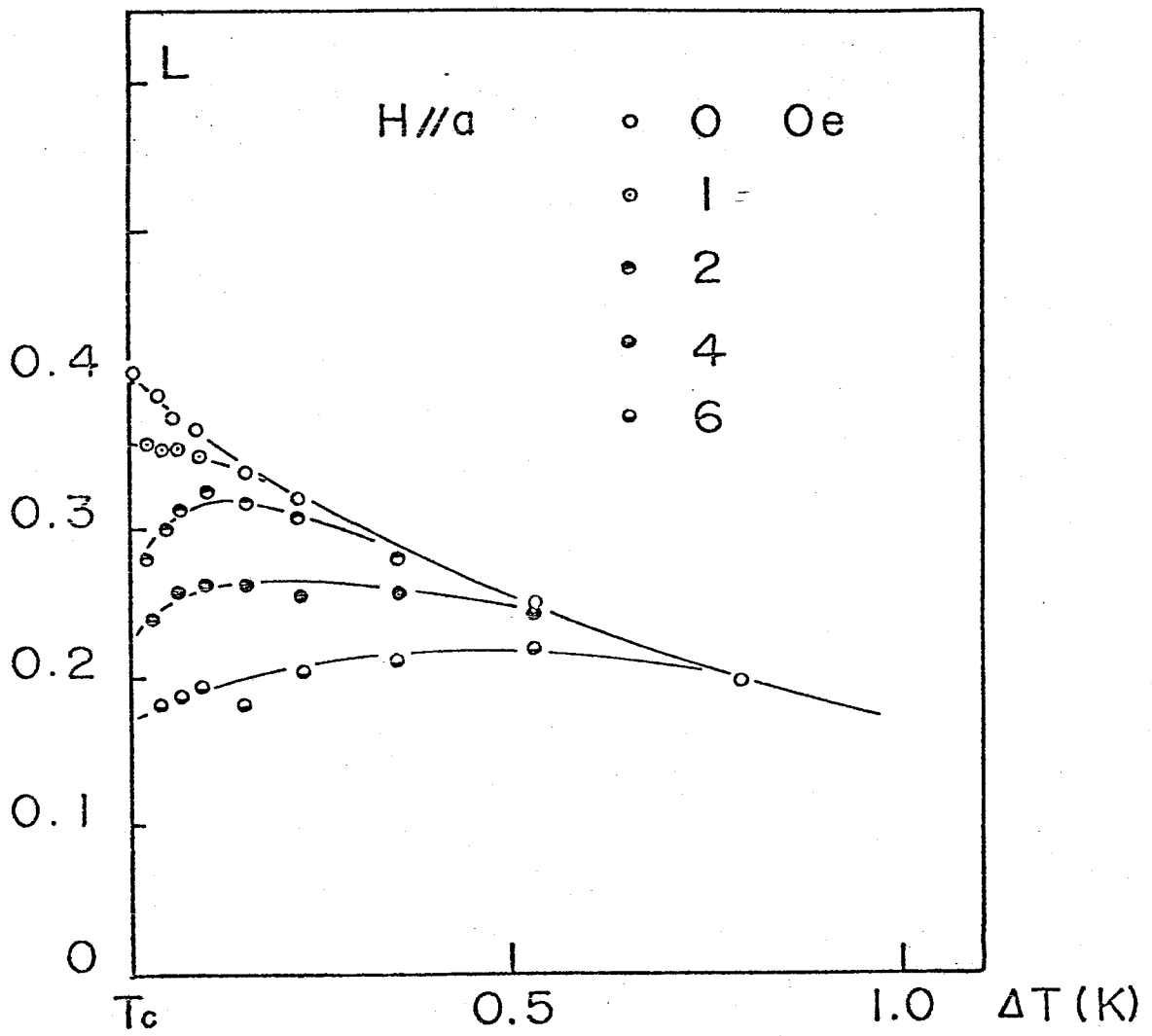

Fig. VI-11. L of $(CH_3NH_3)_2CuCl_4$ plotted against ΔT for various external fields which are applied along the same direction of the measurement of the susceptibility.

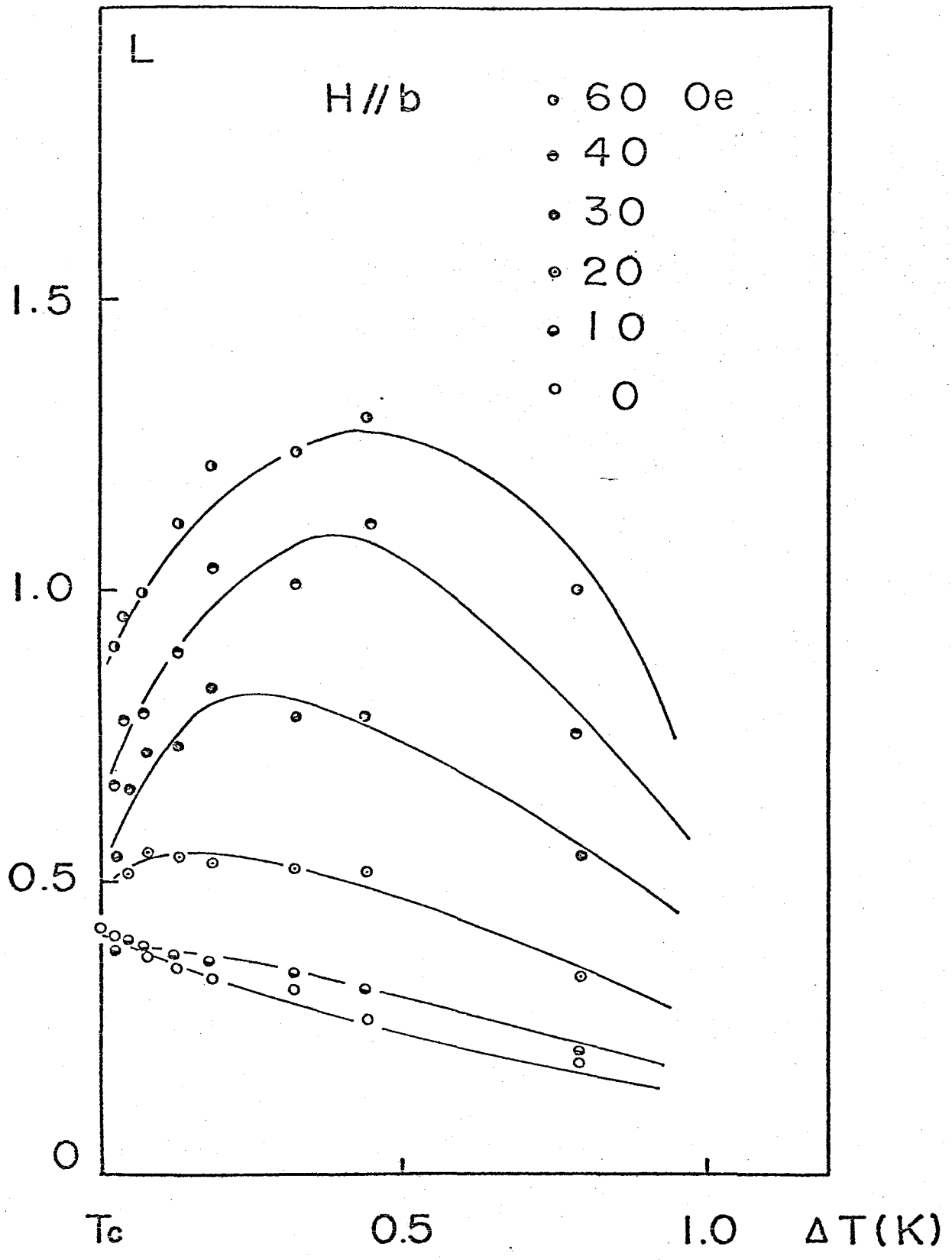

Fig. VI-12. L of $(CH_3NH_3)_2CuCl_4$ plotted against ΔT under external fields which are applied along b-axis, the second easy axis.

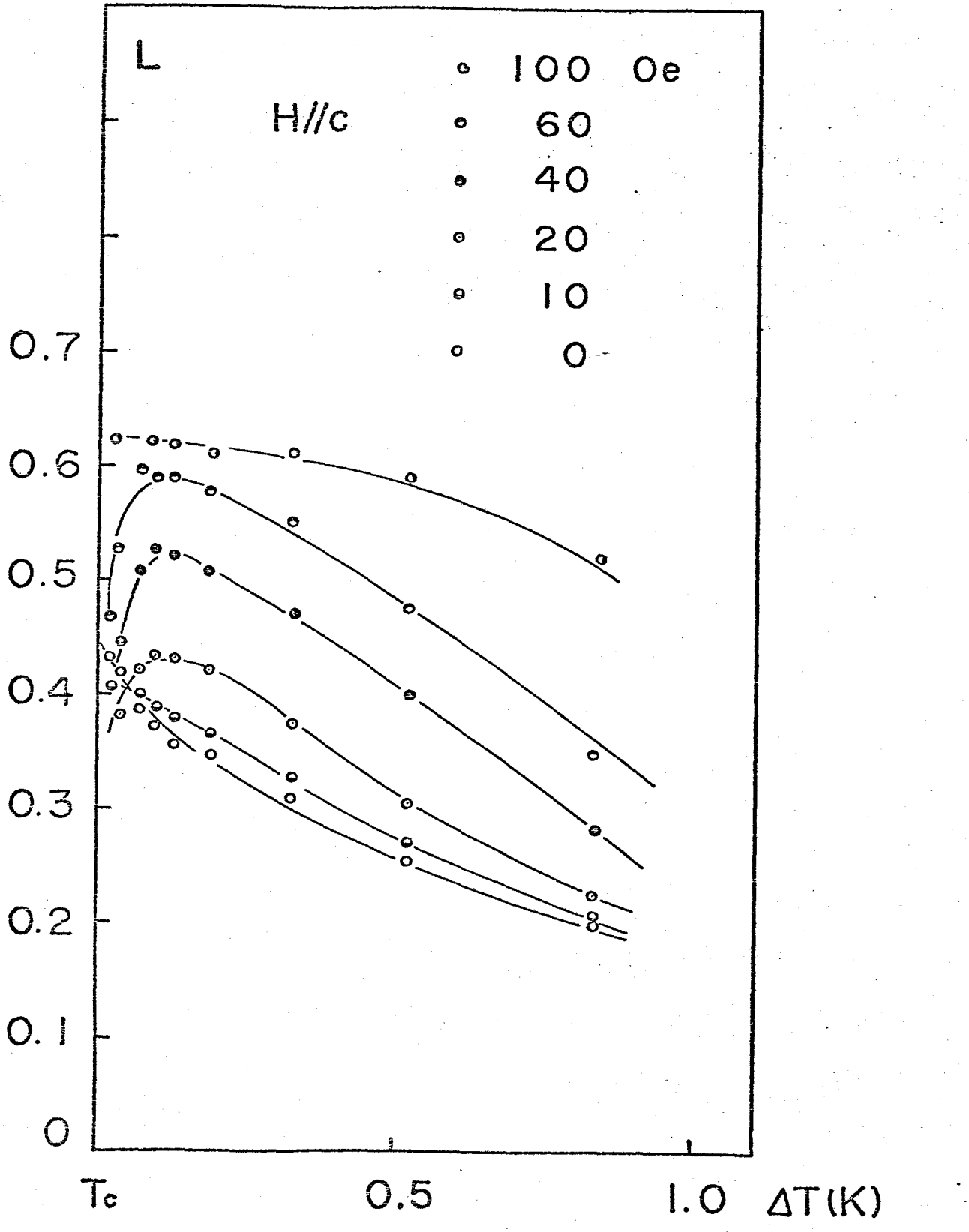

Fig. VI-13. L of $(CH_3NH_3)_2CuCl_4$ plotted against ΔT under external fields which are applied along c-axis, the hard axis.

the result of L when H_c is applied along c axis, the hard axis. For the same value of the field, the value of L in this case is smaller than the case when H_b is applied along b axis.

In both cases of $Mn(CH_3COO)_2 \cdot 4H_2O$ and $(CH_3NH_3)_2CuCl_4$, L increases most drastically when the field is applied along the second easy axis.

References

1) H. Mori and K. Kawasaki: Progr. theor. Phys. 27 (1962) 529.

2) P. G. de Gennes: J. Phys. Chem. Solids 4 (1958) 223.

3) W. M. de Jong: Thesis, Leiden 1975.

4) M. S. Seehra and T. G. Castner, Jr.: Solid State Commun. 8 (1970) 787.

5) D. L. Huber: Phys. Rev. B 6 (1972) 3180.

6) J. Koetzler and H. von Philipsborn: Phys. Rev. Letters 40 (1978) 790.

7) K. Tomita and T. Kawasaki: Progr. theor. Phys. 44 (1970) 1173.

Appendix

Non-linearity and polydispersive relaxation

One phenomenological possibility of non-Debye relaxation is the non-linear effect, as was predicted by Nishikawa,[1] and Suzuki and Kubo.[2] According to them, the relaxation equation of the magnetization can be expressed as follows, using the Ising model and the molecular field approximation.

$$\tau_c \frac{dM}{dt} = -\lambda M - \eta M^3 + \cdots \quad , \tag{A-1}$$

where τ_c is the microscopic characteristic relaxation time. The relaxation time for high temperature is given by τ_c. The elementary relaxation mechanisms are included in τ_c in this model; they might be interactions with a heat bath. λ and η are the molecular field coefficients, and λ corresponds to the static susceptibility. As the transition point is approached, λ gets smaller to introduce the enhancement of the non-linear term. If we take the non-linear term into consideration, the normalized decay function is obtained as follows.

$$\Psi(t) = \frac{\sqrt{\varepsilon}}{\sqrt{(\varepsilon+k)\exp[2\varepsilon t/\tau_c]-k}} \quad , \tag{A-2}$$

where ε is $(1-T_c/T)$, and k is the measure of the strength of the non-linear term and is equal to $(1/3)M_0^2(T_c/T)^3$, (M_0 is the initial value of M).

(A-2) can be expanded as

$$\Psi(t) = \frac{\sqrt{\varepsilon}}{\sqrt{(\varepsilon+k)\exp[2\varepsilon t/\tau_c]-k}} \tag{A-3}$$

$$= \sum_{n=0}^{\infty} \frac{\varepsilon}{\varepsilon+k} \frac{(2n-1)!!}{n!2^n} \left[\frac{k}{\varepsilon+k}\right]^n e^{-(2n+1)\varepsilon t/\tau_c} .$$

Thus, $\Psi(t)$ is expressed as a superposition of $e^{-(2n+1)\varepsilon t/\tau_c}$ —— a polydispersive relaxation. However, the asymptotic behavior of $\Psi(t)$ for $t\to\infty$ is $e^{-\varepsilon t/\tau_c}$. This comes from the fact that the longest relaxation time is τ_c/ε. This character will be visually found in the Cole-Cole plot in Fig. A-1. This function does not explain the low frequency phenomenon of the experimental results.

Just at T_c, the leading term of the right hand side of the equation (A-1) is M^3 term. In this case the relaxation function is

$$\Psi(t) = \frac{1}{\sqrt{1+2kt}}$$

$$= \int_0^\infty e^{-t/\tau_c} G(\tau)d\tau \ , \qquad \text{(A-4)}$$

$$G(t) = \frac{1}{\tau_c\sqrt{2k\pi}}(\tau/\tau_c)^{-3/2}\exp[-\frac{1}{2k(\tau/\tau_c)}] \ . \qquad \text{(A-5)}$$

The asymptotic form for $t\to\infty$ of this function is $t^{-1/2}$. The corresponding Cole-Cole plot and the distribution function $G(\tau)$ are given in Fig. A-2 and A-3. $t^{-1/2}$ dependence gives rise to the angle $\pi/4$ between the abscissa and the tangent at $\omega=0$. This is much slower than the experimental case. The experimental results will lie between (A-3) and (A-4).

References

1) K. Nishikawa: Progr. theor. Phys. 38 (1967) 305.

2) M. Suzuki and R. Kubo: J. Phys. Soc. Japan 24 (1968) 51.

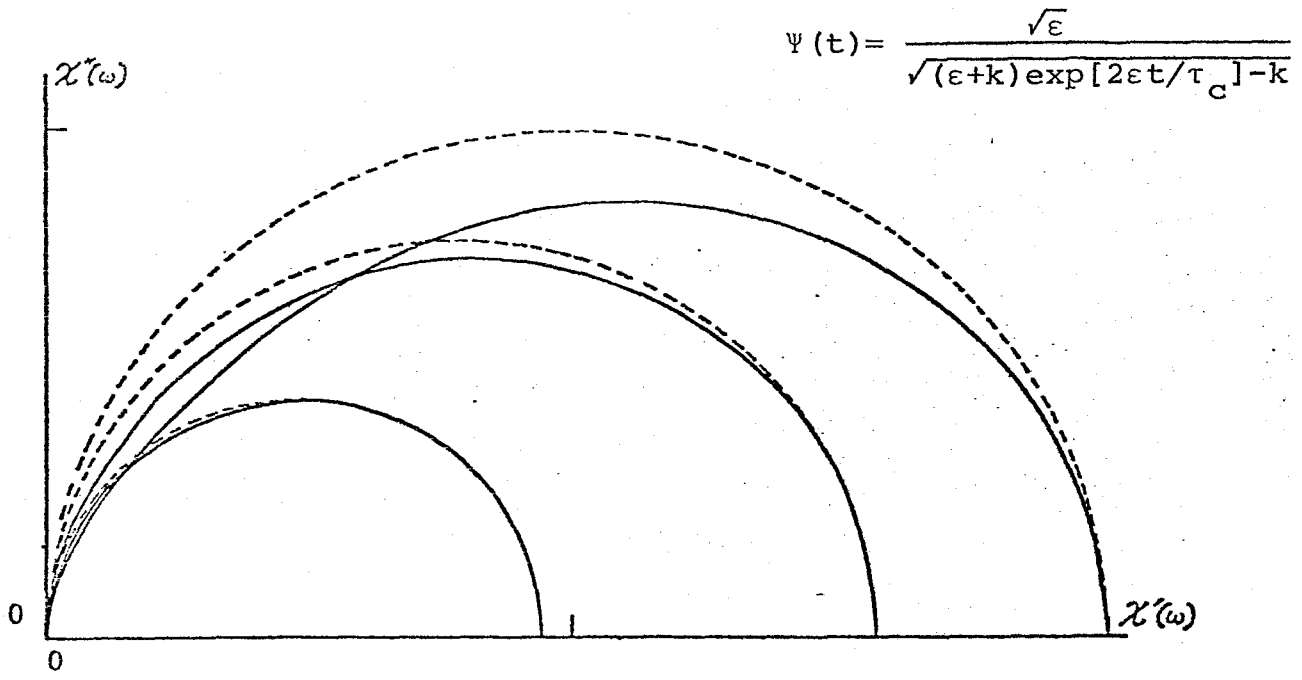

Fig. A-1. Cole-Cole plot corresponding to the decay function which is obtained from the non-linear relaxation equation.

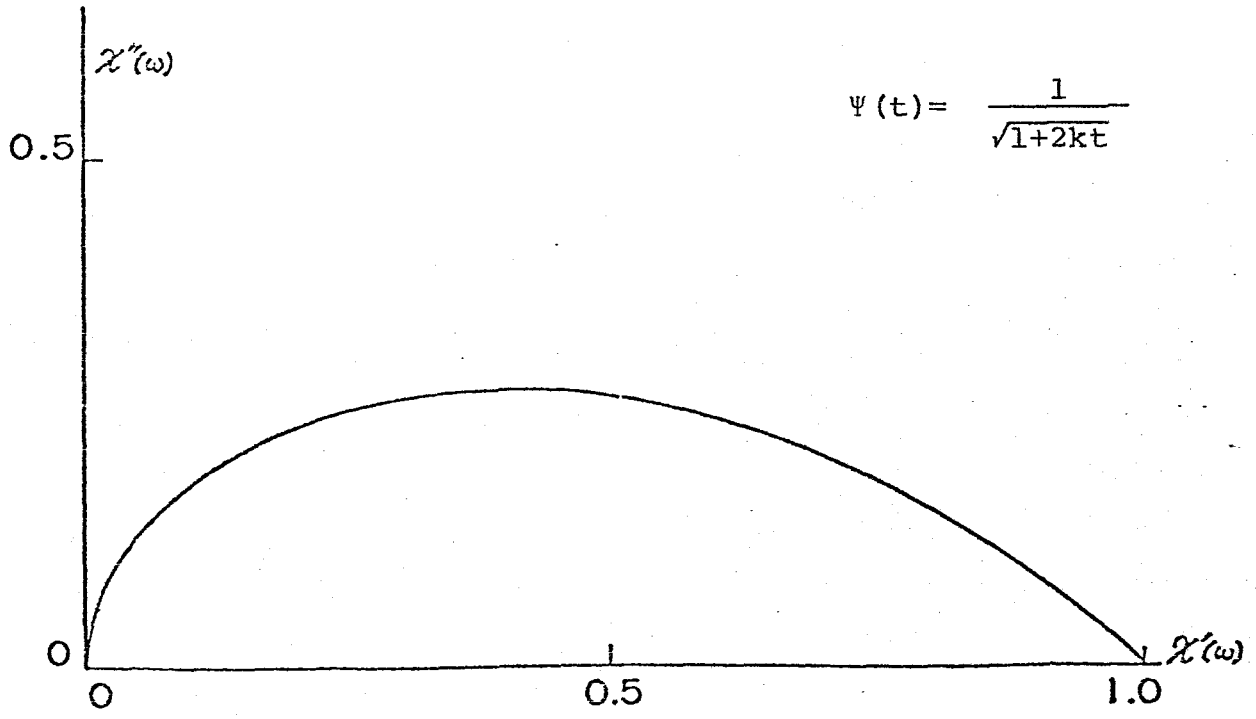

Fig. A-2. Cole-Cole plot corresponding to the decay function of $\Psi(t)=\frac{1}{\sqrt{1+2kt}}$ which is obtained from the critical case of the non-linear equation.

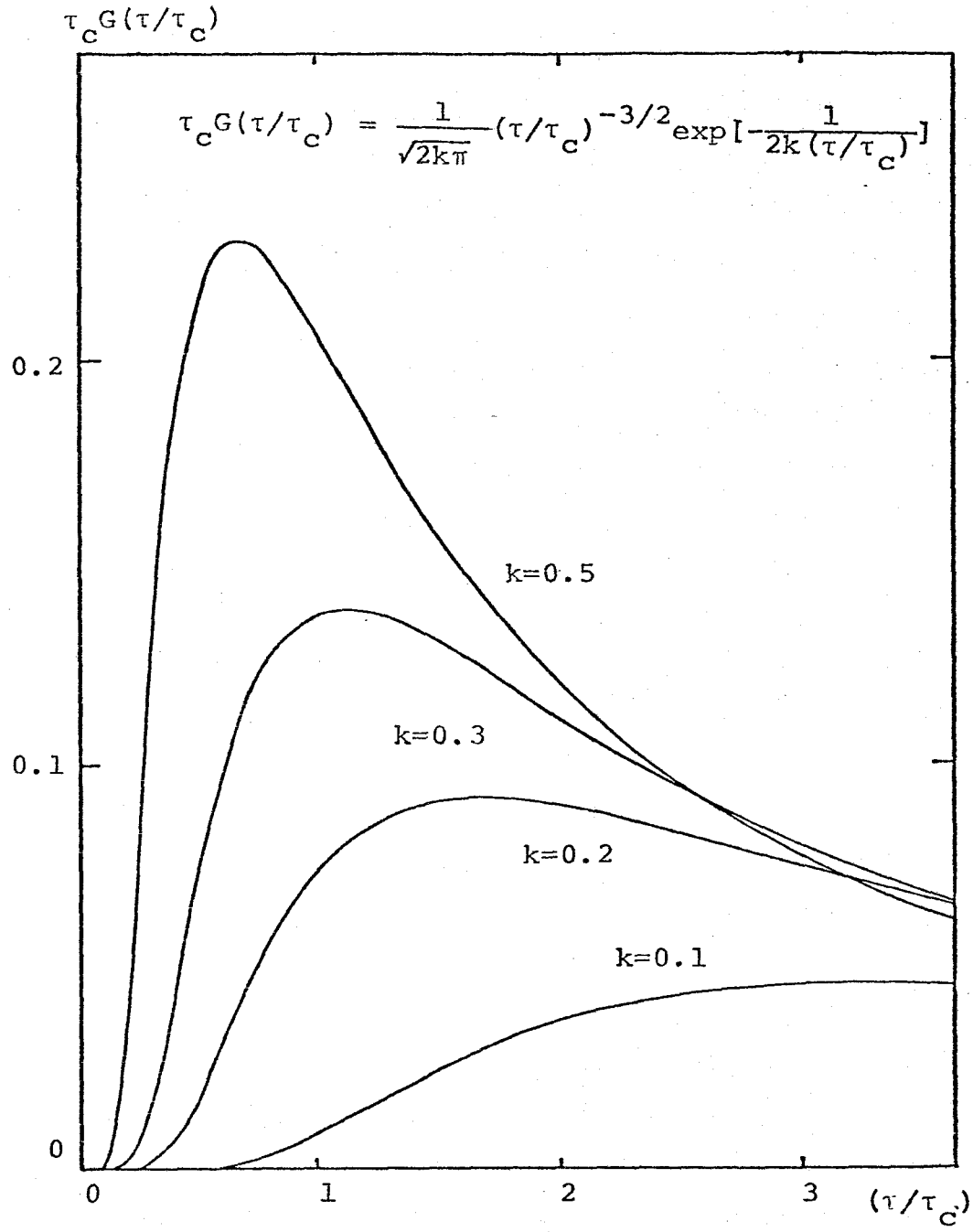

Fig. A-3. The distribution function of the polydispersive relaxation corresponding to the decay function of $\frac{1}{\sqrt{1+2kt}}$ which is obtained from the critical case of the non-linear equation

Acknowledgments

The author would like to express his thanks for the hearty encouragement and stimulating discussions of Professor T. Haseda and Professor M. Matsuura in the course of this study. He also thanks Dr. K. Amaya and Dr. K. Takeda for many fruitful discussions and advices. He thanks Mr. H. Kobayashi for his technical aid, and the colleagues of the Haseda group for their help in the experiments.